Figure 1
H-Coal PDU Reactor

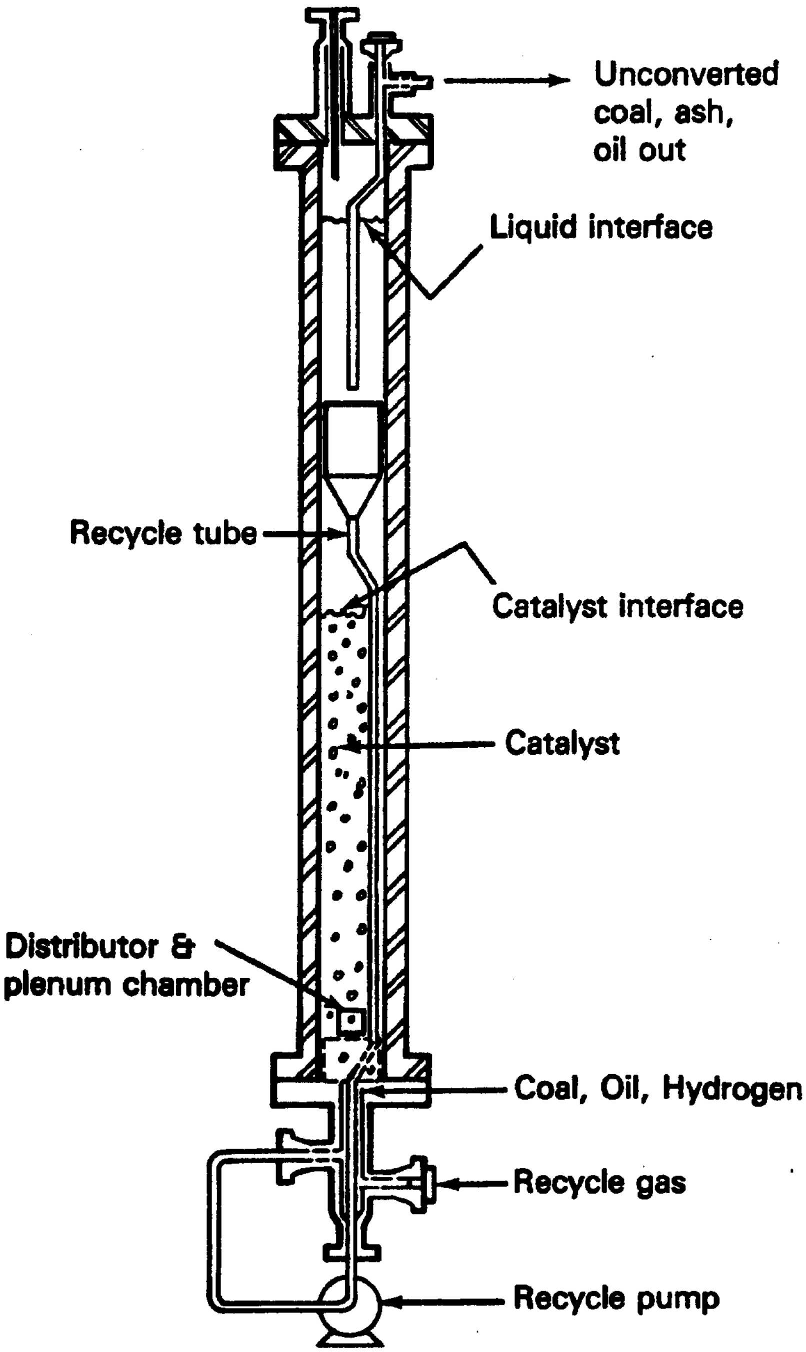

Figure 2

Ebullated Bed Composed of 3 Phases

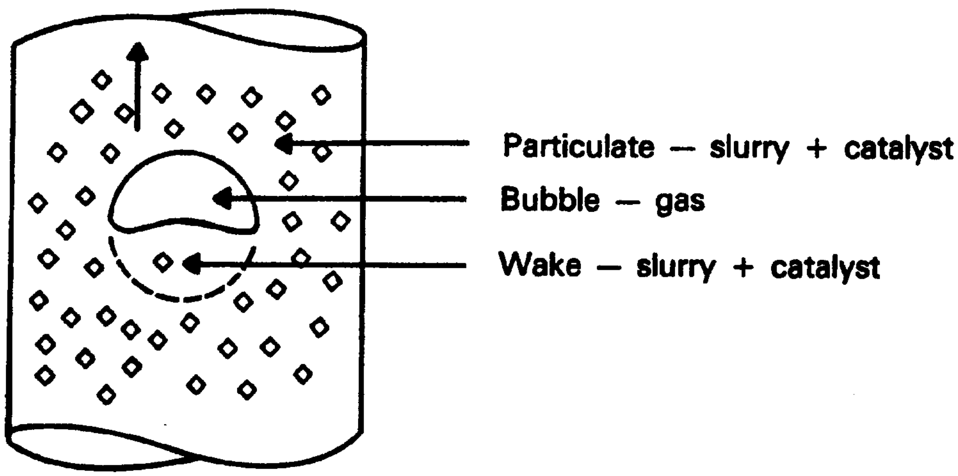

Figure 3
Schematic Diagram of the Fluid Dynamics Unit

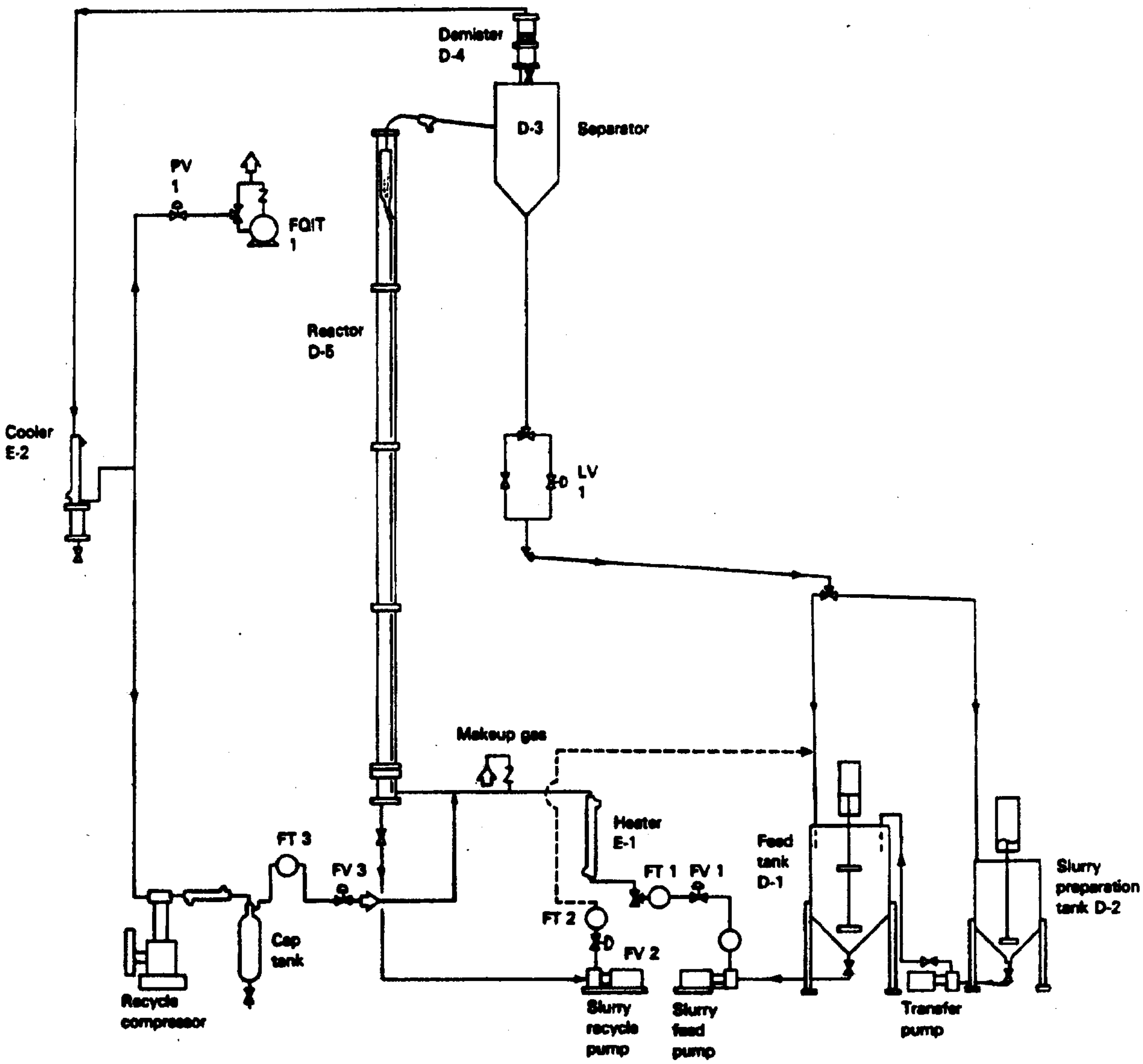

Figure 4

Gamma Ray Scans
Liquid Velocity 0.07 ft/sec

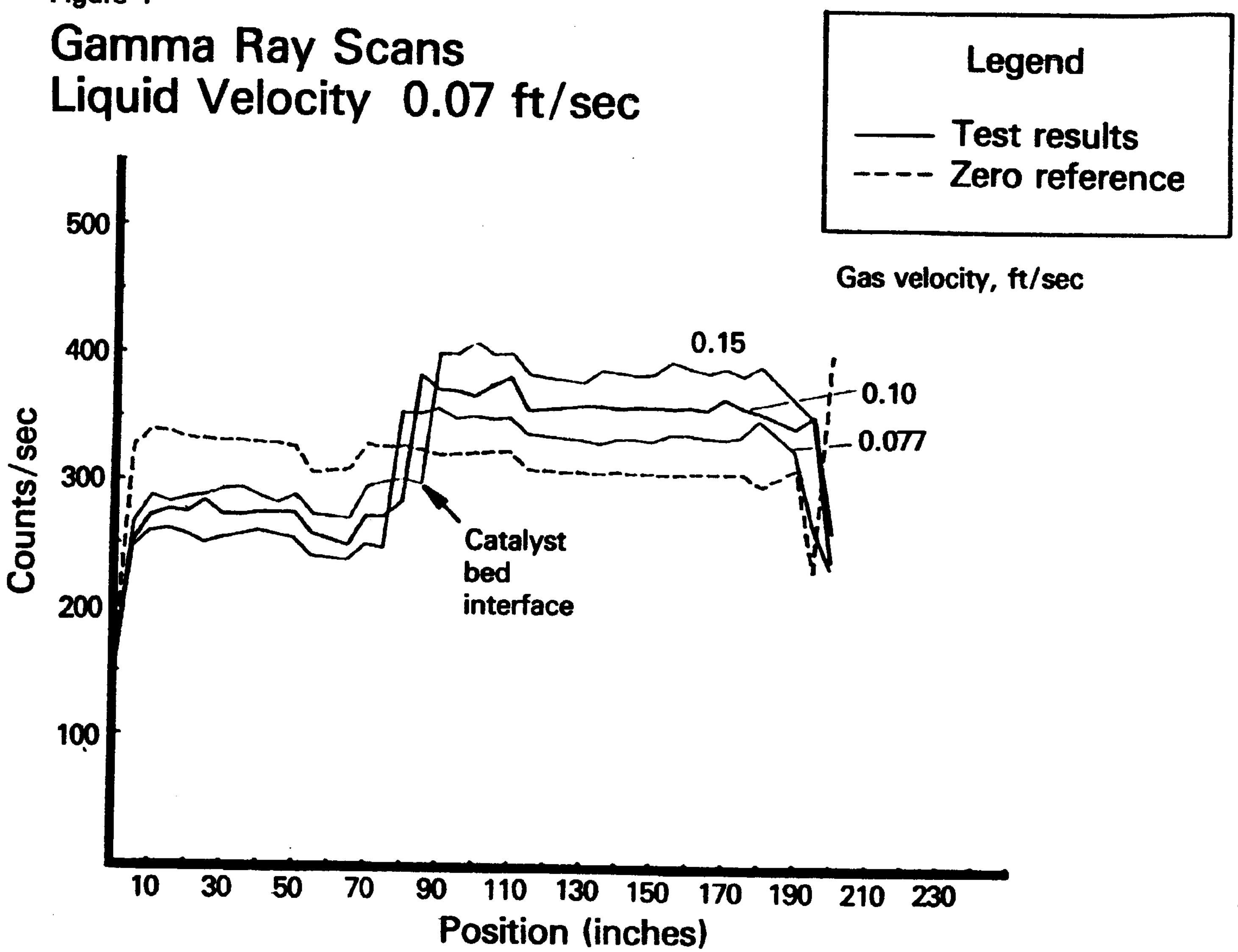

FIGURE 5

RICHARDSON ZAKI CORRELATION
RUN AU77-223
KEROSENE / 20.7 VOL % COAL CHAR / HDS-2A CATALYST

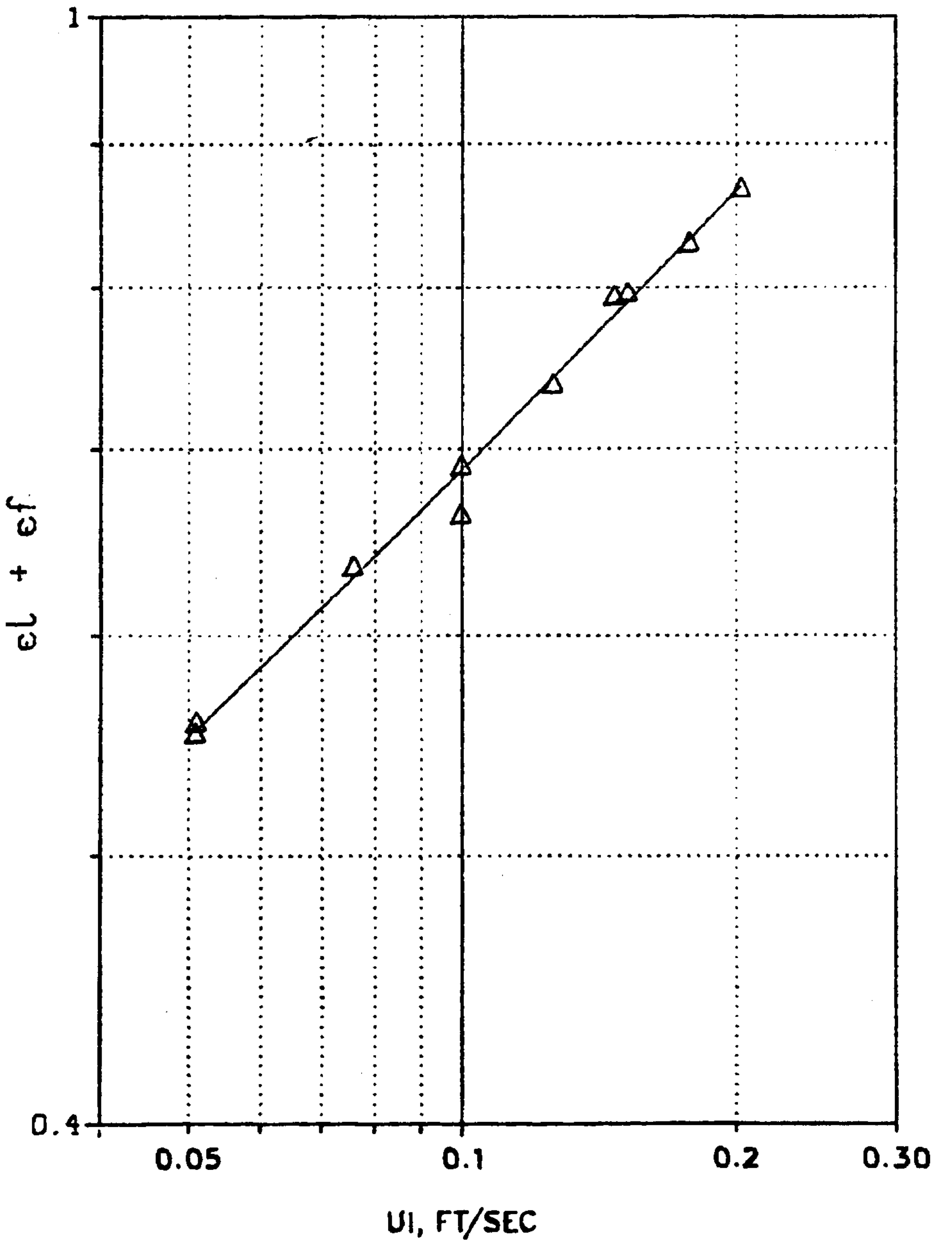

Figure 6

Schematic Diagram of Drift Flux vs. Gas Holdup: Darton and Harrison (3)

(Gas/liquid/solid fluidization)

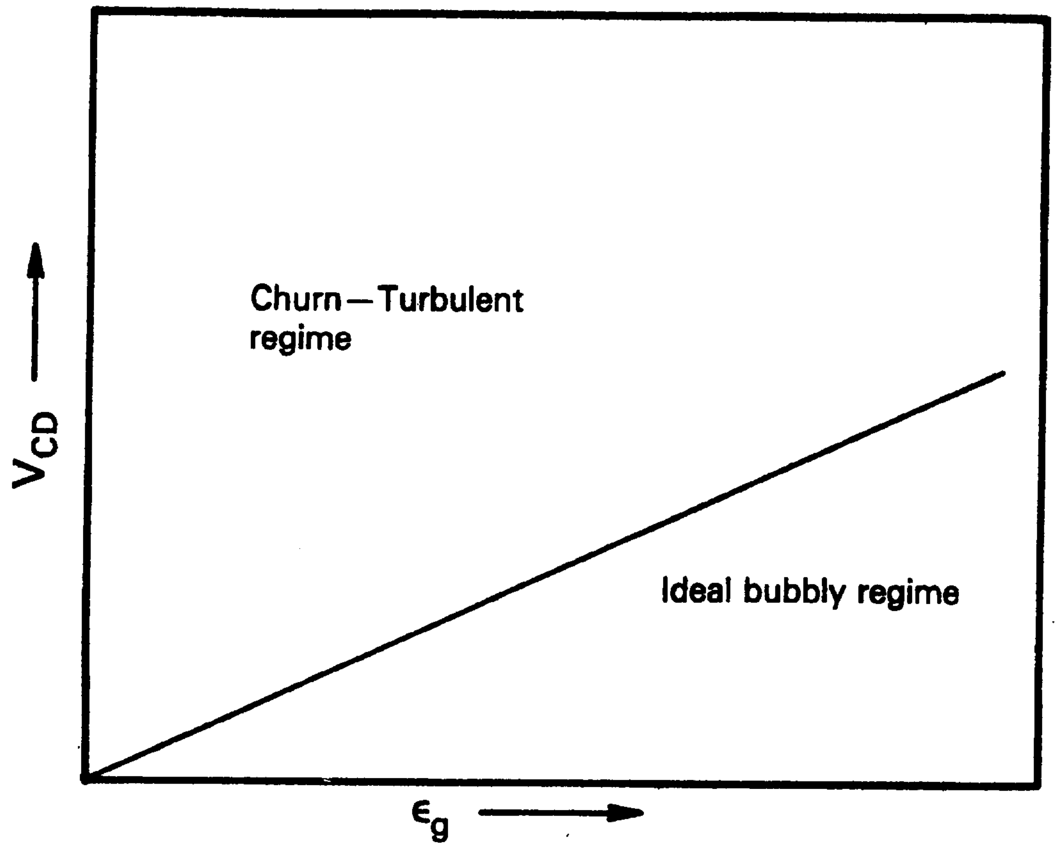

FIGURE 7

DRIFT FLUX DENSE PHASE,COLD FLOW RUN 218
KEROSENE / NO FINES / HDS-2A CATALYST

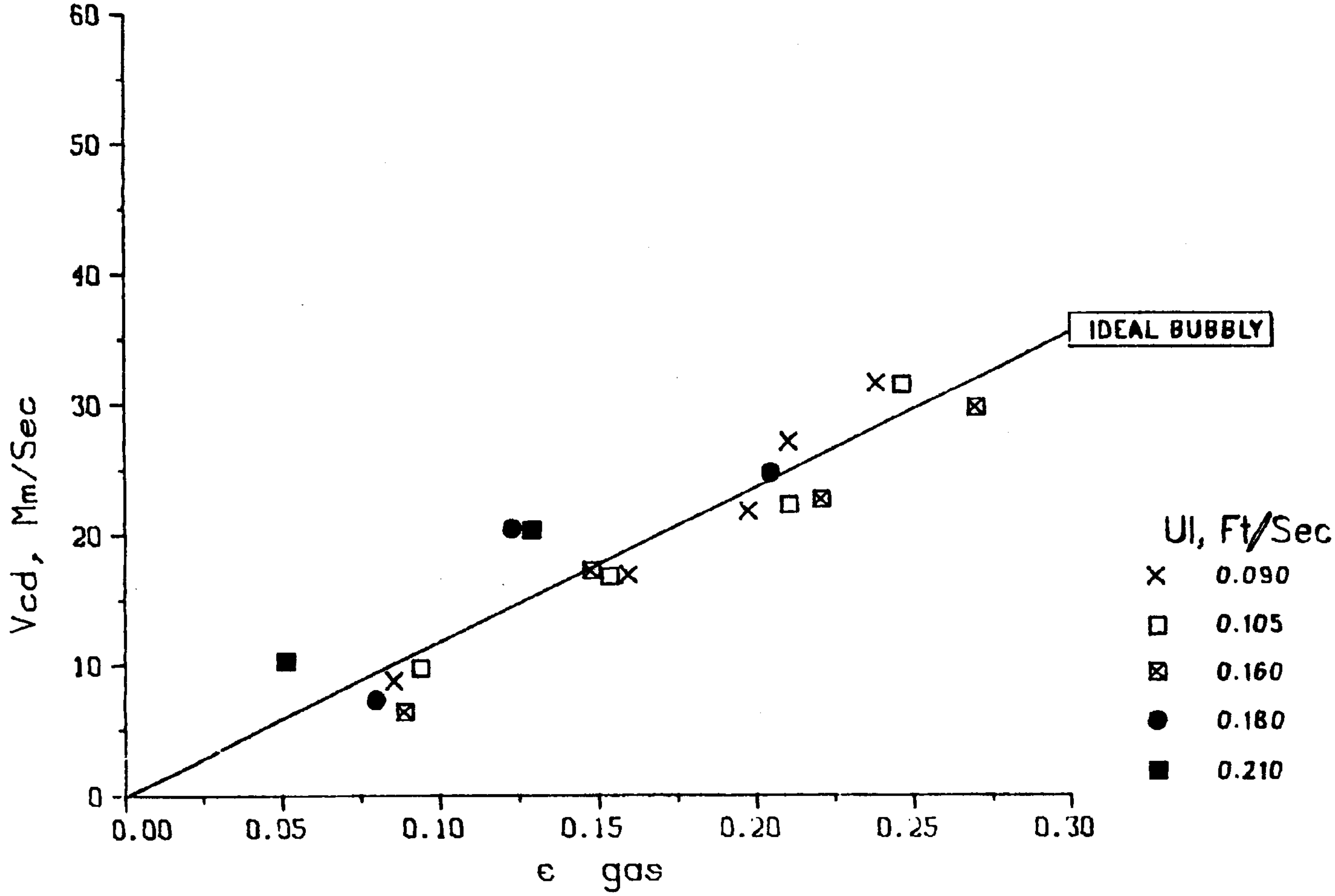

FIGURE 8

DRIFT FLUX DENSE PHASE ,COLD FLOW RUN 221
KEROSENE / 4 VOL % COAL CHAR FINES / HDS-2A CATALYST

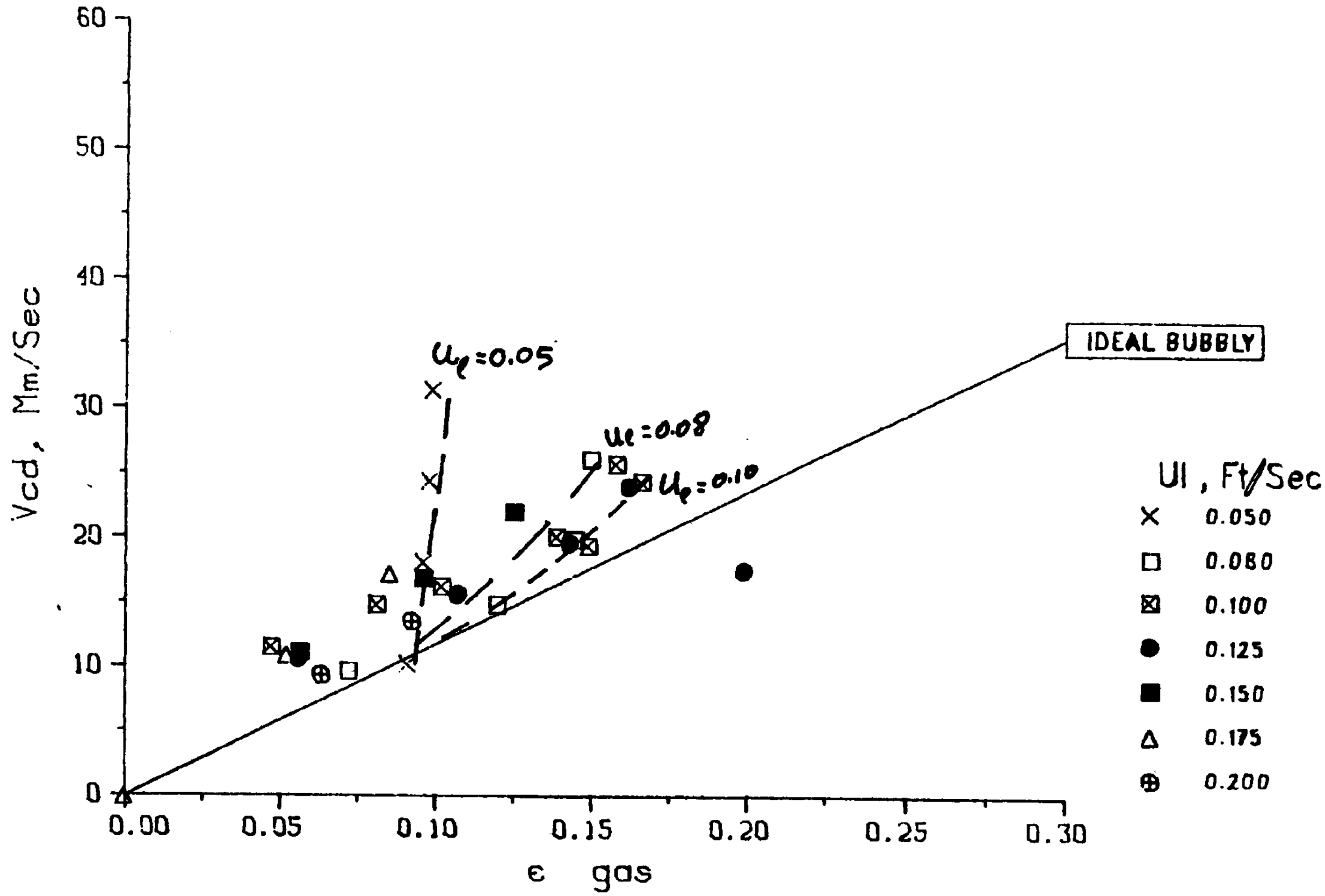

FIGURE 9

DRIFT FLUX DENSE PHASE, COLD FLOW RUN 222
KEROSENE / 9.8 VOL % COAL CHAR FINES / HDS-2A CATALYST

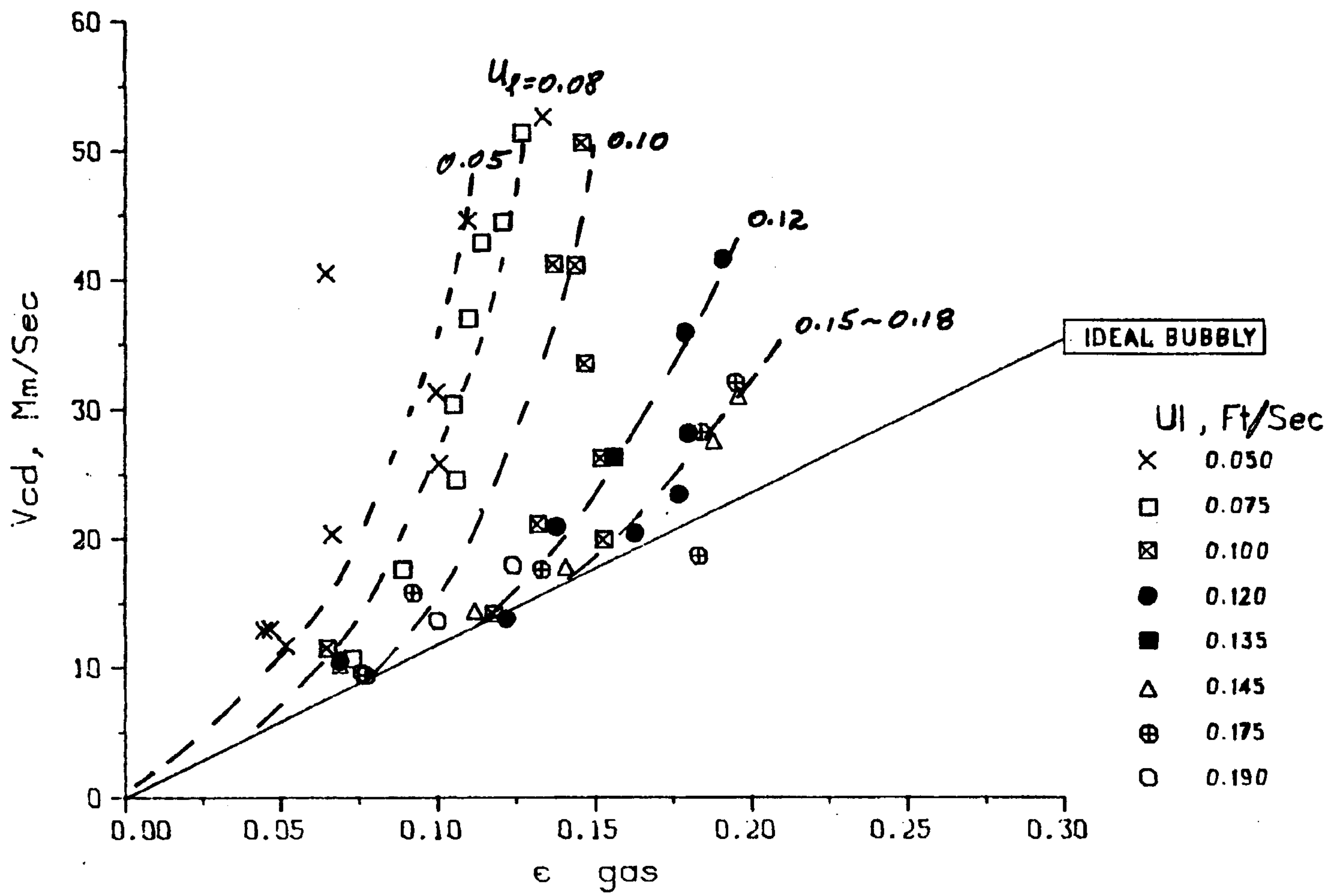

FIGURE 10

DRIFT FLUX DENSE PHASE,COLD FLOW RUN 223
KEROSENE / 20.7 VOL % COAL CHAR FINES / HDS-2A CATALYST

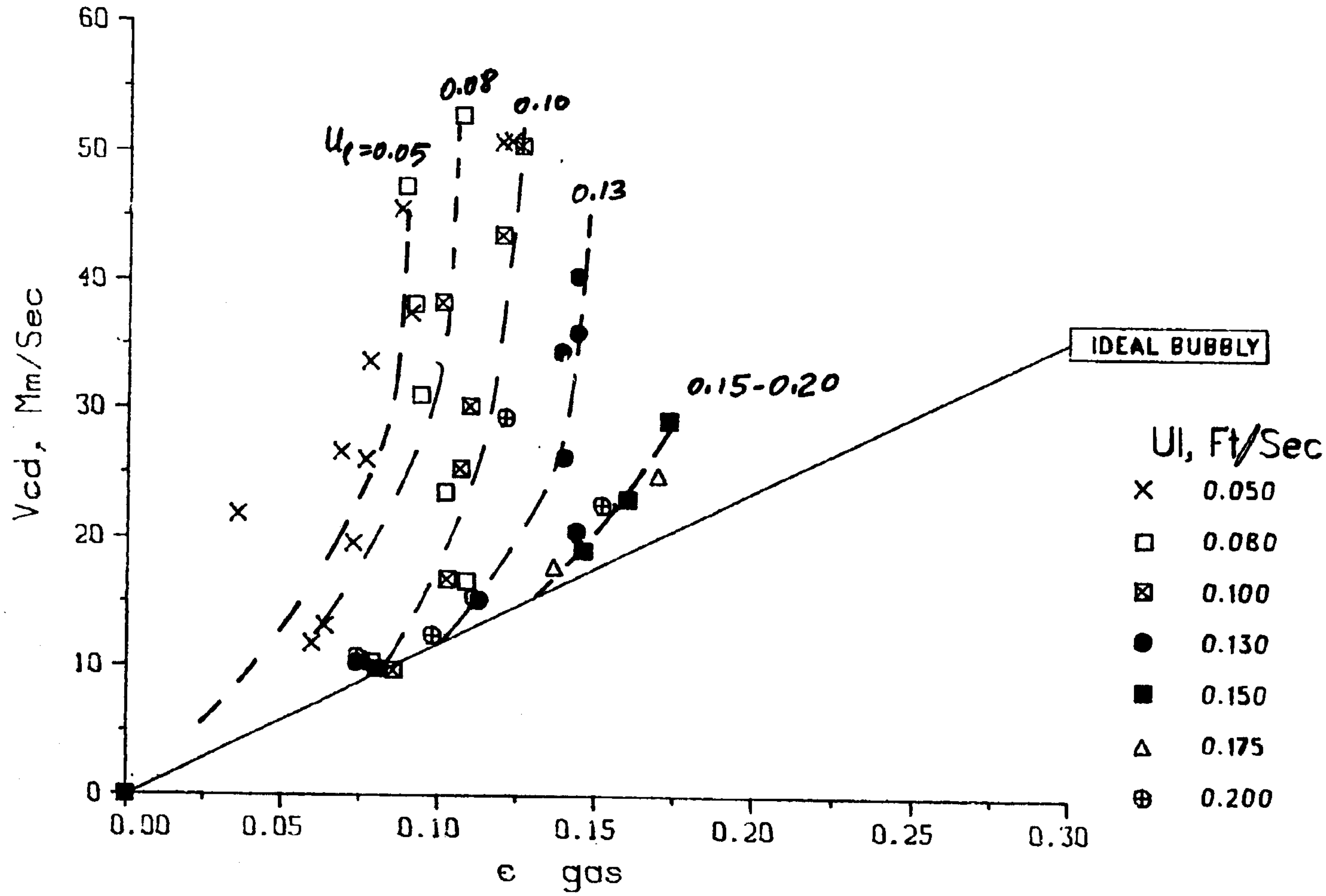

FIGURE 11

DRIFT FLUX DENSE PHASE,COLD FLOW RUN 224
KEROSENE / 15.4 VOL % COAL CHAR FINES / AMOCAT-1A CATALYST

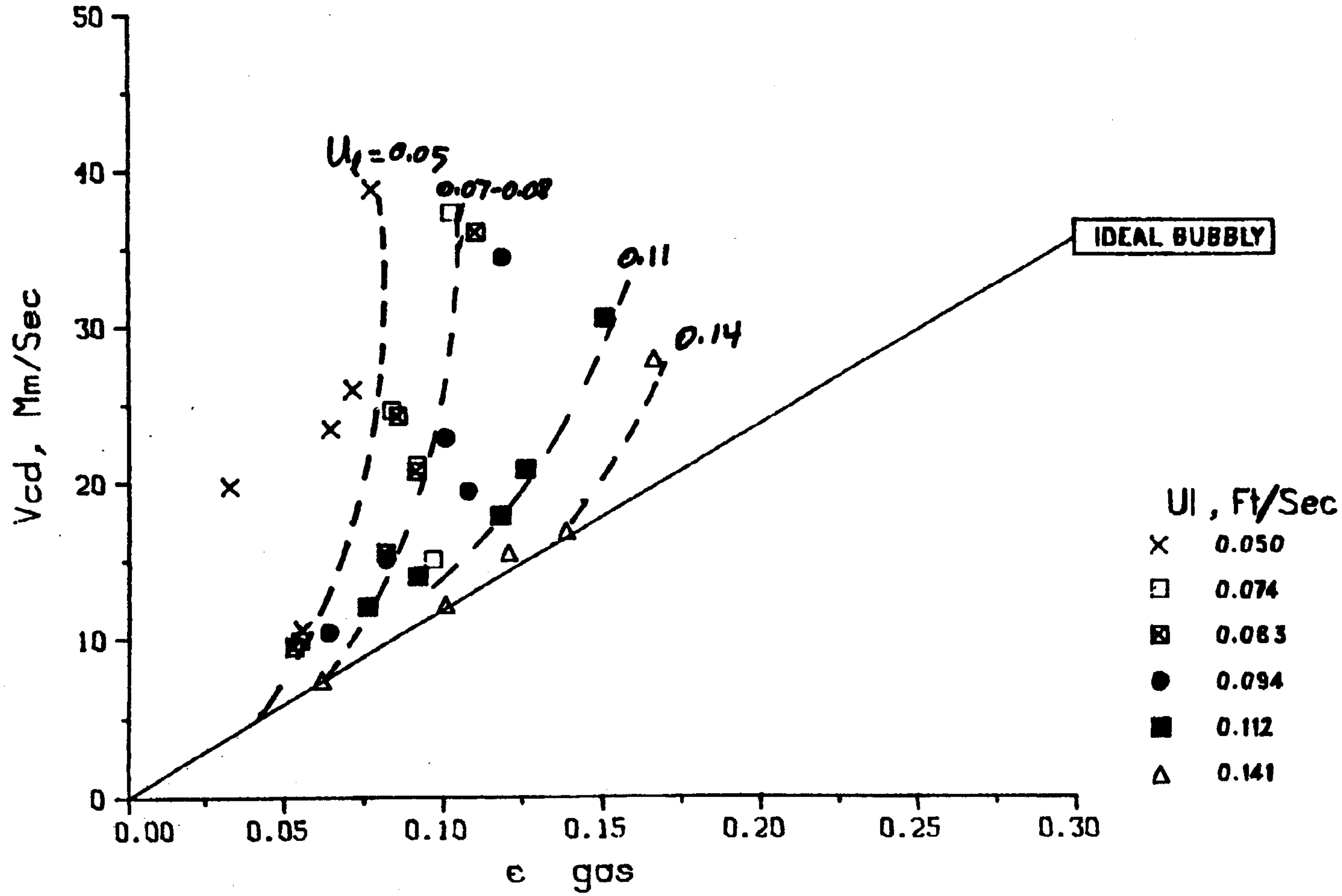

Figure 12

Fines Concentration Effect on Gas Holdup

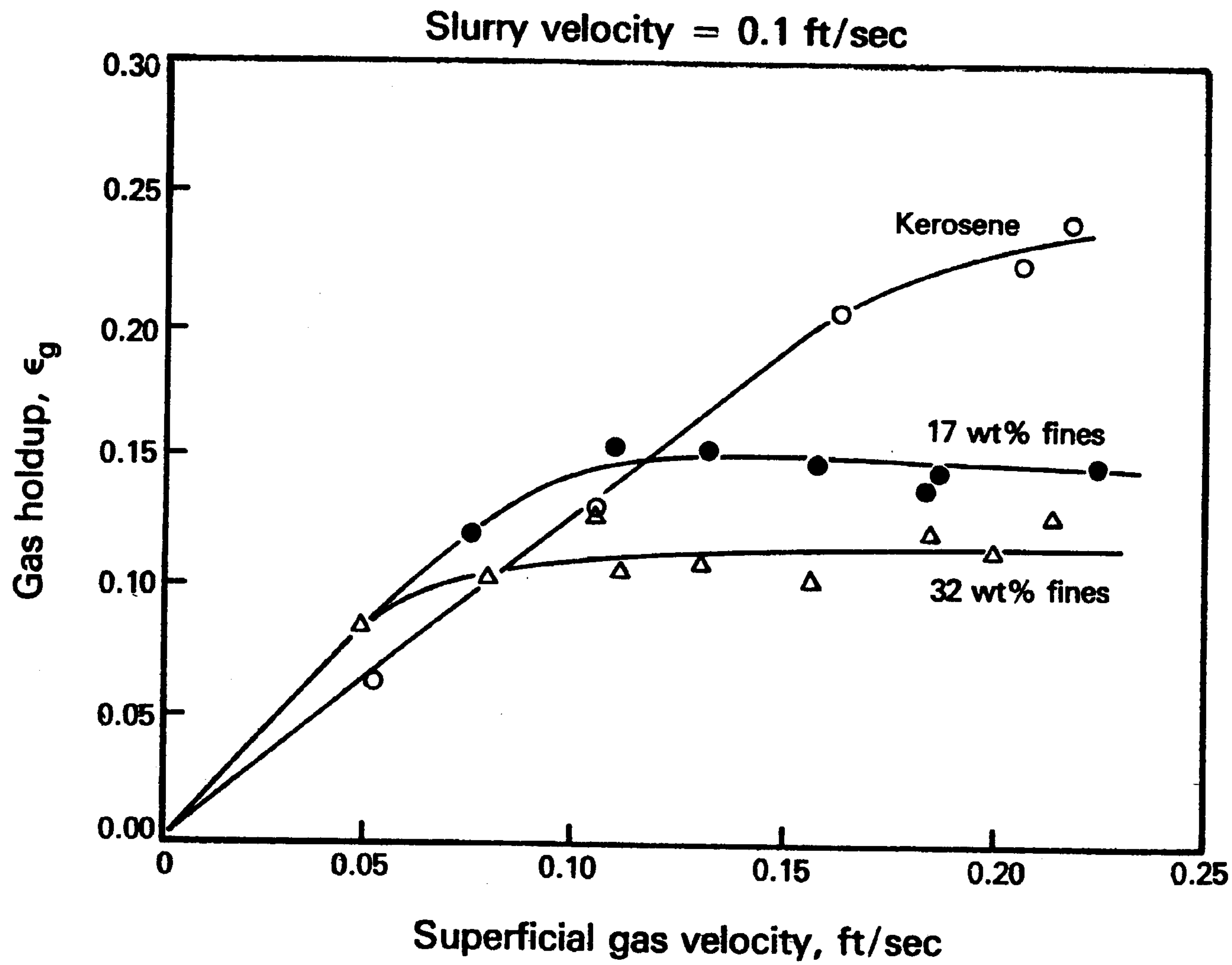

FIGURE 13

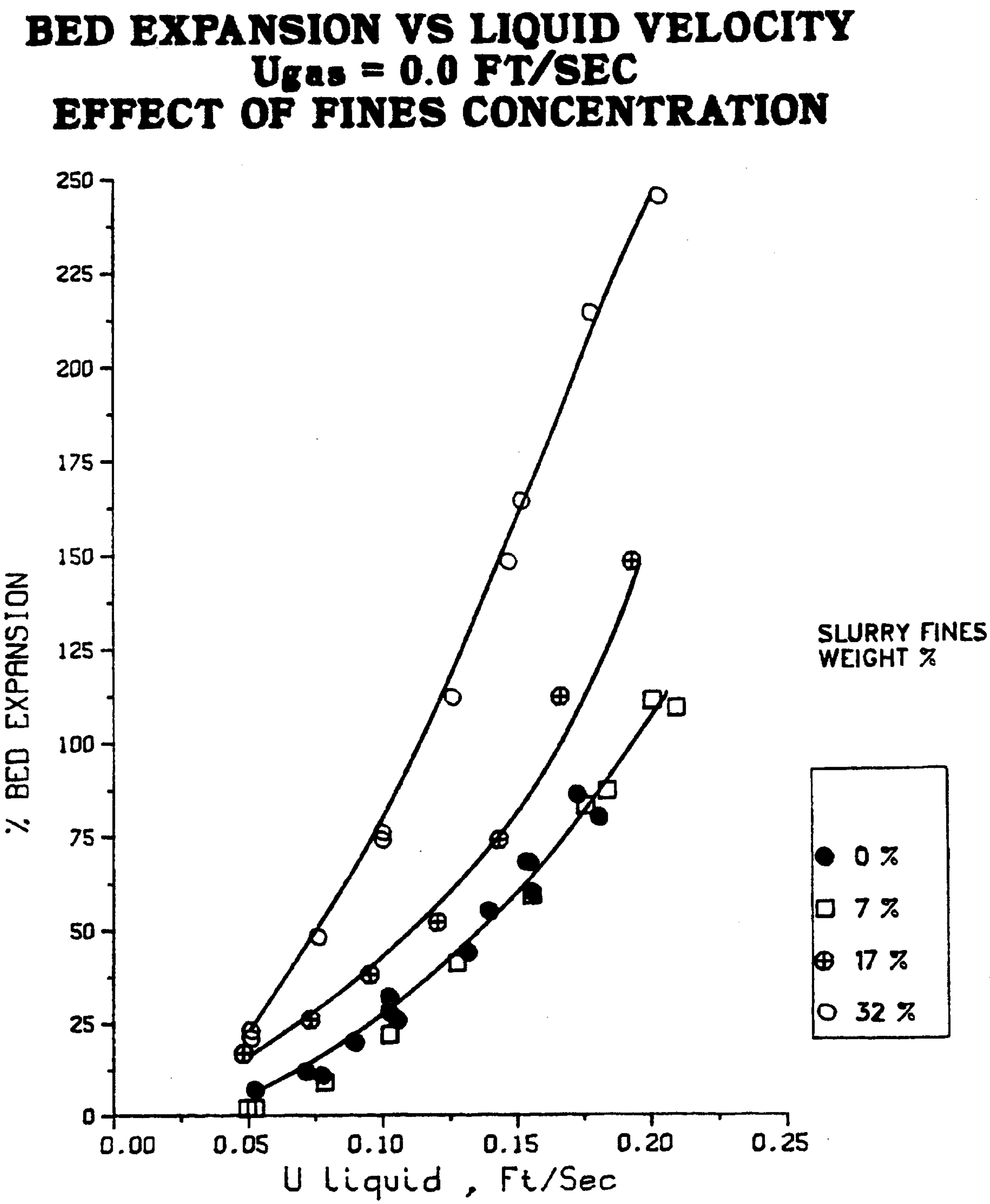
BED EXPANSION VS LIQUID VELOCITY
Ugas = 0.0 FT/SEC
EFFECT OF FINES CONCENTRATION
250
225
200
175
150
125
100
75
50
25
0
% BED EXPANSION
0.00
0.05
0.10
0.15
0.20
0.25
U Liquid , Ft/Sec
SLURRY FINES
WEIGHT %
0 %
7 %
17 %
32 %

FIGURE 14

BED EXPANSION VS LIQUID VELOCITY
Ugas = 0.100 FT/SEC
EFFECT OF FINES CONCENTRATION

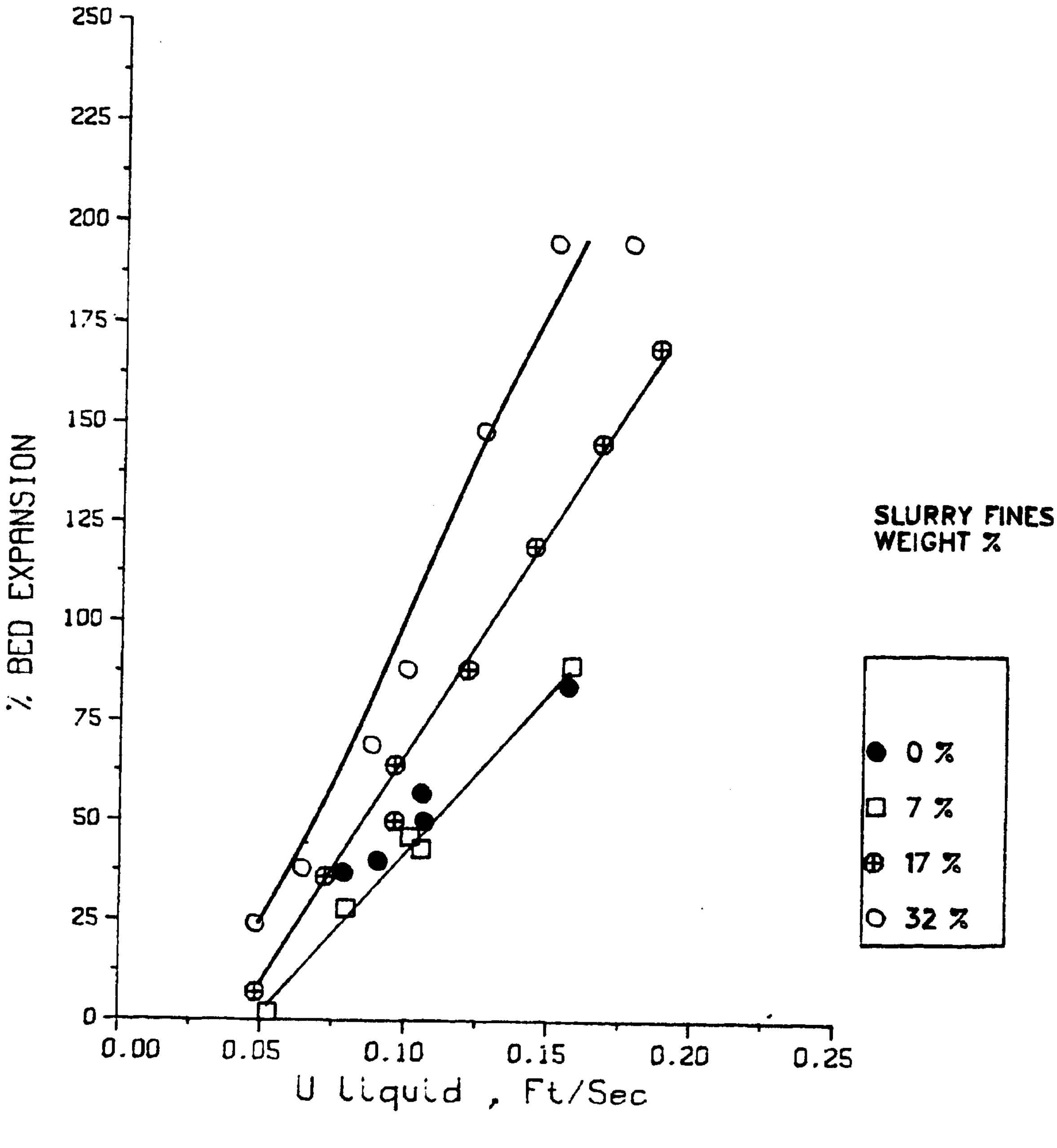

FIGURE 15

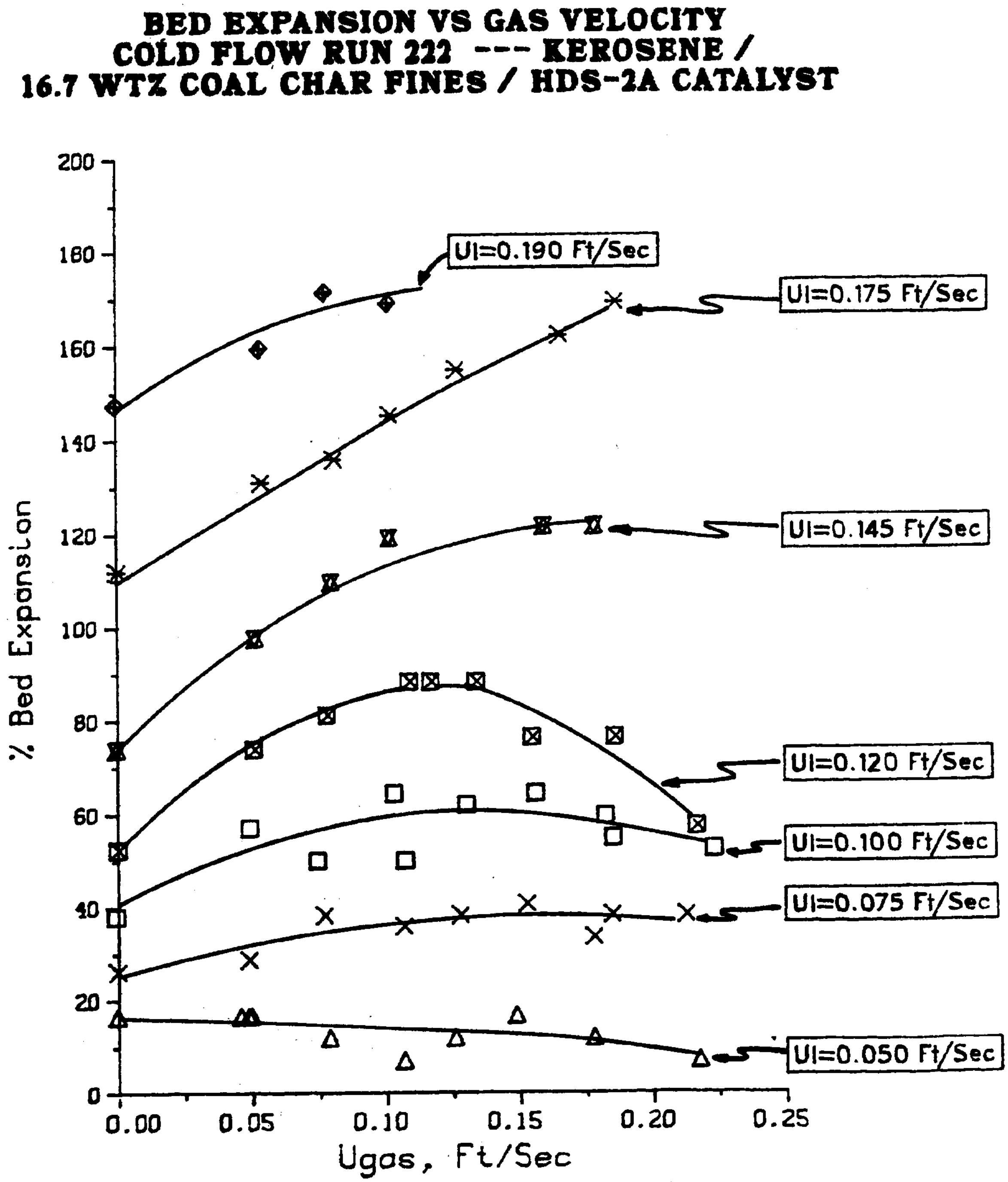

BED EXPANSION VS GAS VELOCITY
COLD FLOW RUN 222 --- KEROSENE /
16.7 WT% COAL CHAR FINES / HDS-2A CATALYST
Ul=0.190 Ft/Sec
Ul=0.175 Ft/Sec
Ul=0.145 Ft/Sec
Ul=0.120 Ft/Sec
Ul=0.100 Ft/Sec
Ul=0.075 Ft/Sec
Ul=0.050 Ft/Sec
% Bed Expansion
Ugas, Ft/Sec
200
180
160
140
120
100
80
60
40
20
0
0.00
0.05
0.10
0.15
0.20
0.25

FIGURE 16

**BED EXPANSION VS GAS VELOCITY
COLD FLOW RUN 224 -- KEROSENE /
25.0 WT % COAL CHAR FINES / AMOCAT-IA CATALYST**

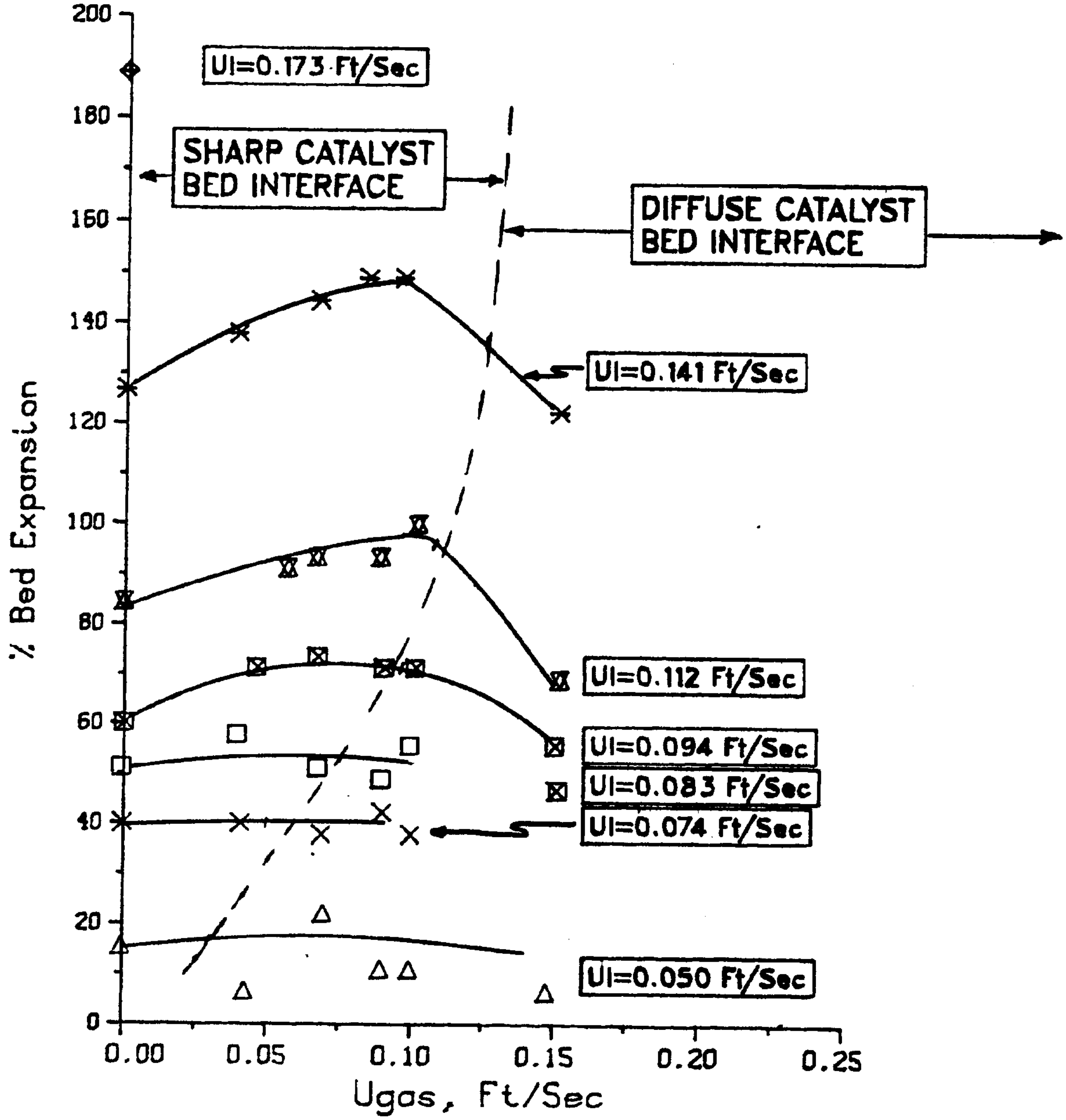

Figure 17

Comparison of Axial Dispersion Coefficient for Various Multi-Phase Fluidization Systems

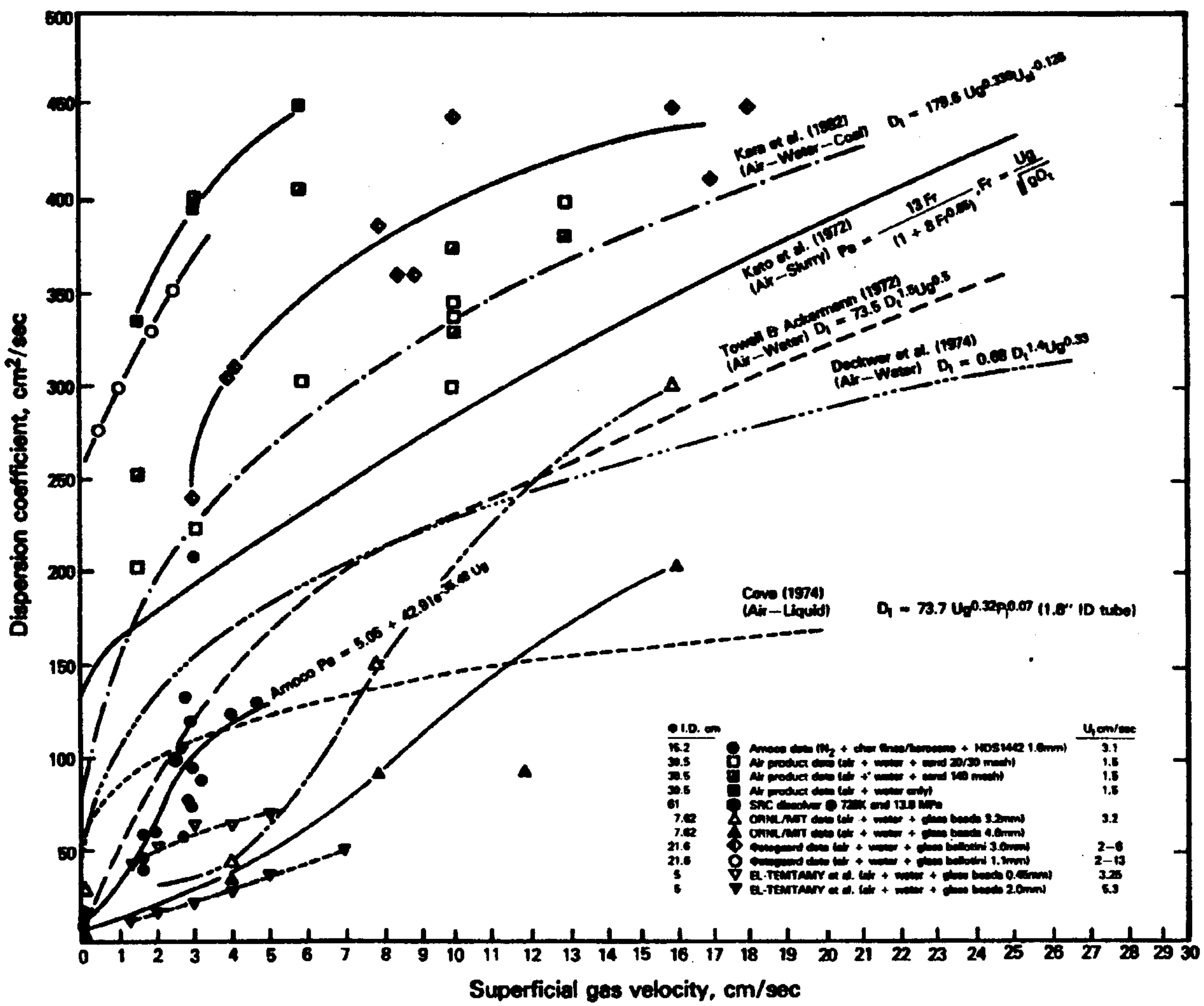

Figure 18

Adsorption of Thiophene by Coal Char Fines

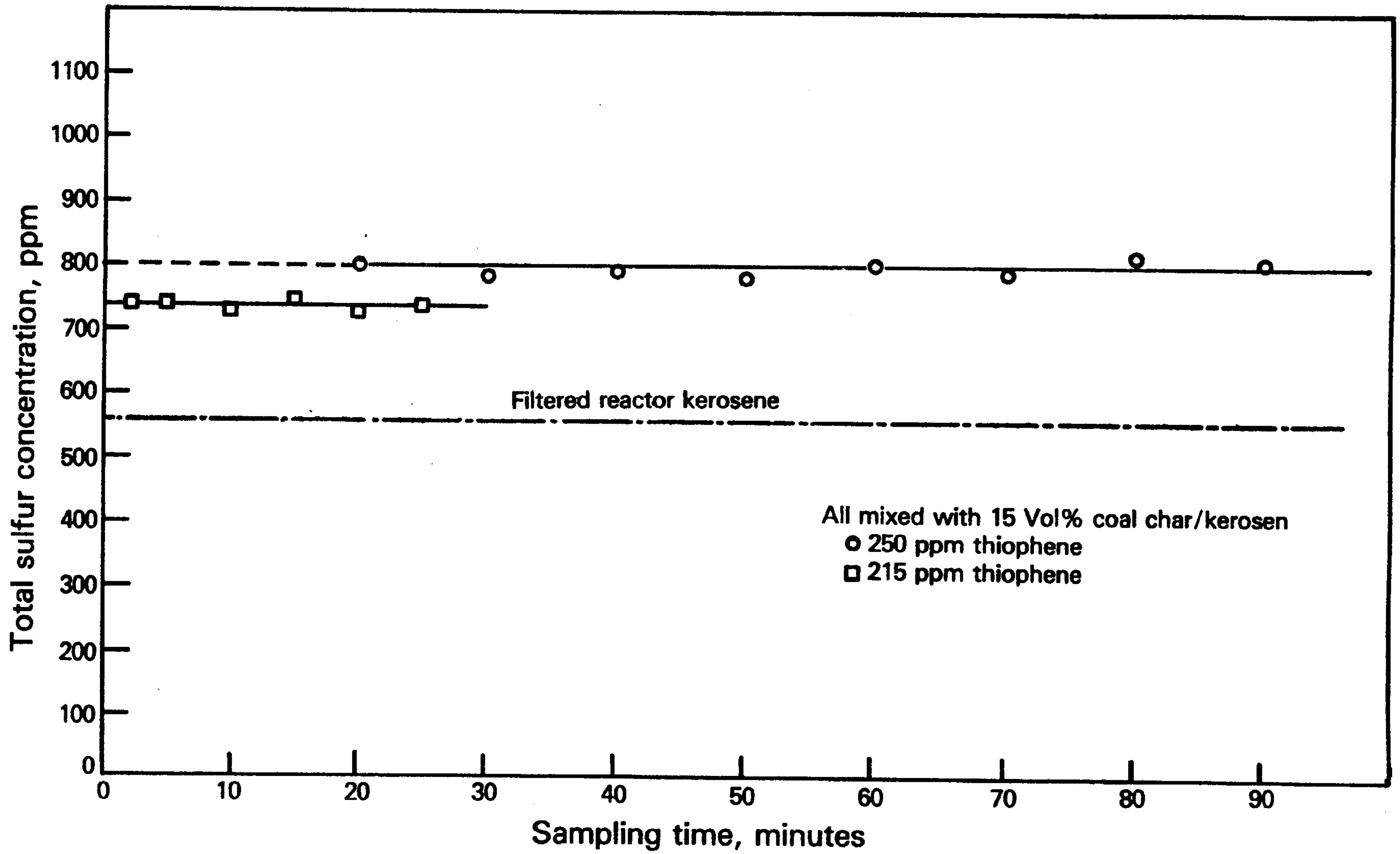

Figure 19

Input Pulse and the Resulting C-Curves for Tracer Injection at the Slurry Inlet Before the Bubble Cap Distributor

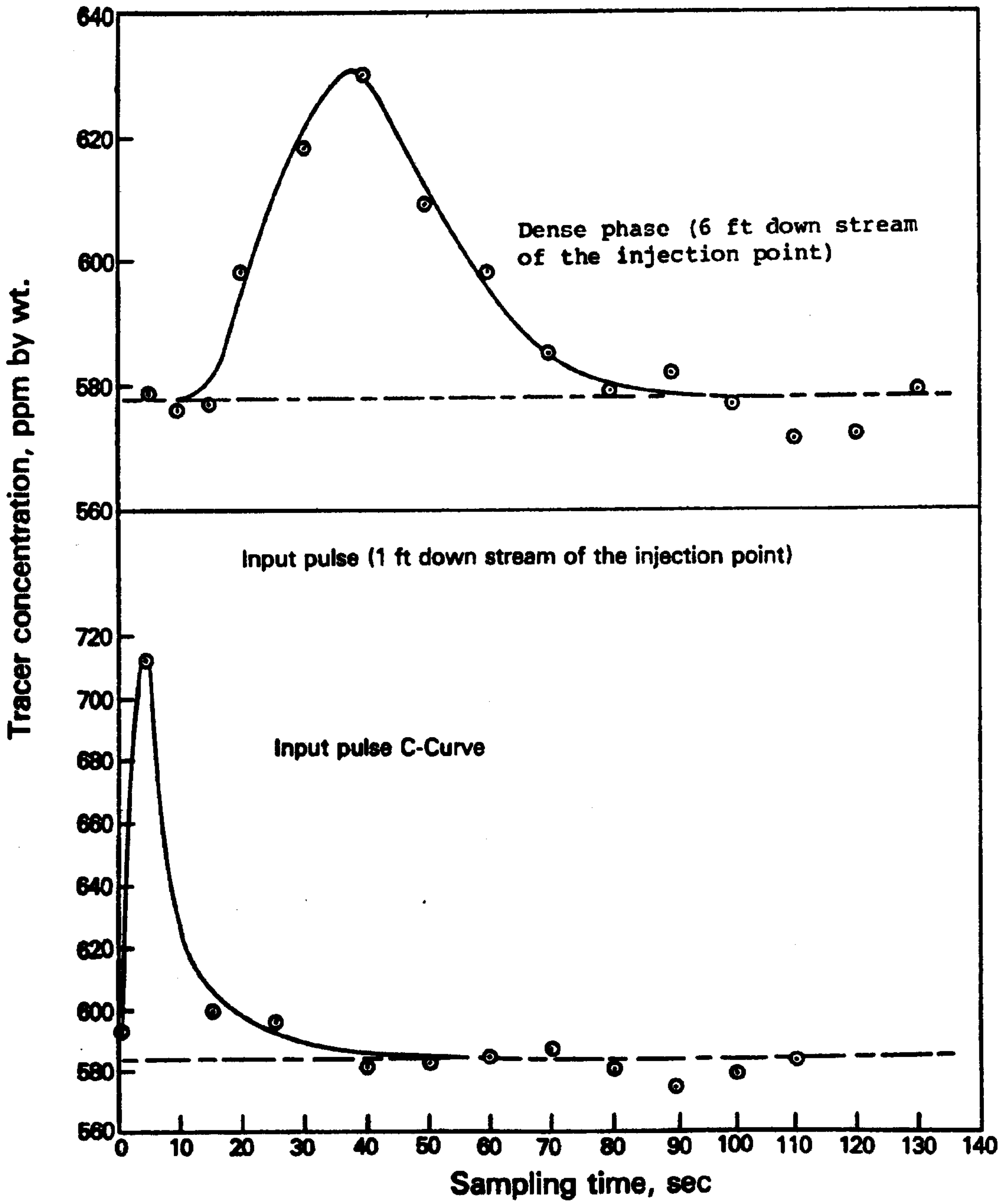

Figure 20

Schematic Diagram of Amoco Cold Flow Unit Modified for Liquid Mixing Experiment

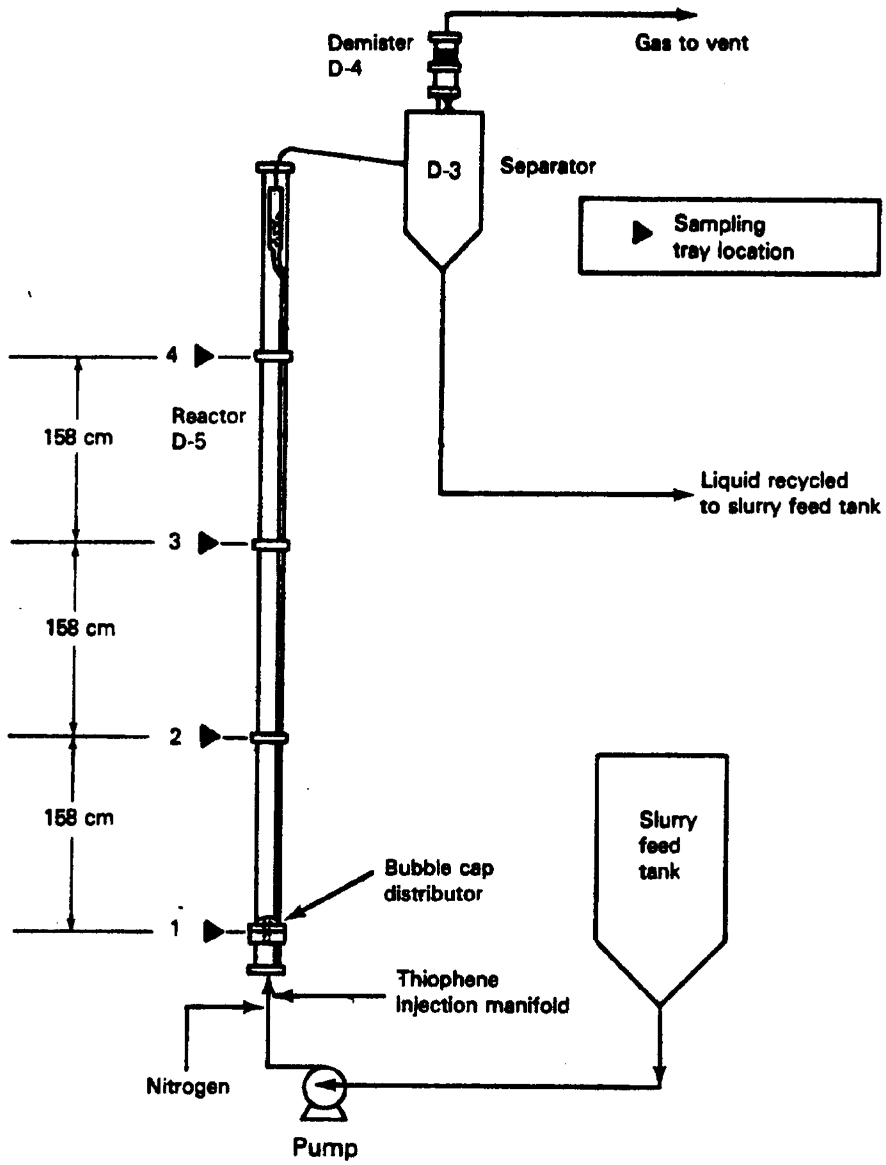

Figure 21

AMOCO PILOT PLANT SAMPLING SYSTEM DETAILS

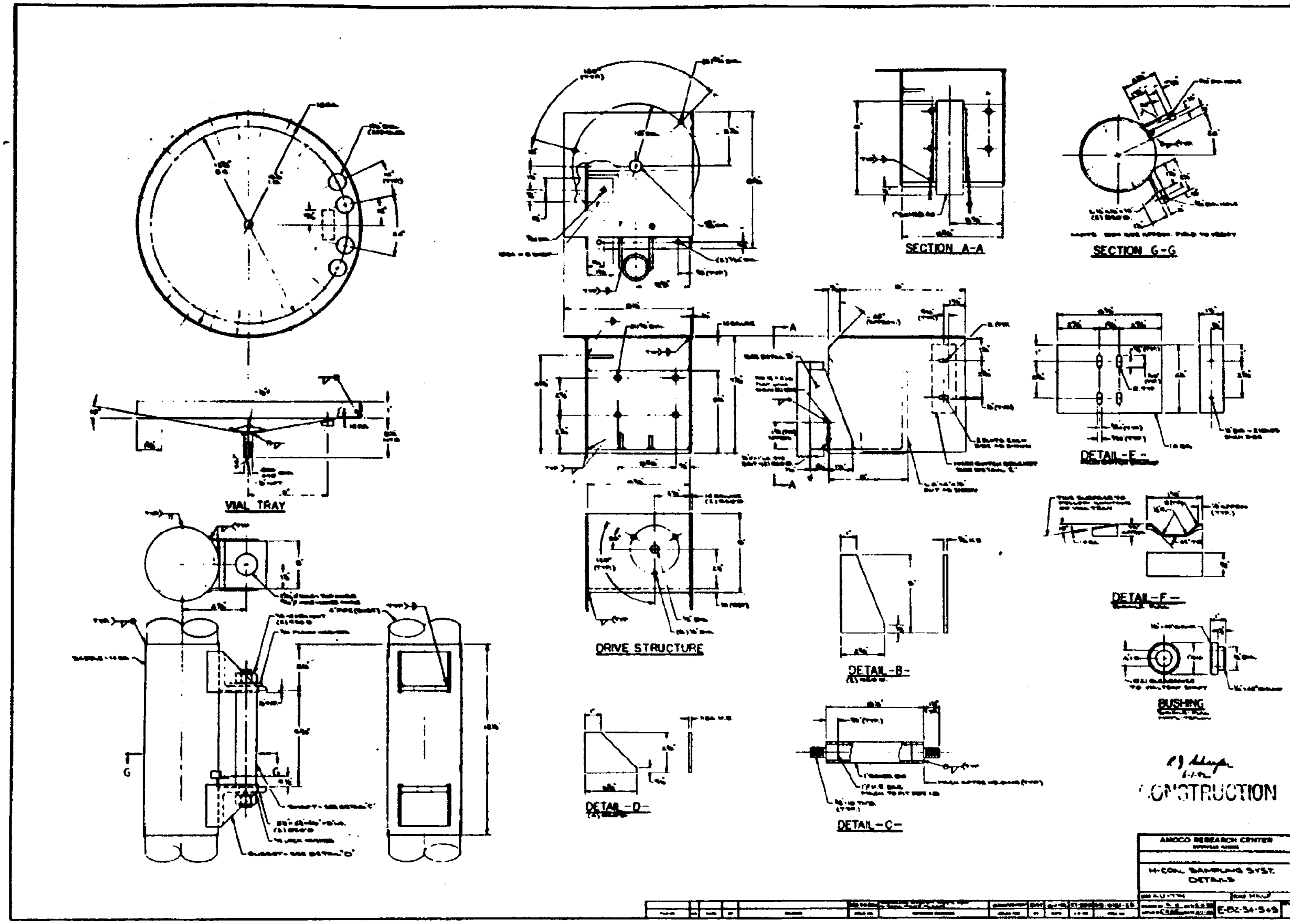

Figure 22

AMOCO PILOT PLANT SAMPLING SYSTEM TRAY

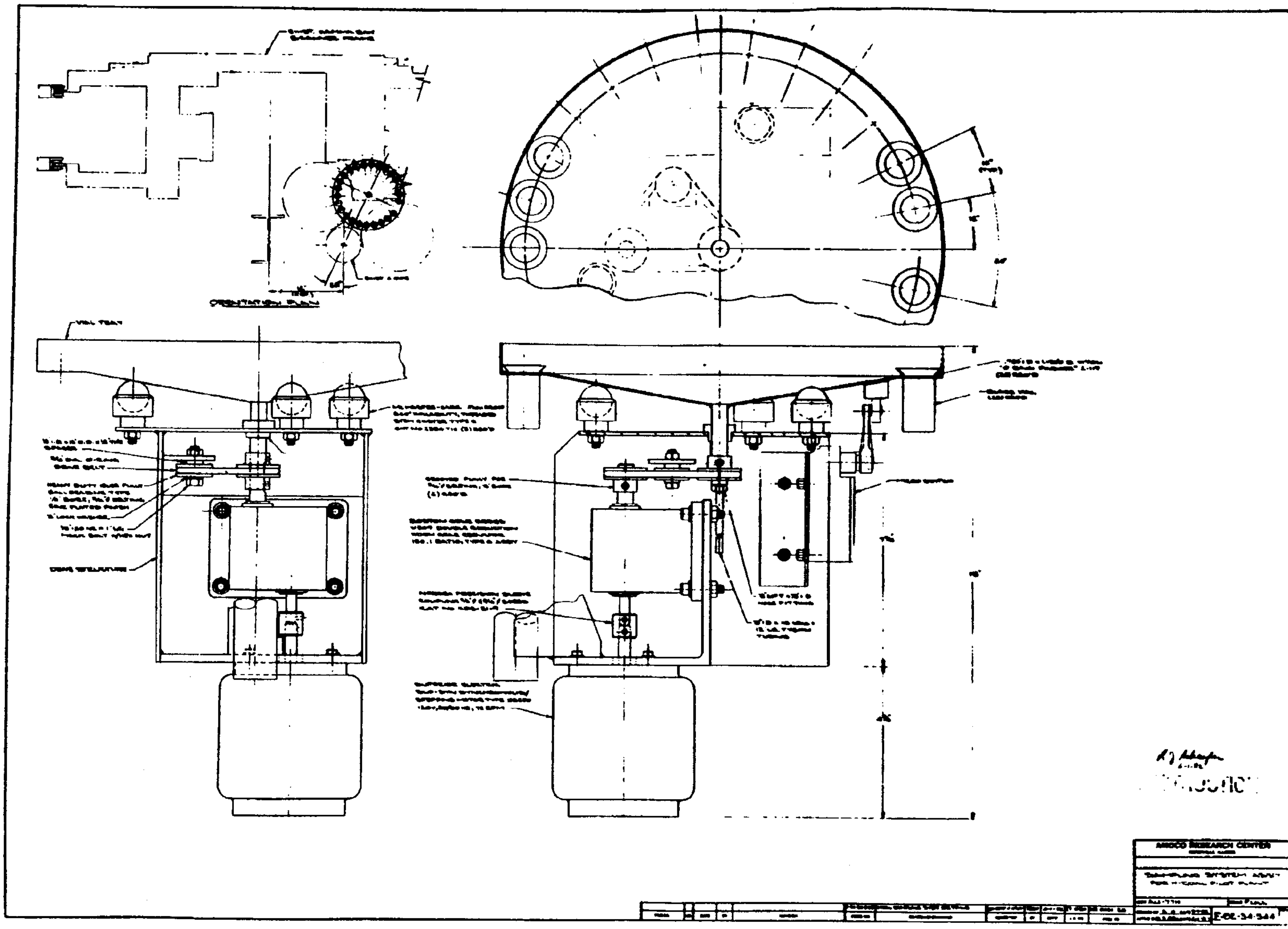

Figure 23

AMOCO PILOT PLANT TRACER INJECTOR

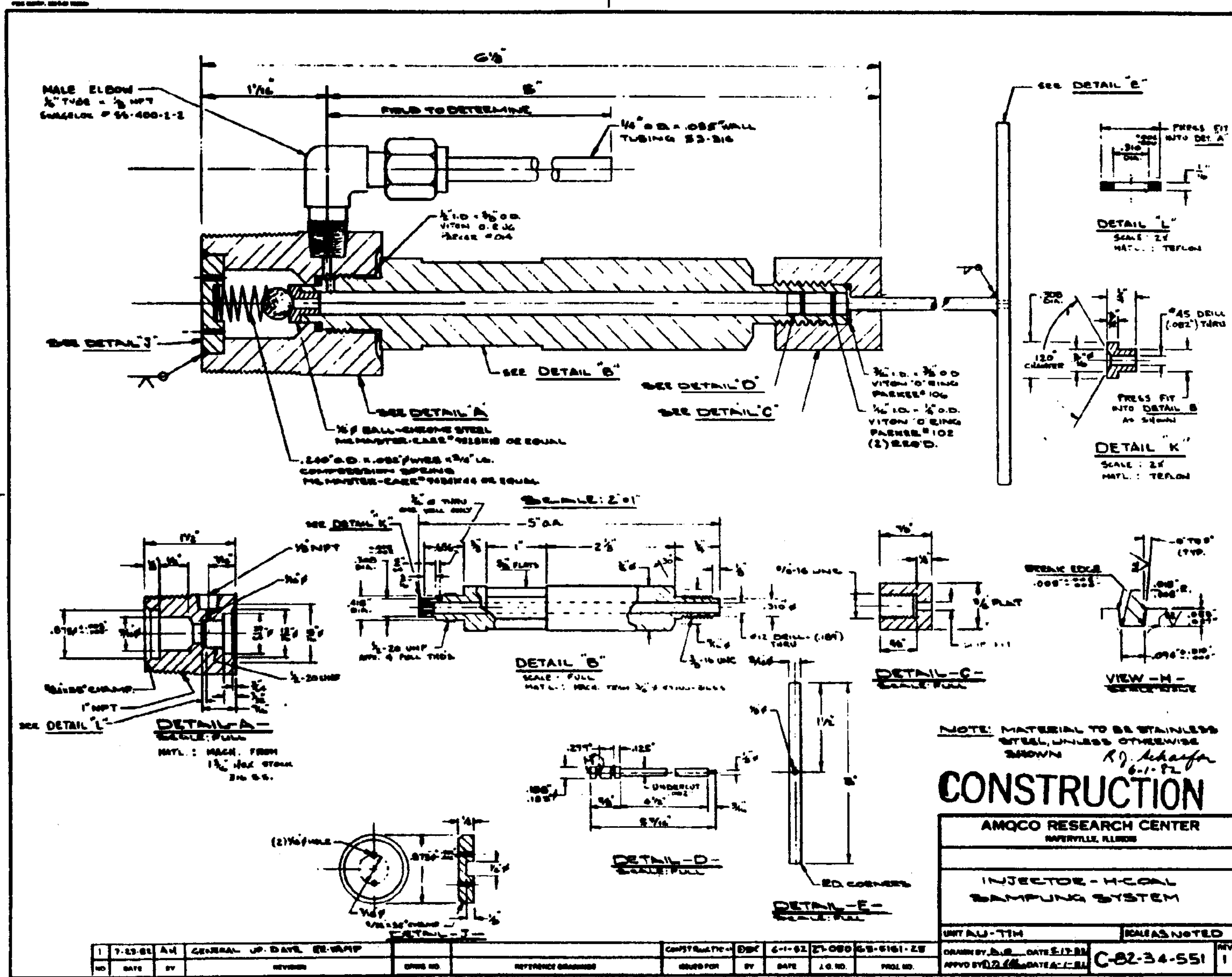

Figure 24

AMOCO PILOT PLANT SAMPLING PROBE

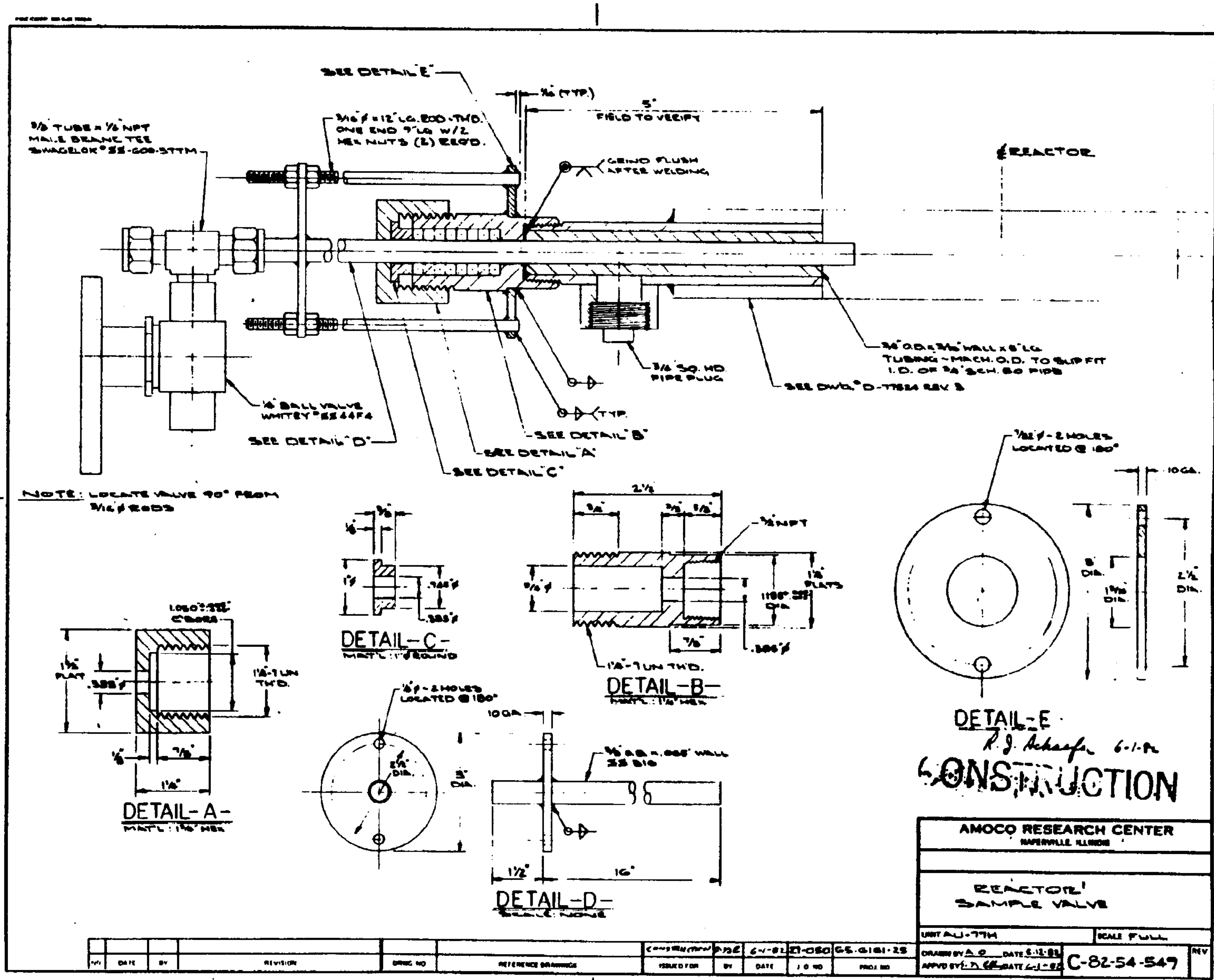

FIGURE 25
CONCENTRATION—TIME DISTRIBUTION CURVE FOR LIQUID MIXING RUN 490—8

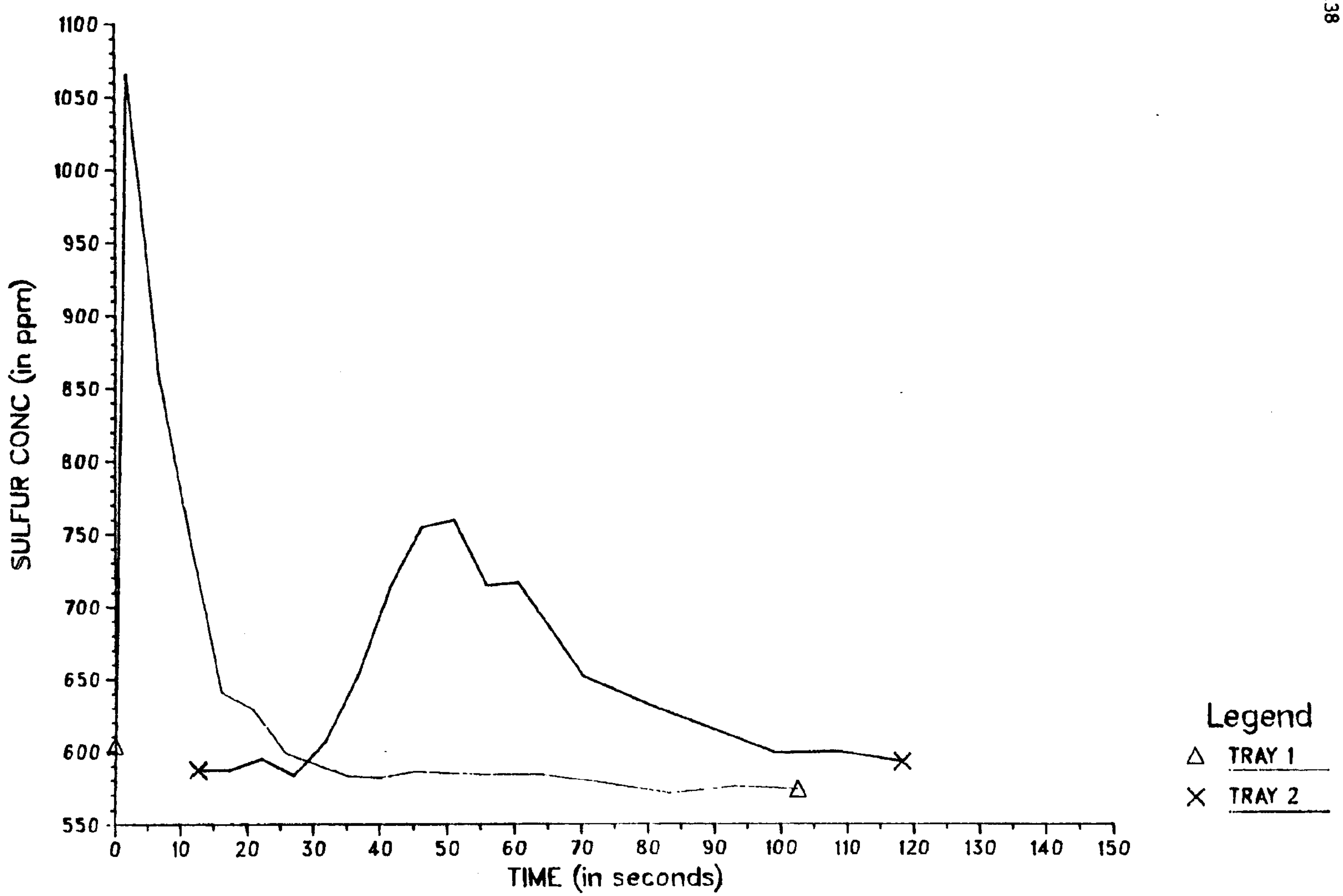

Figure 26

Slurry Dispersion Data Analysis

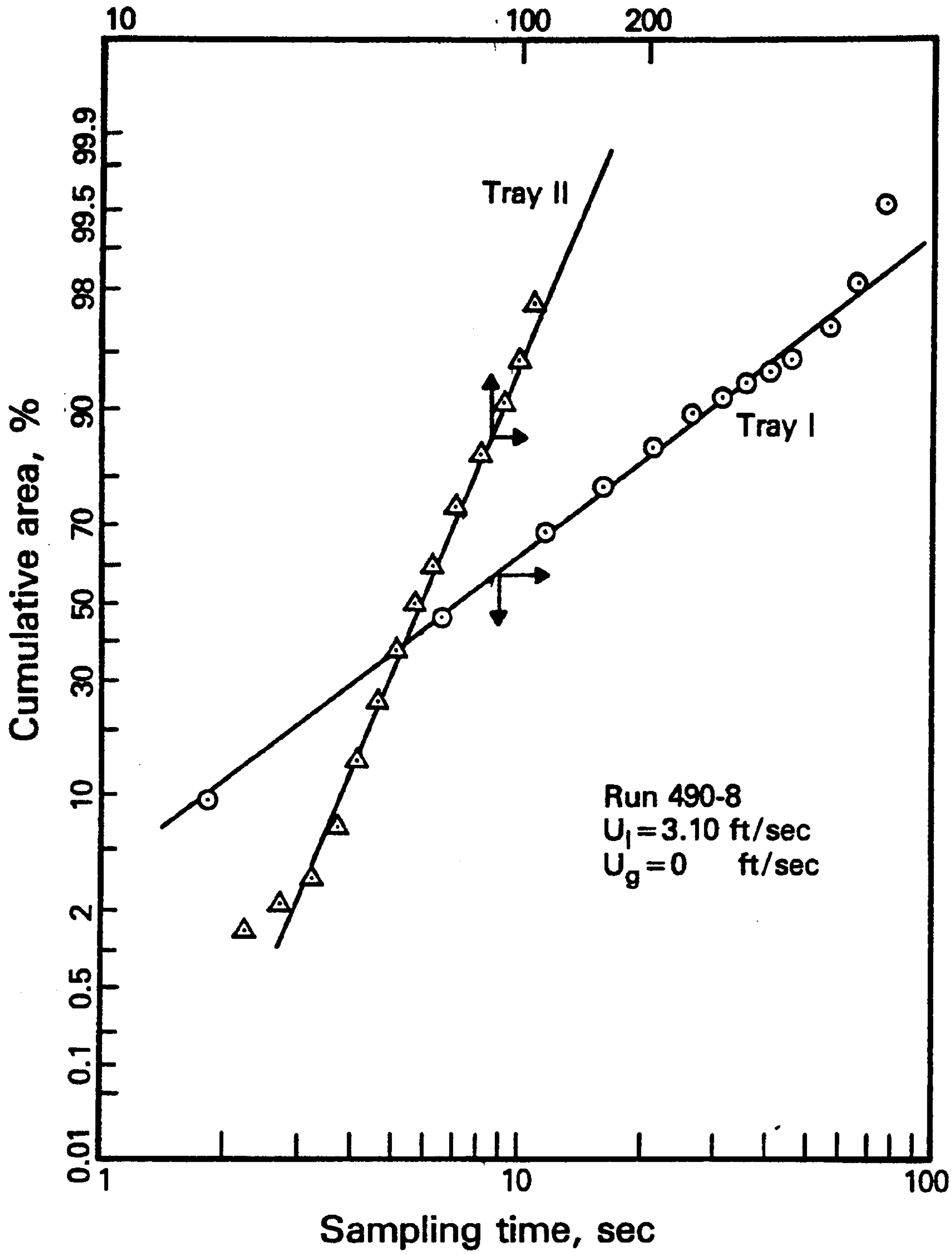

Figure 27

H-Coal Slurry Dispersion Correlations

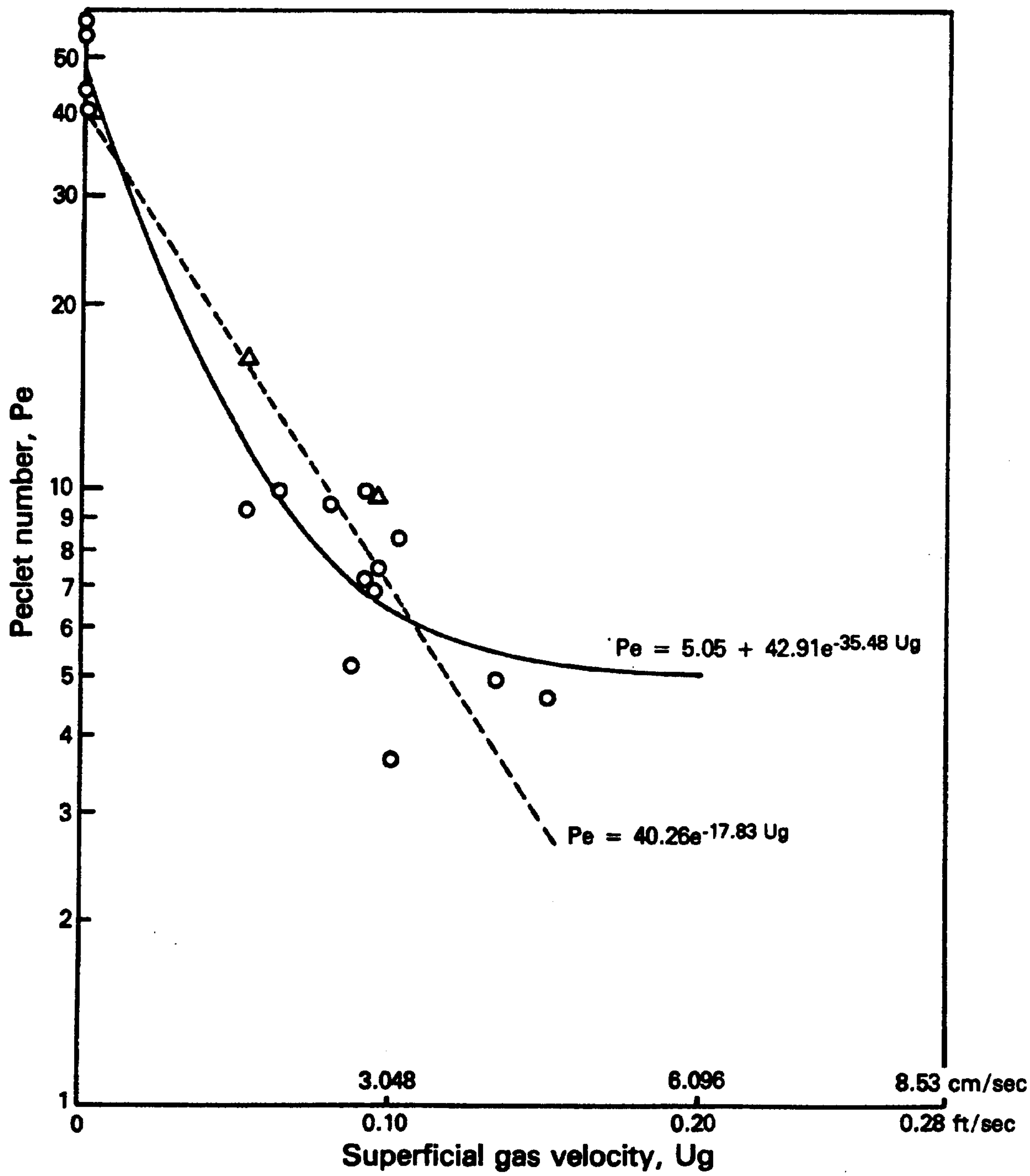

Figure 28

Liquid Mixing Material Balance

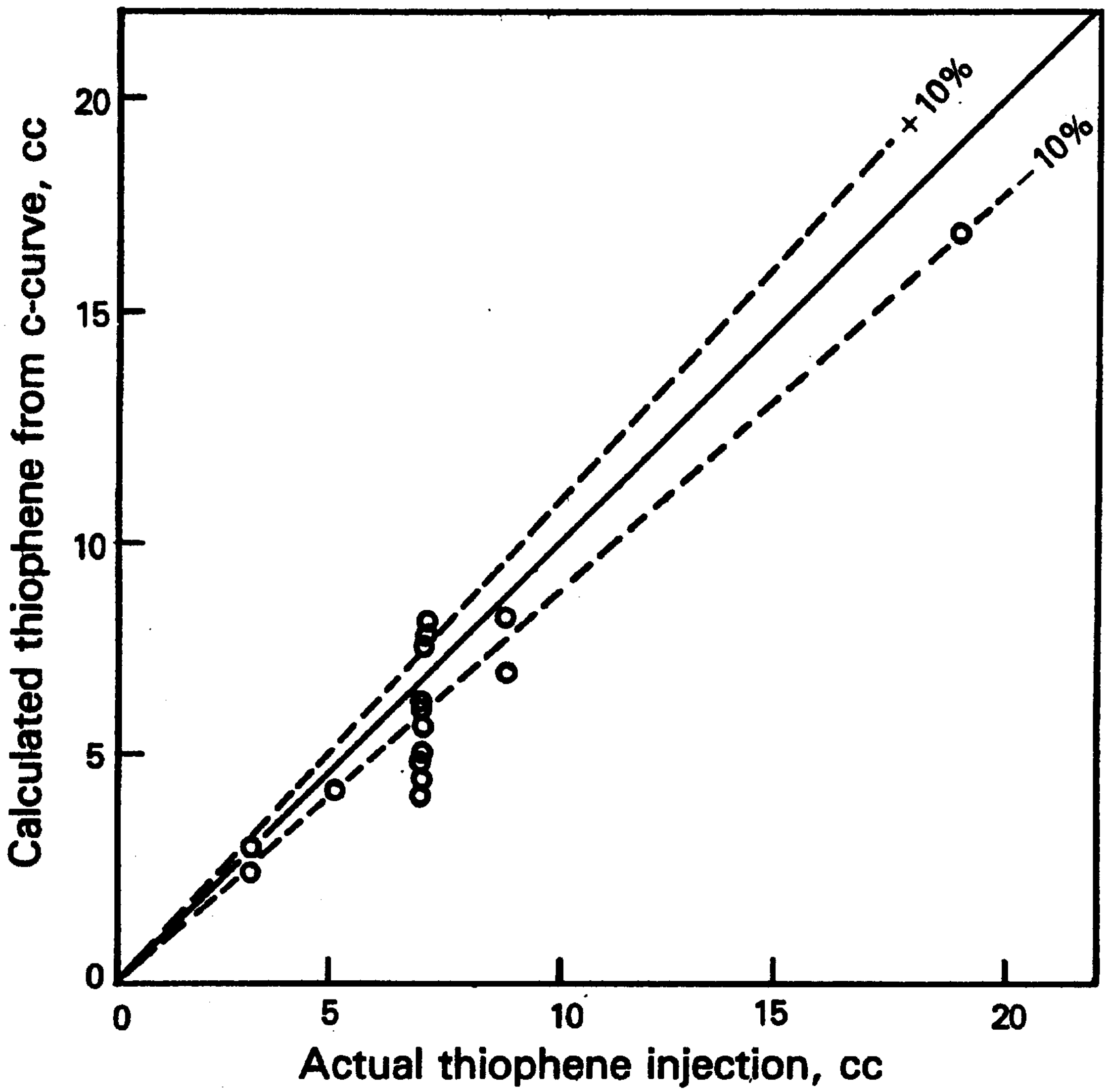

FIGURE 29
CONCENTRATION—TIME DISTRIBUTION CURVE FOR LIQUID MIXING RUN 490—17

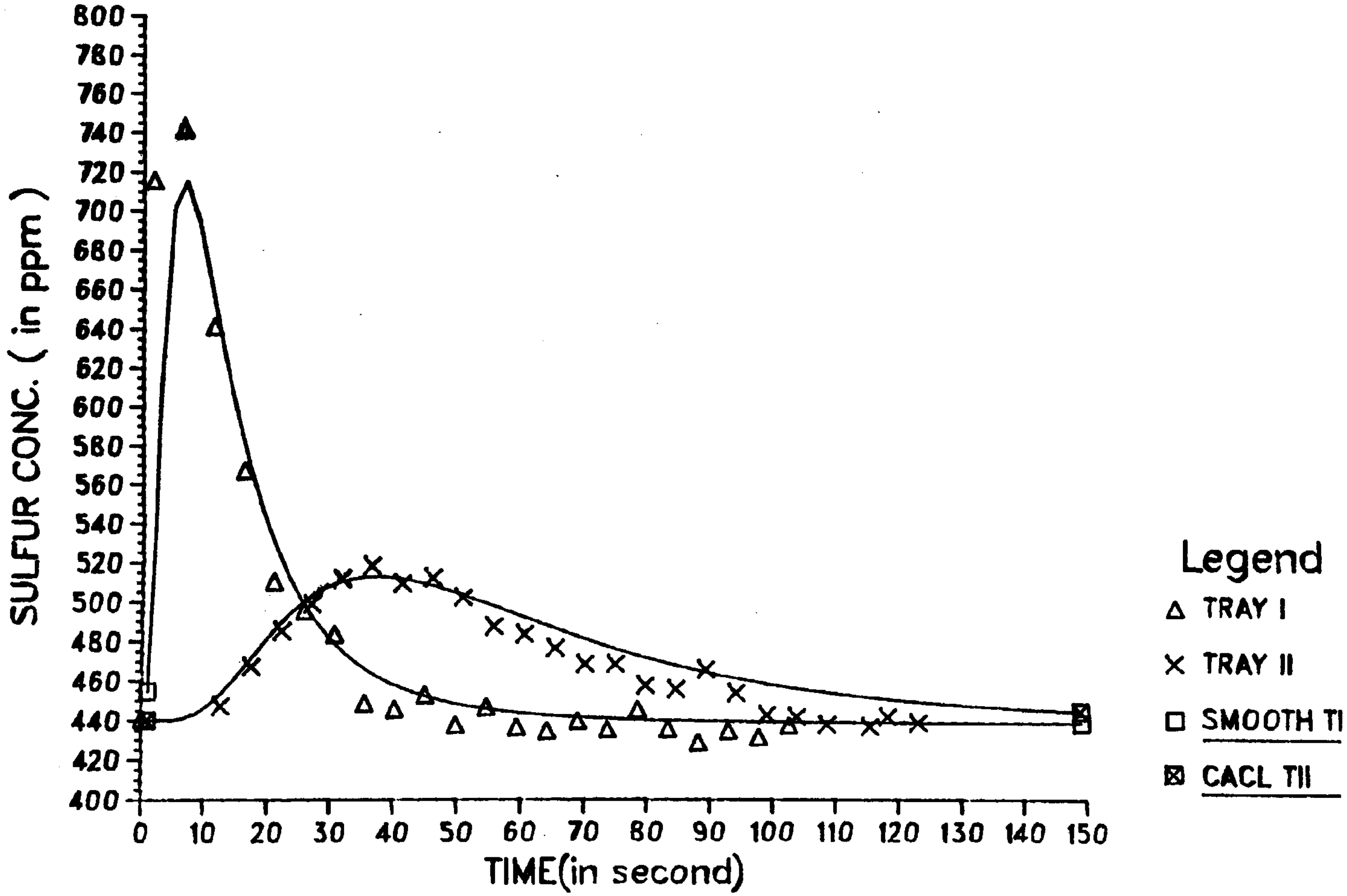

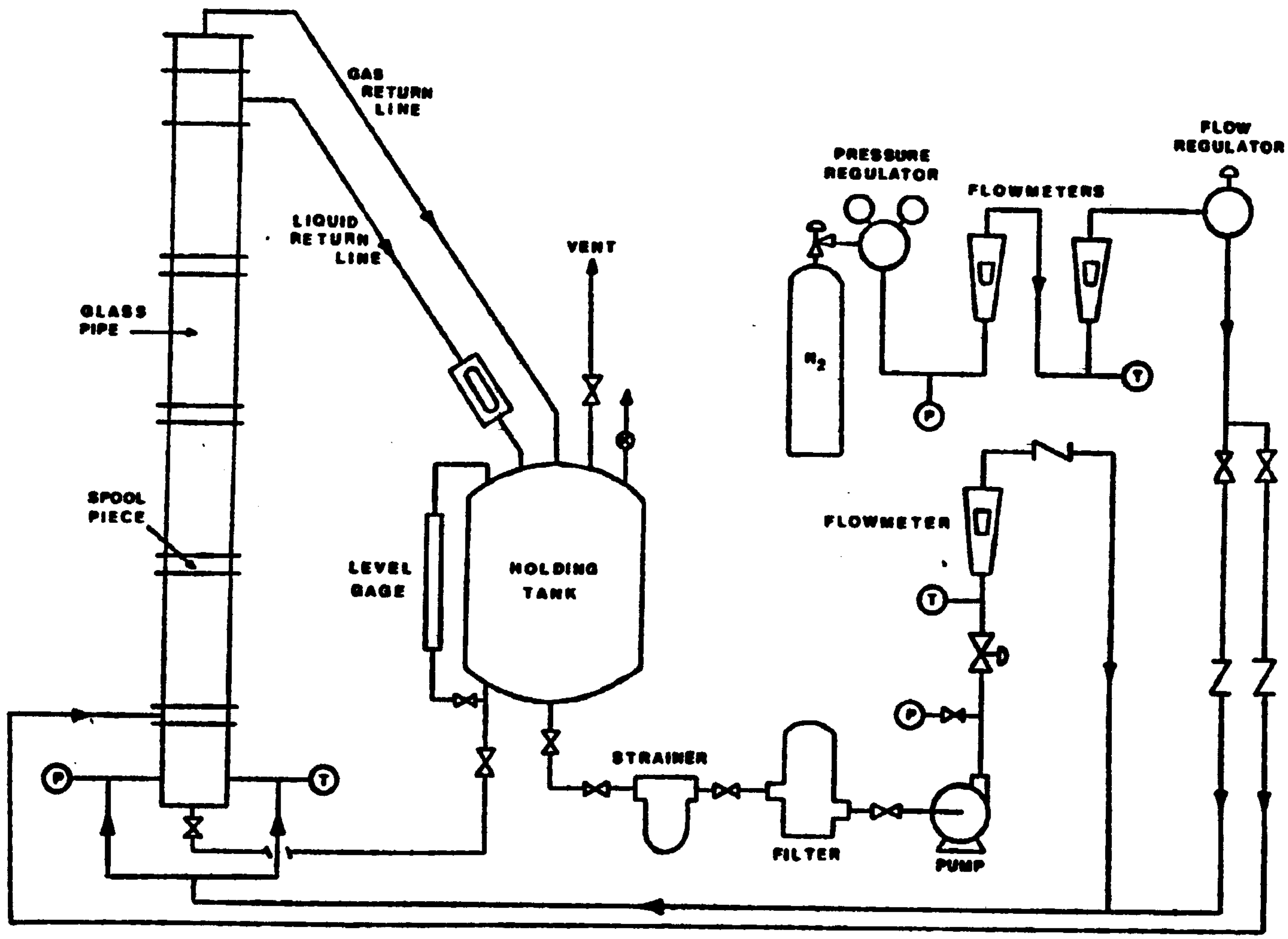

Figure 30 - Schematic Diagram of Experimental Apparatus.

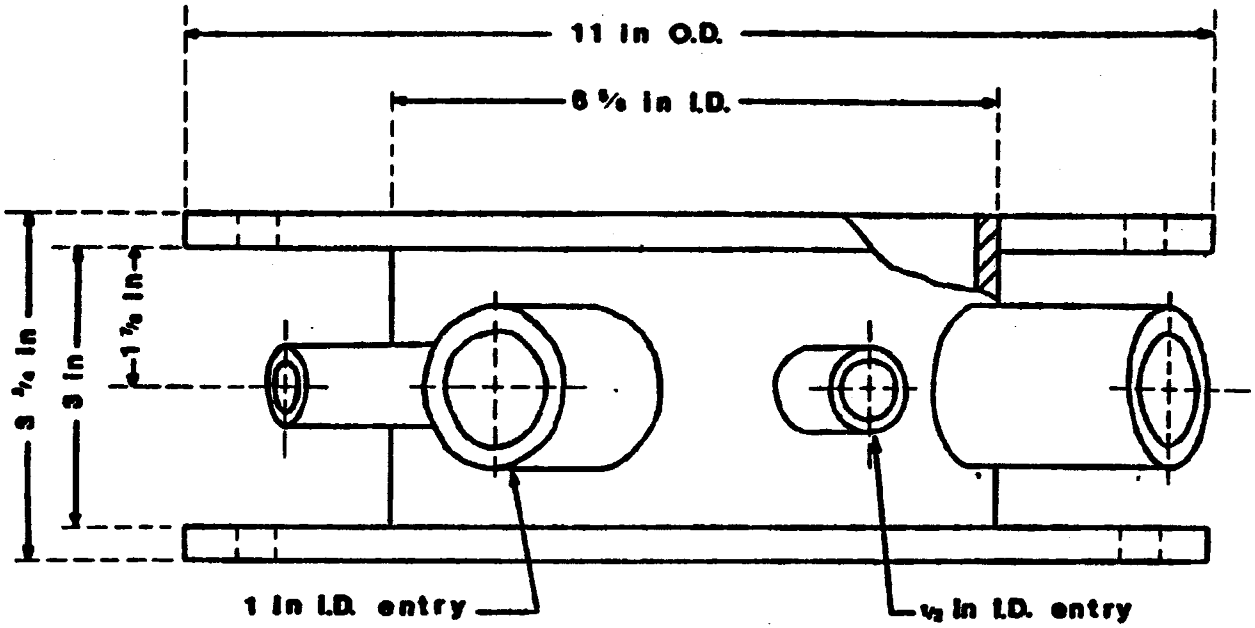

Figure 31 - Metal Spool Piece.

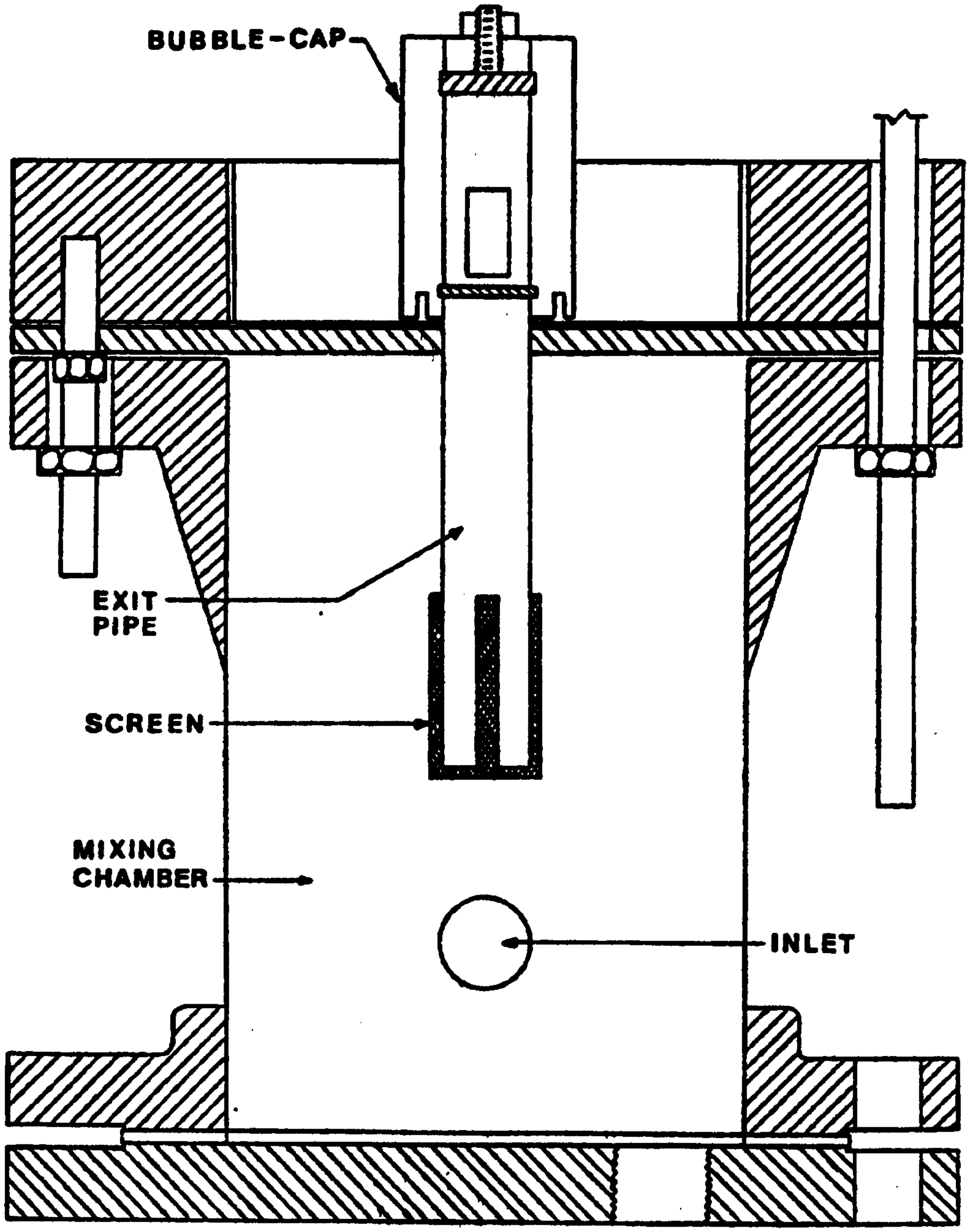

Figure 32 - Inlet Distributor Section.

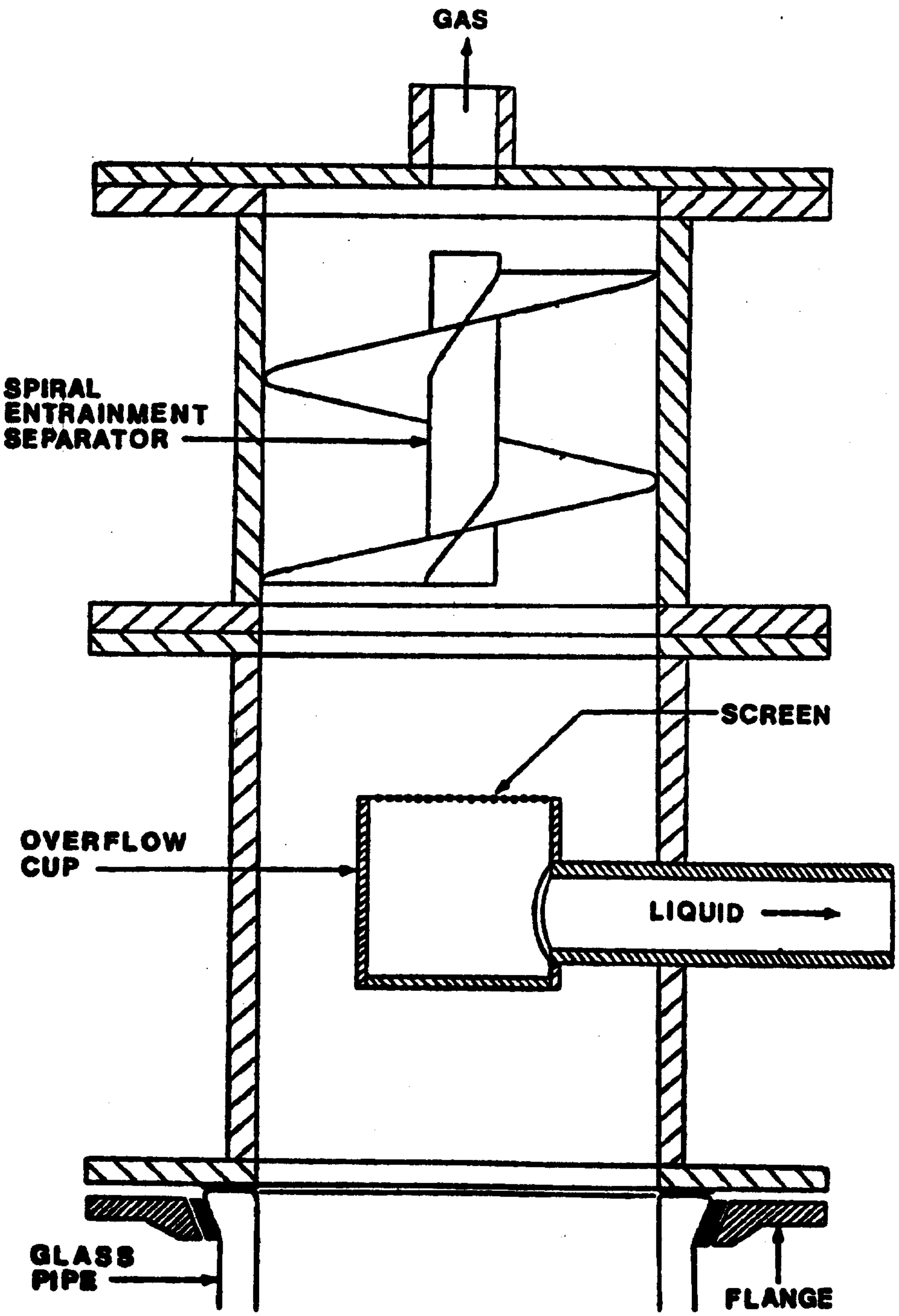

Figure 33 - Overflow Cup and Spiral Entrainment Separator.

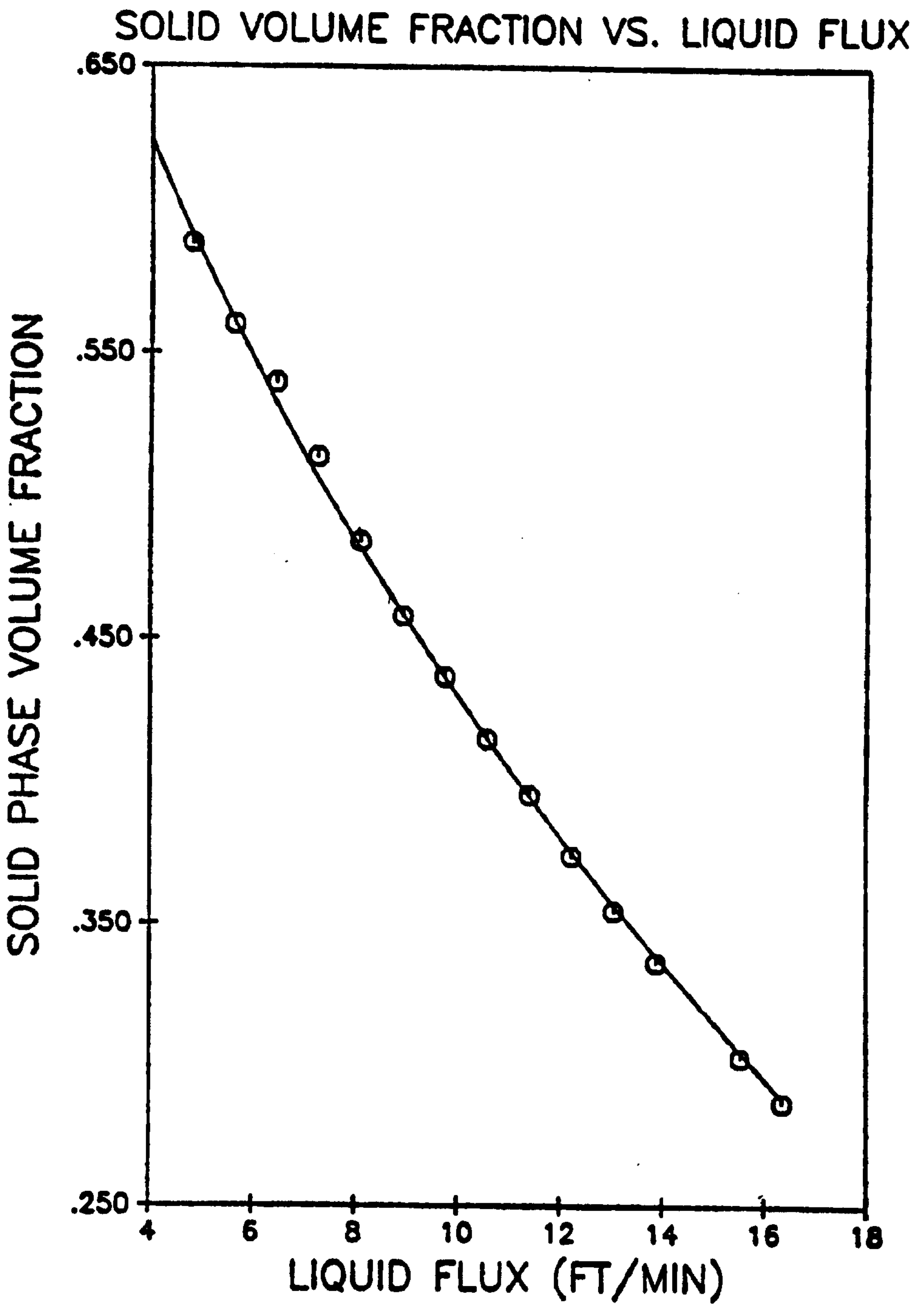

Figure 34 - **Solid Phase Volume Fraction**

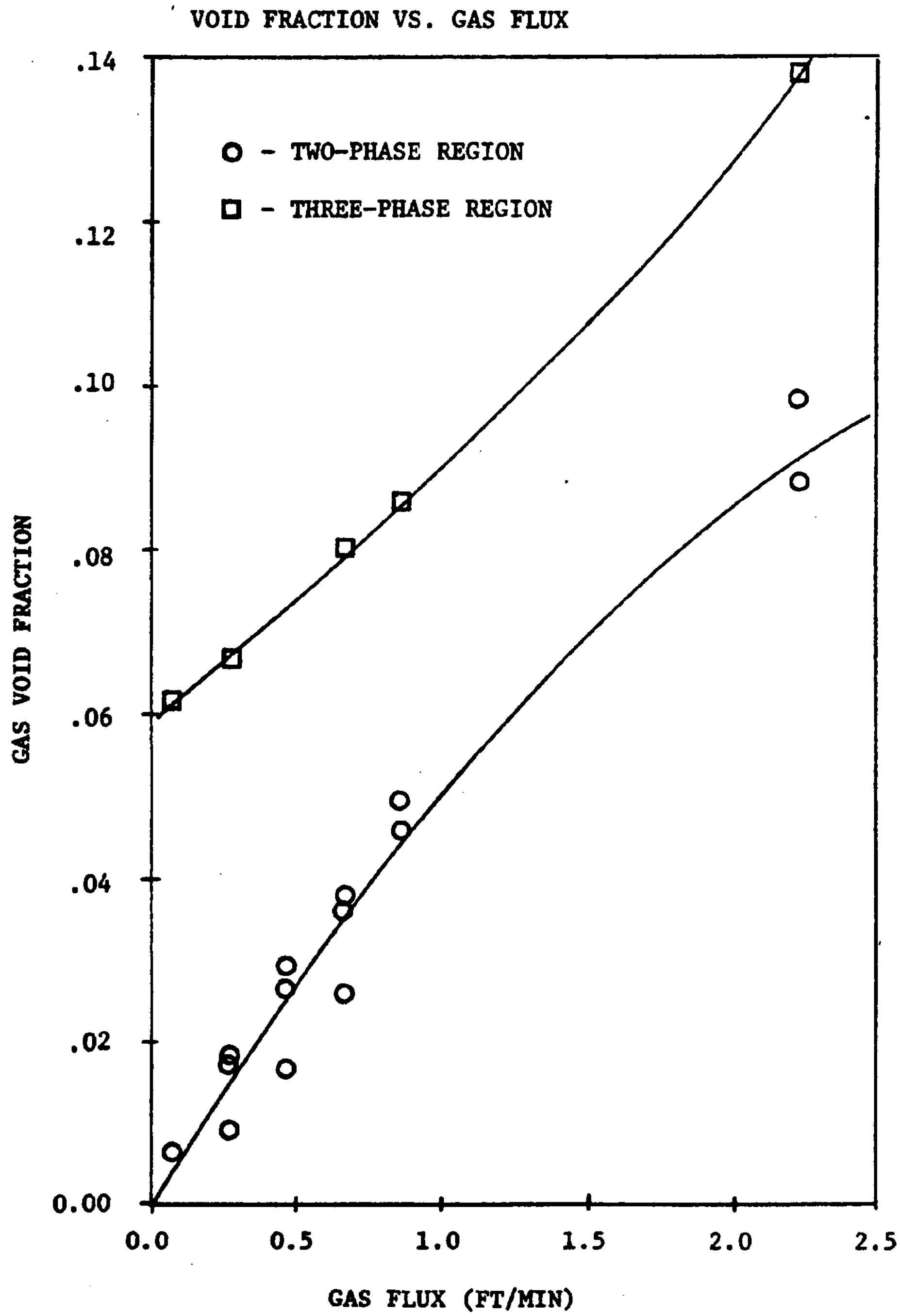

FIGURE 34A. **Gas Holdup**
(Liquid Flux = 4.80 ft/min.)

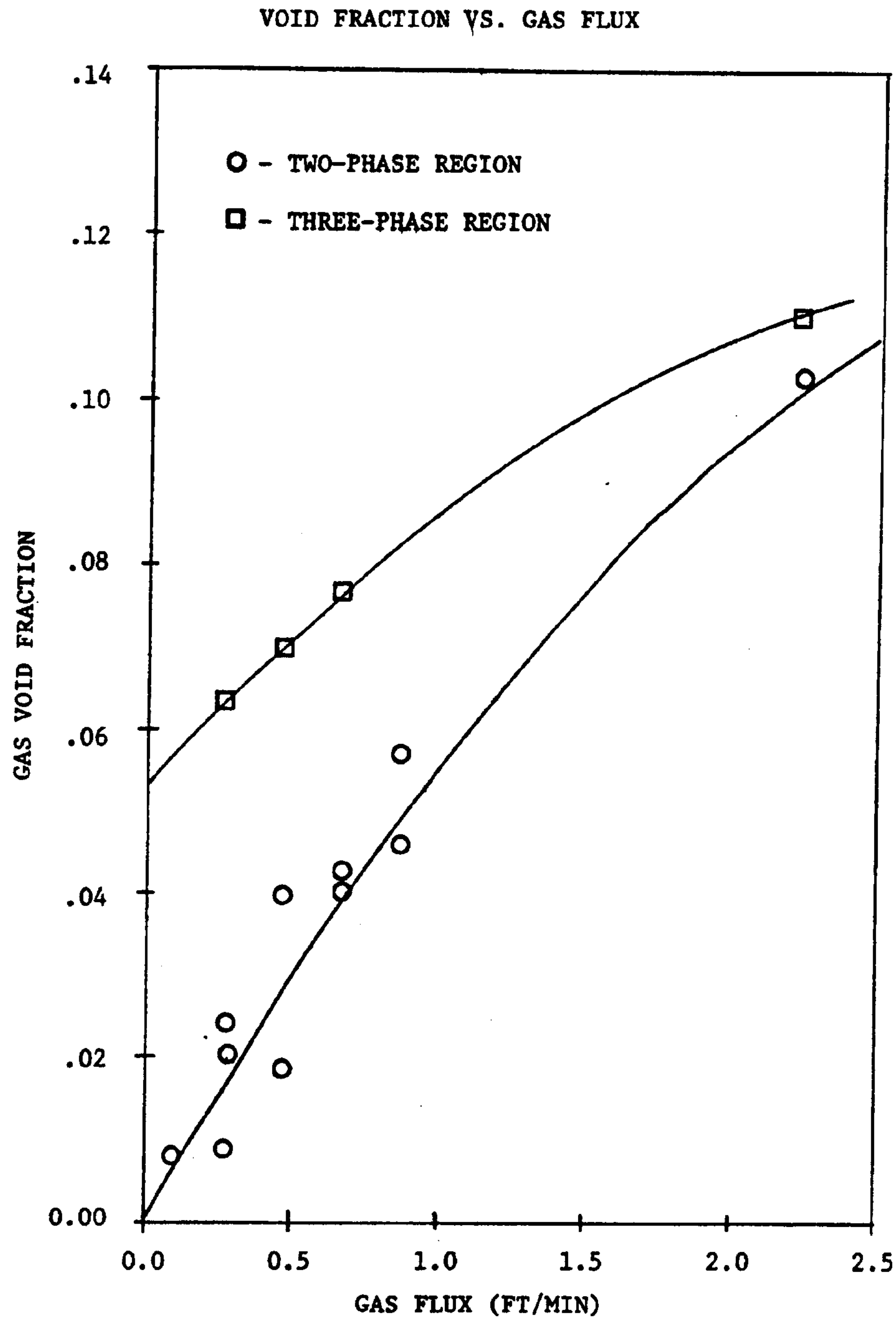

FIGURE 34B. Gas Holdup
(Liquid Flux = 6.45 ft/min.)

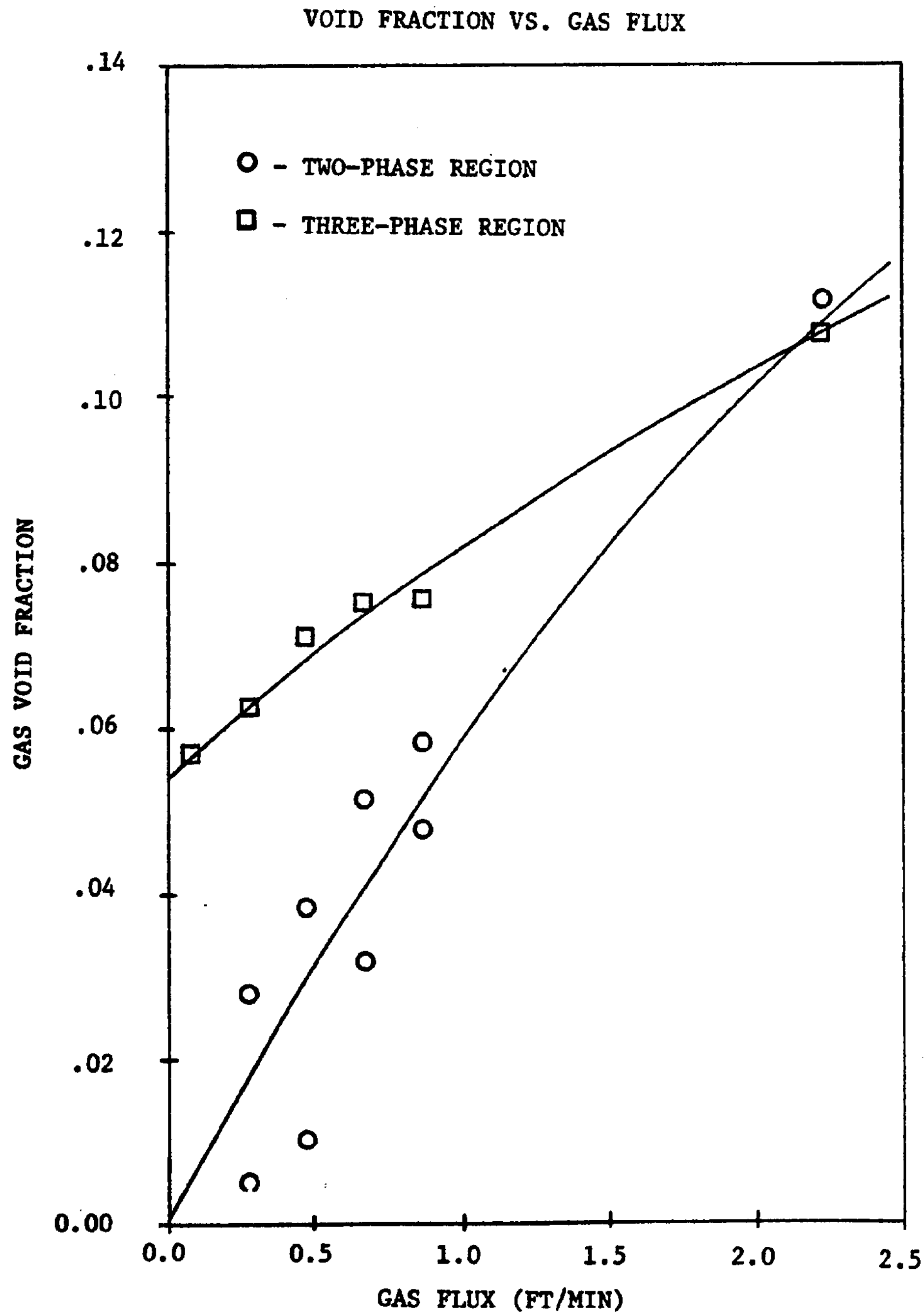

FIGURE 34C. Gas Holdup
(Liquid Flux = 8.10 ft/min.)

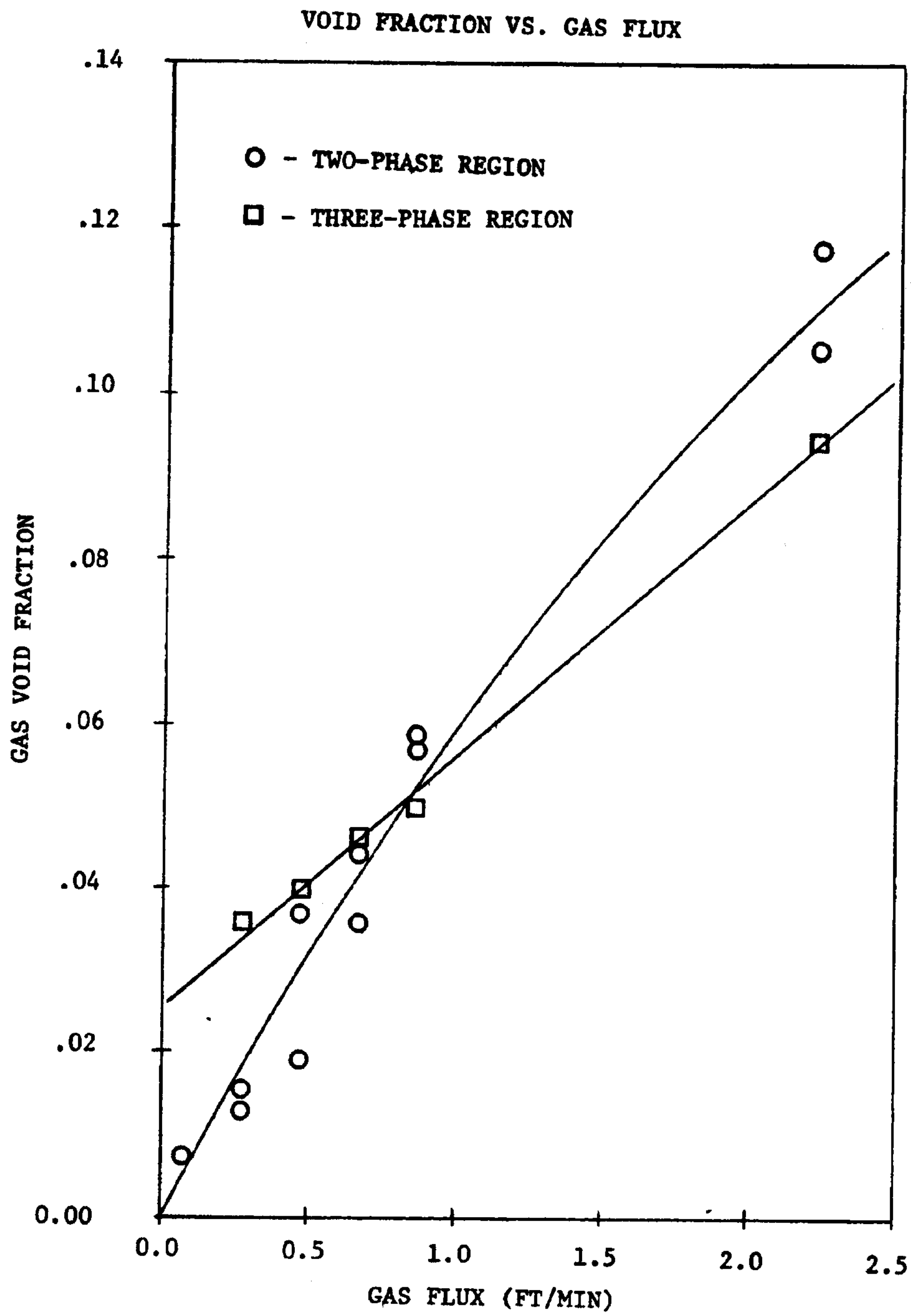

FIGURE 34D. Gas Holdup

(Liquid Flux = 9.75 ft/min.)

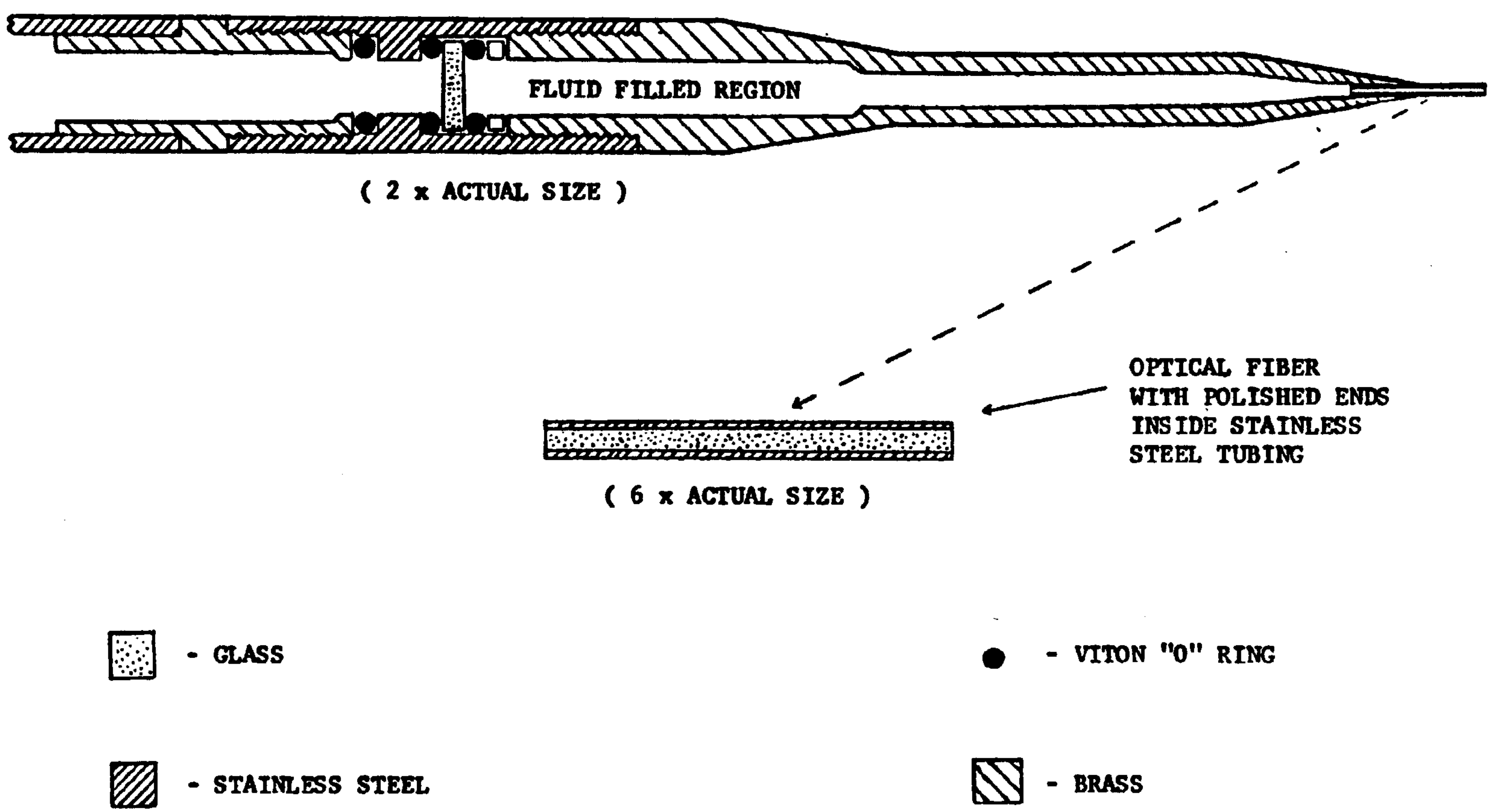

Figure 35 - Cross-Sectional View of a Light Beam Probe

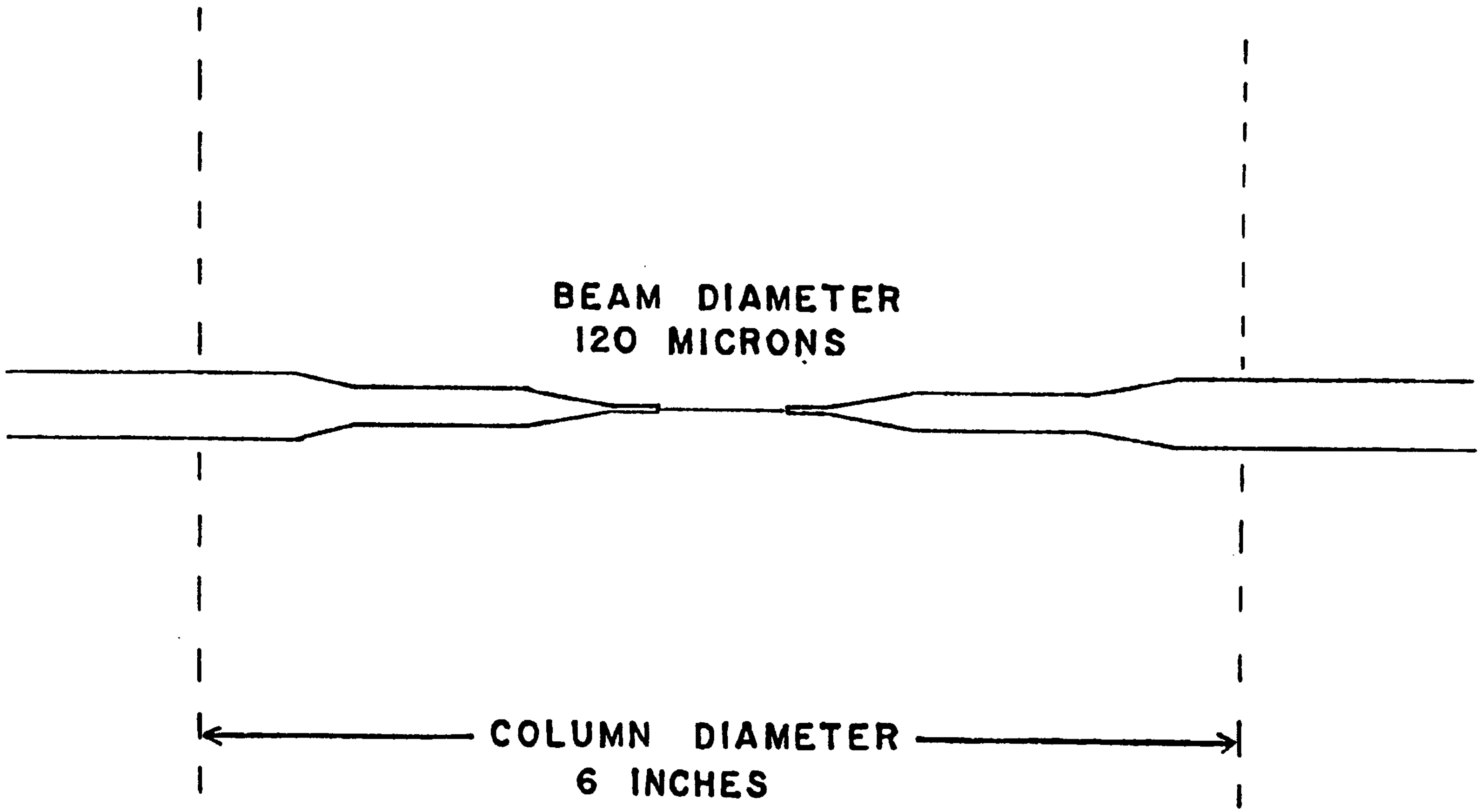

Figure 36 - Schematic of Light Beam Probes Inserted into the Column

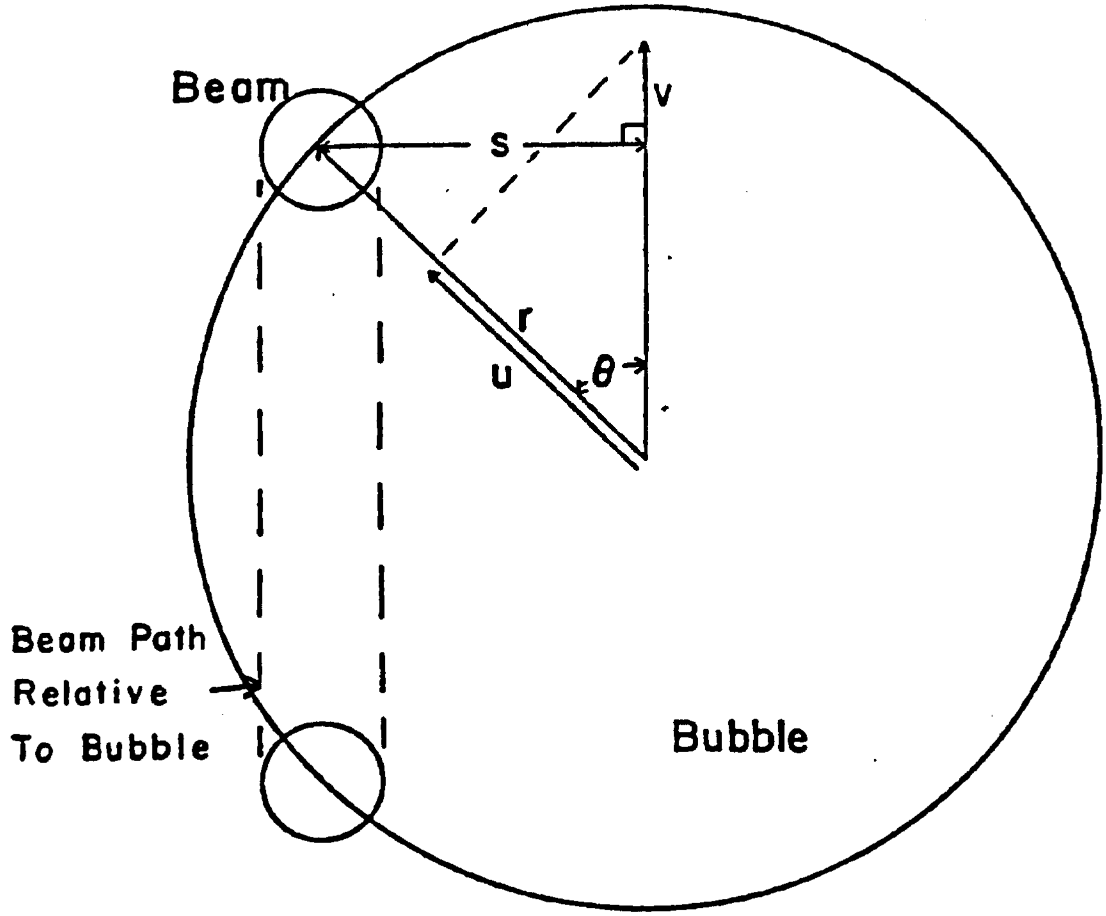

$$u = v \cdot \cos(\theta)$$

$$\tau = 2 \cdot r \cdot \cos(\theta)/v$$

Figure 37 - Bubble/Beam Intersection Geometry

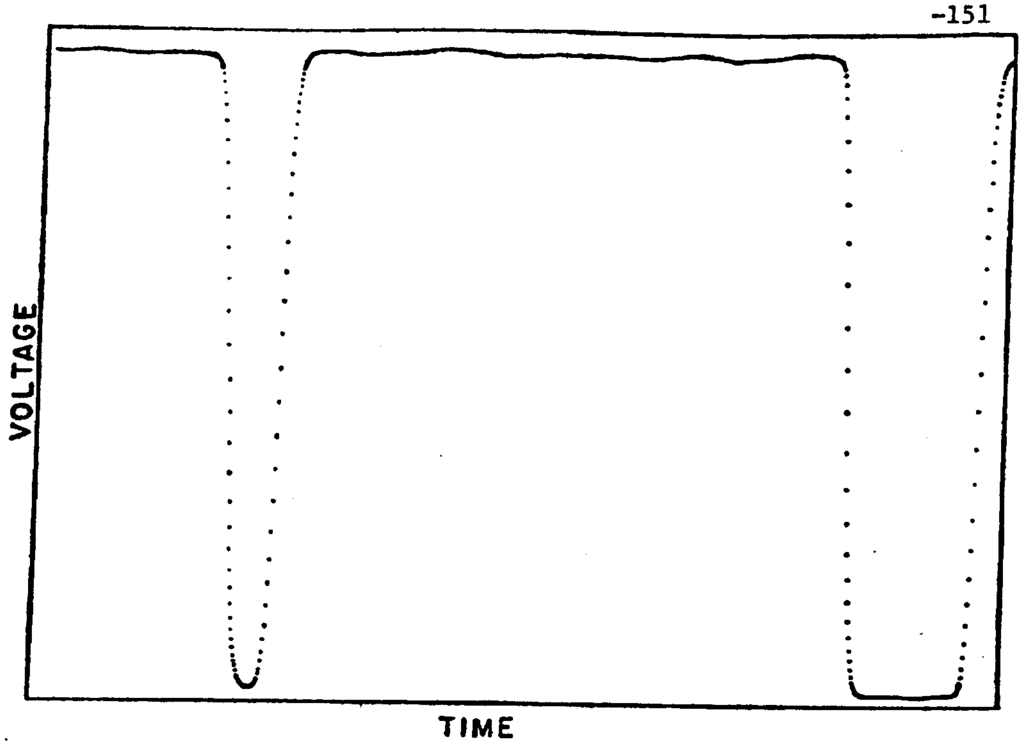

(a)

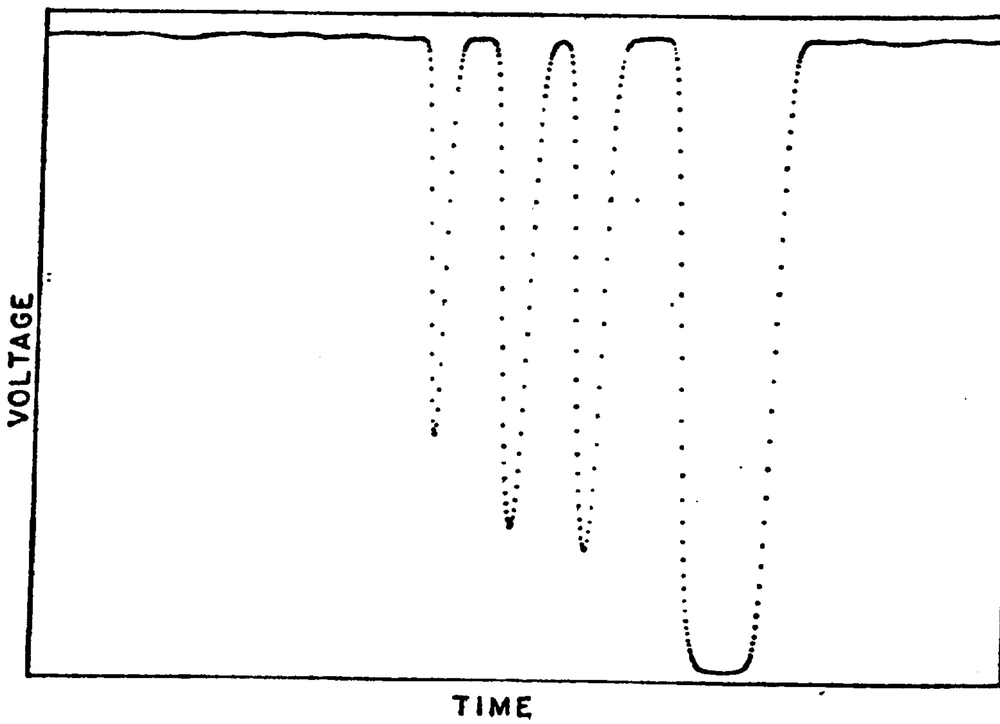

(b)

Figure 38 - Typical Signals from Light Beam Probe
(50 Microseconds between Data Points)

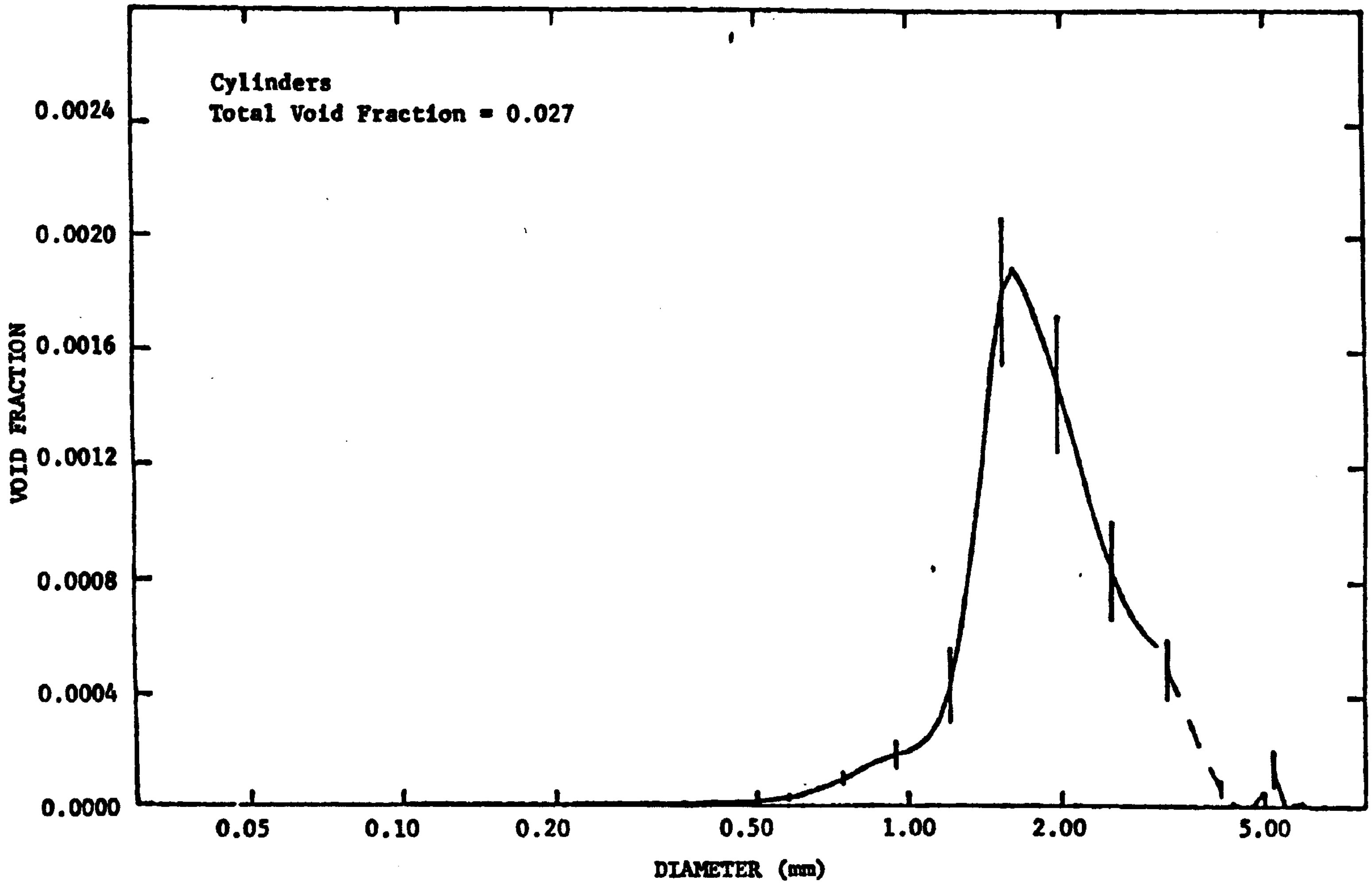

Figure 39 - Bubble Size Distribution (Cylinders , LF = 4.01 cm/sec , GF = 0.44 cm/sec)

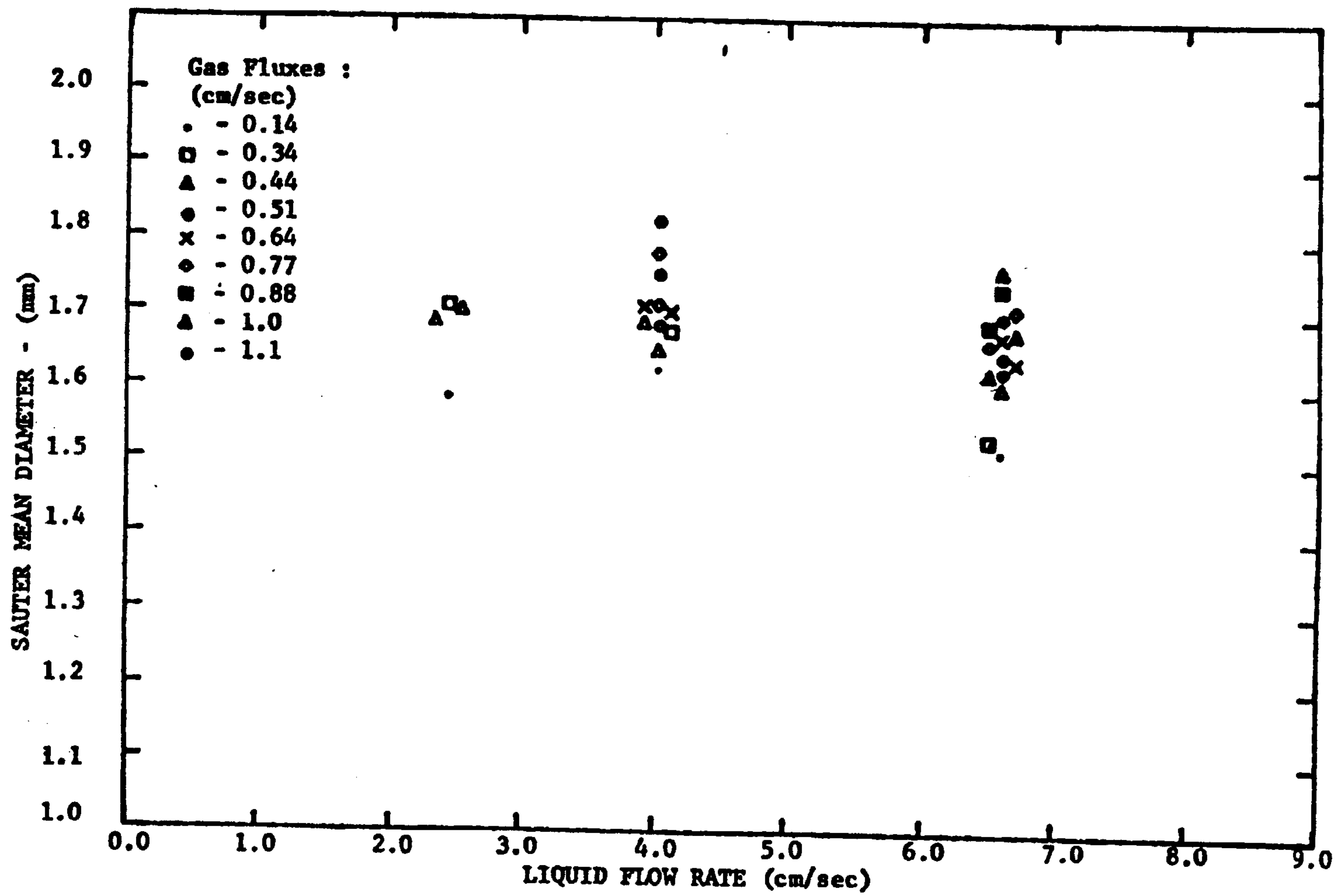

Figure 40 - Sauter Mean Diameters (Cylinders)

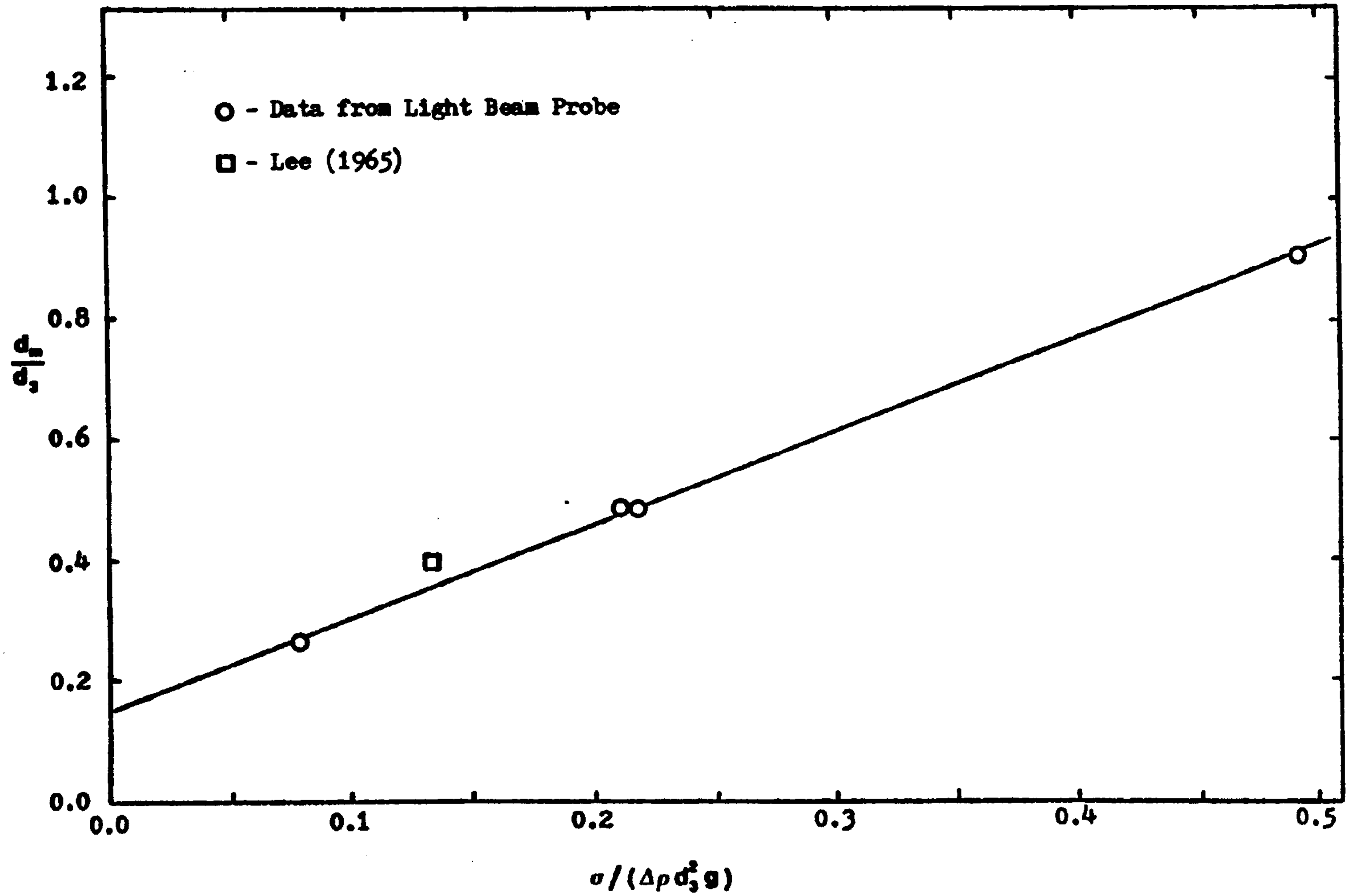

Figure 41 - Dimensionless Mean Bubble Diameter Versus the Inverse of the Eotvos Number

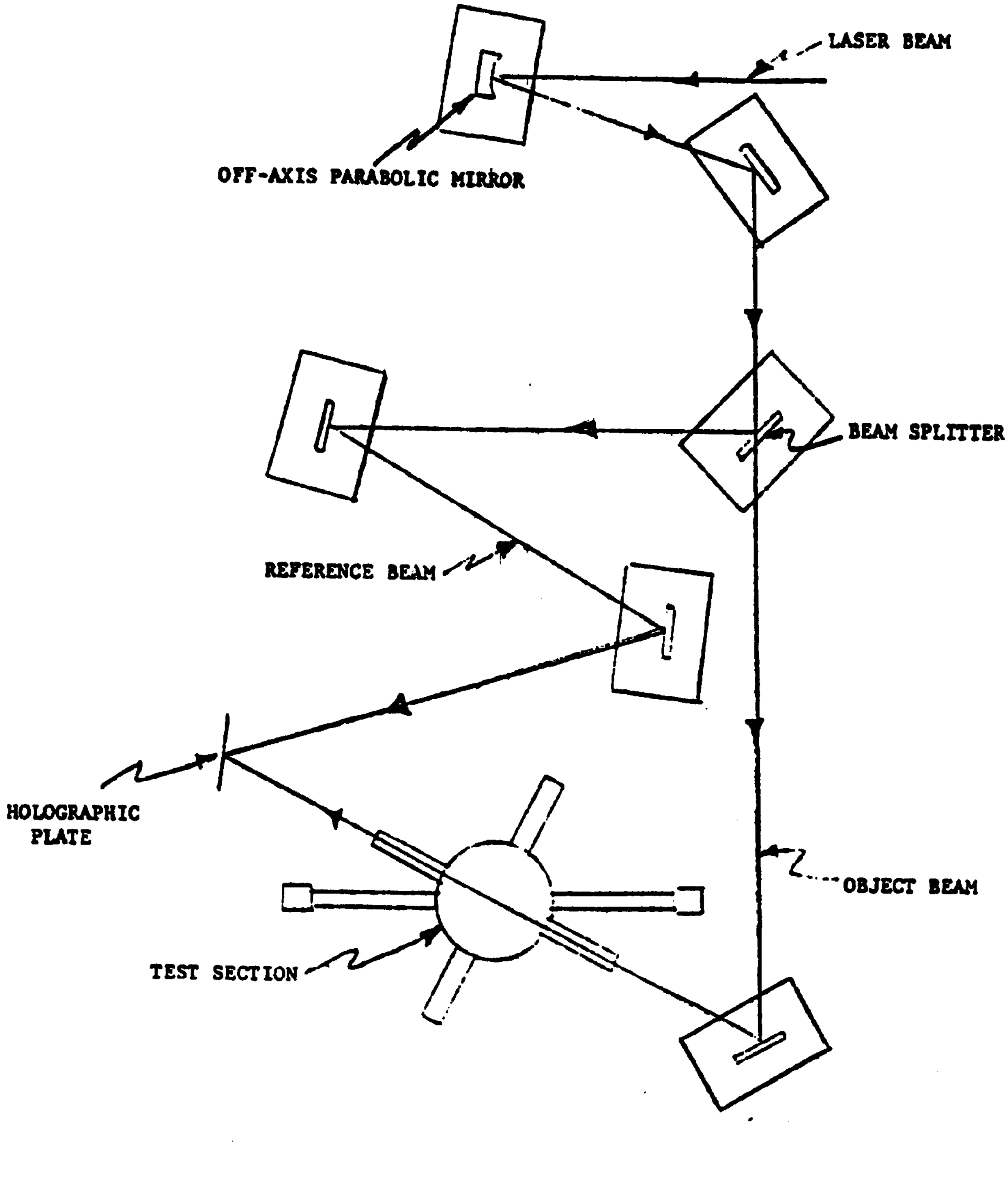

Figure 42 - OPTICAL SET-UP (OFF-AXIS HOLOGRAPHY) TO DETERMINE BUBBLE SIZES AND DISTRIBUTIONS.

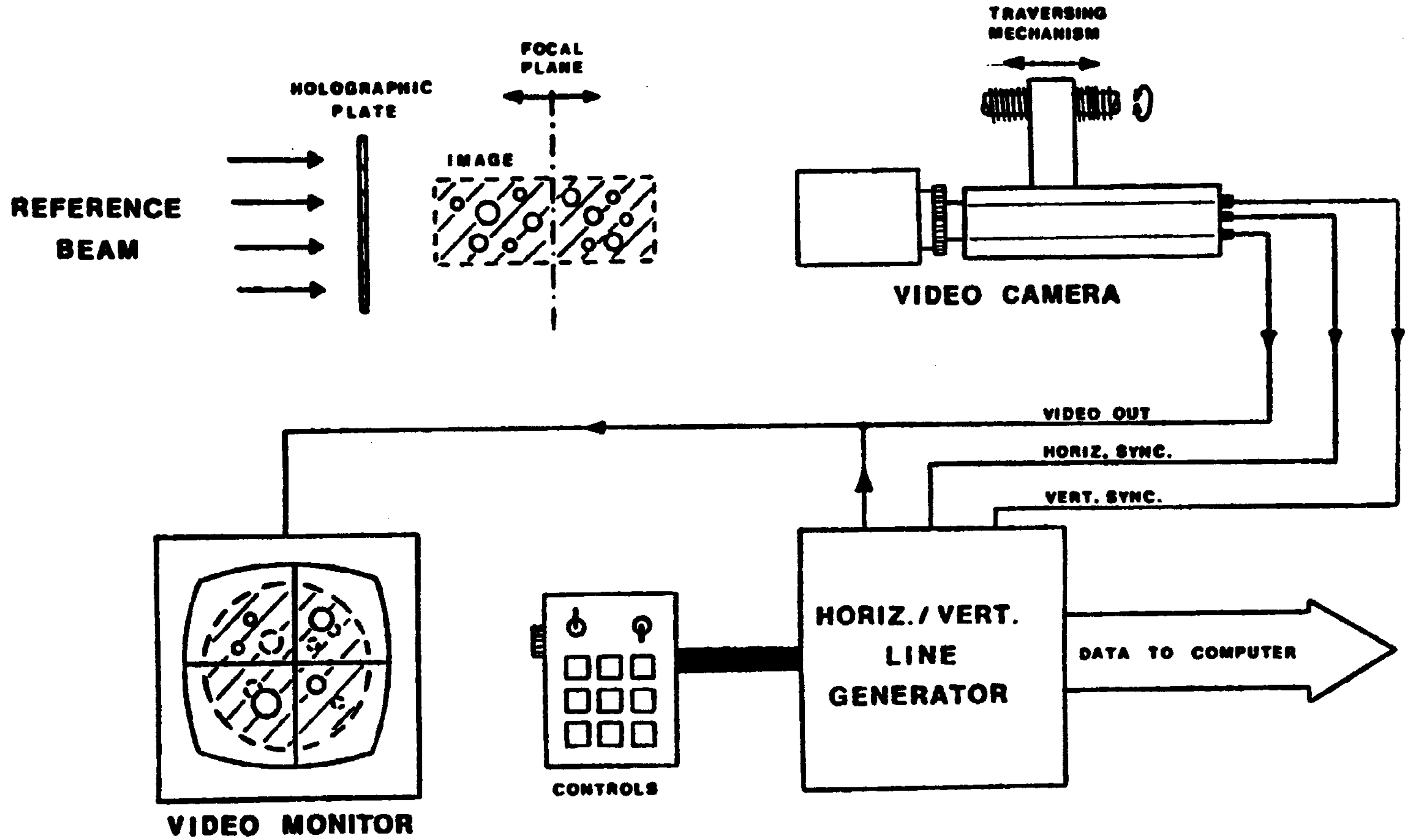

Figure 43 - Holographic Analysis System

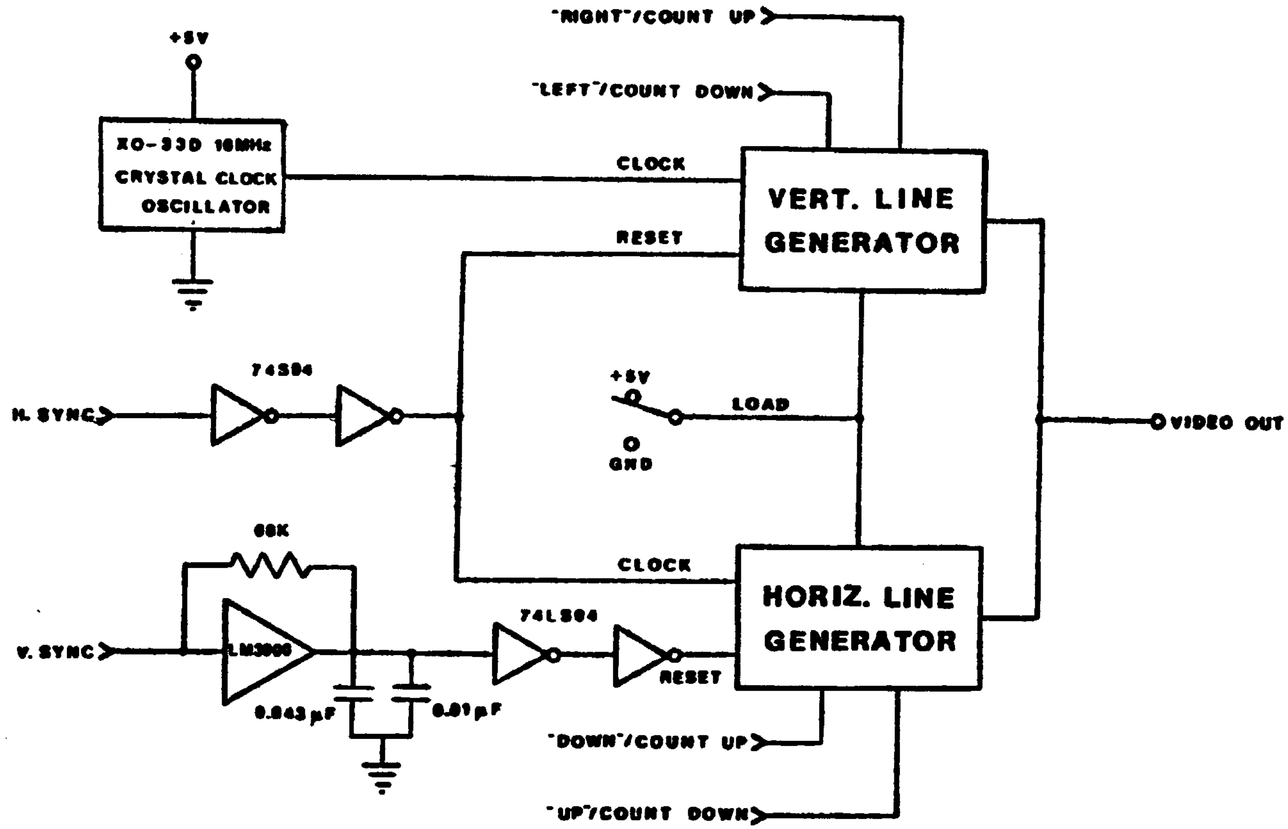

Figure 44 - Horizontal/Vertical Line Generator - External Connections and Signal Conditioning

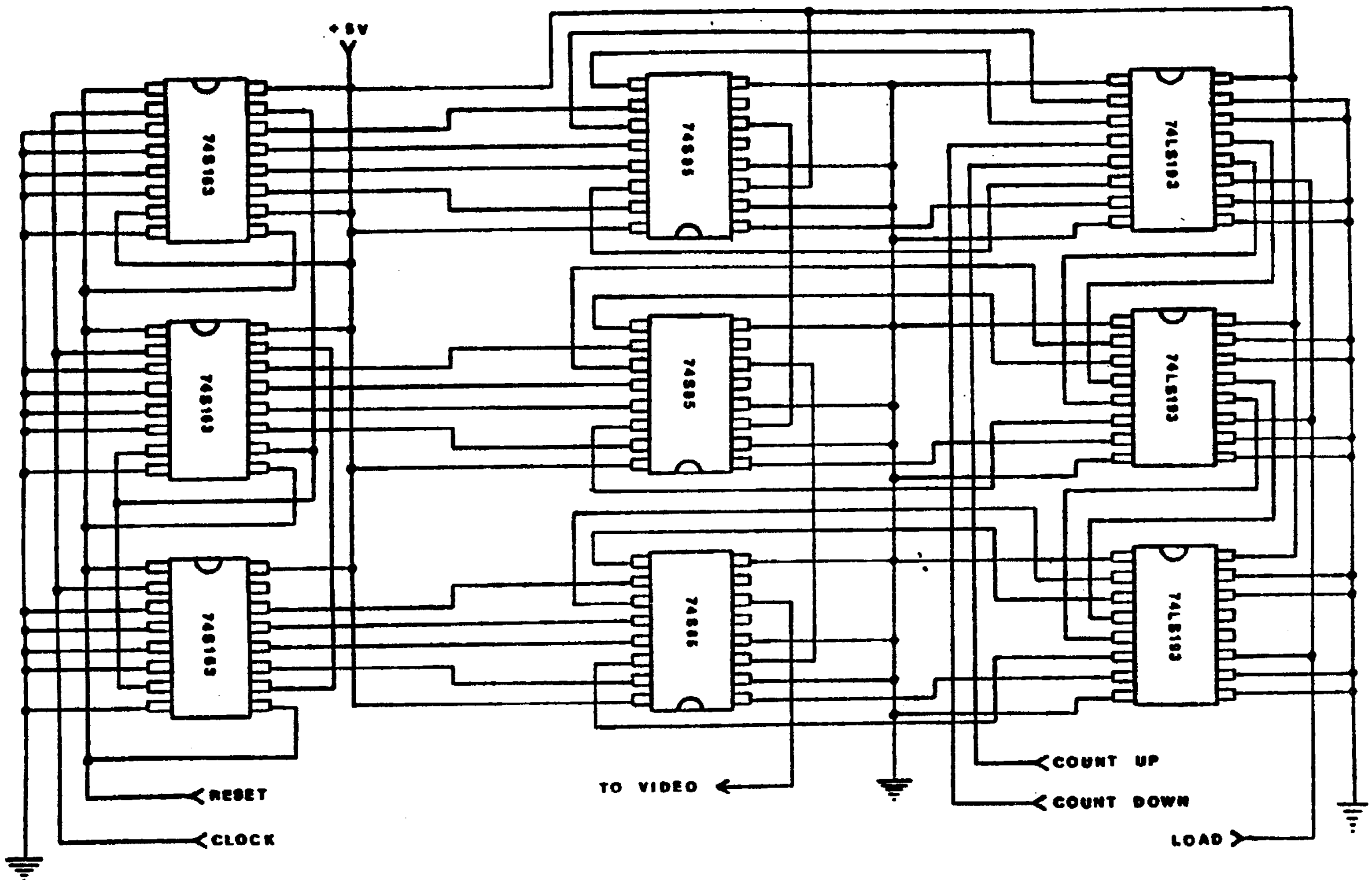

Figure 45 - Horizontal/Vertical Line Generator Circuit Diagram

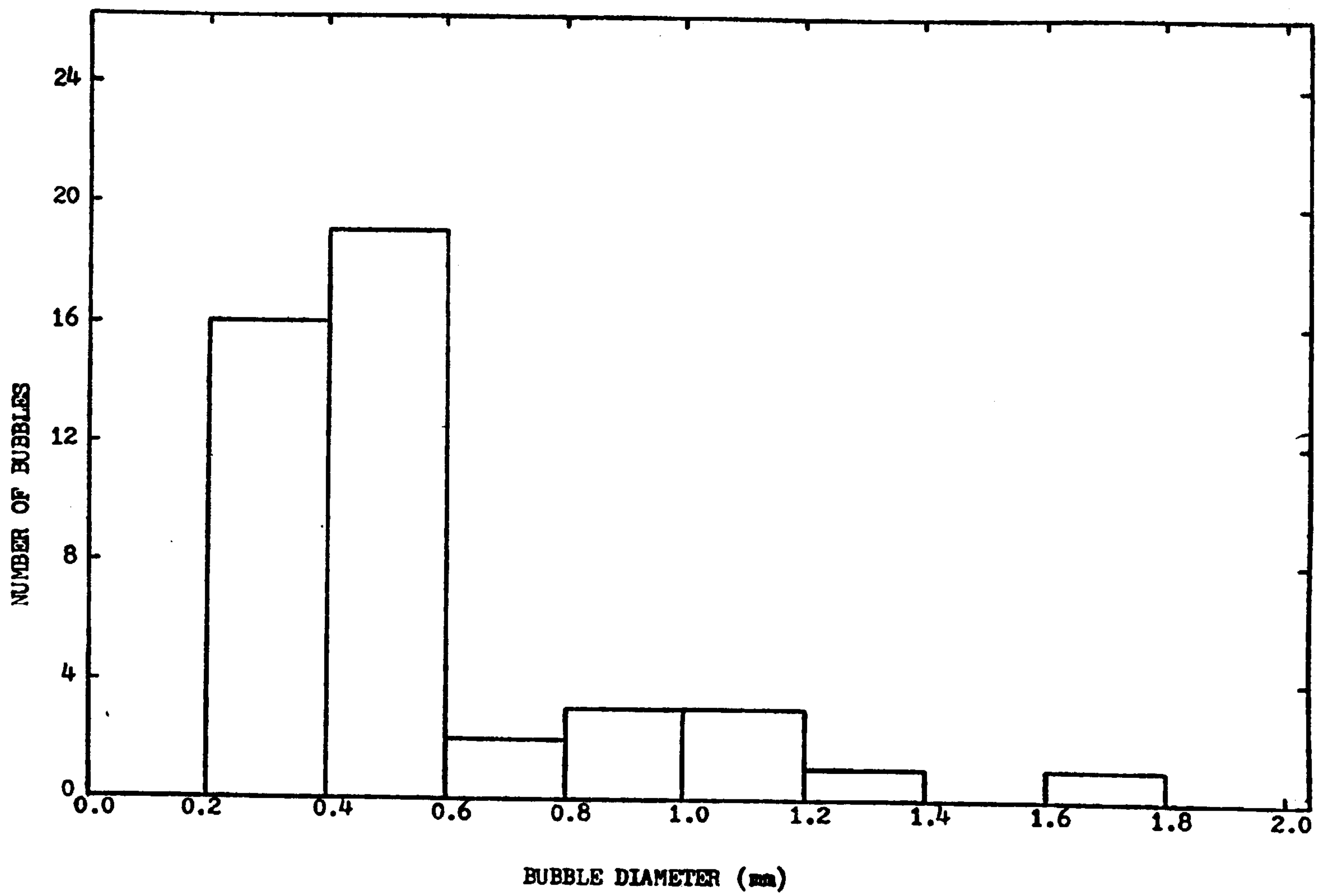

Figure 46 - Bubble Size Distribution with Gas Injection into the Liquid Inlet Line (U_1 = 1.60 cm/sec, U_g = 0.05 cm/sec)

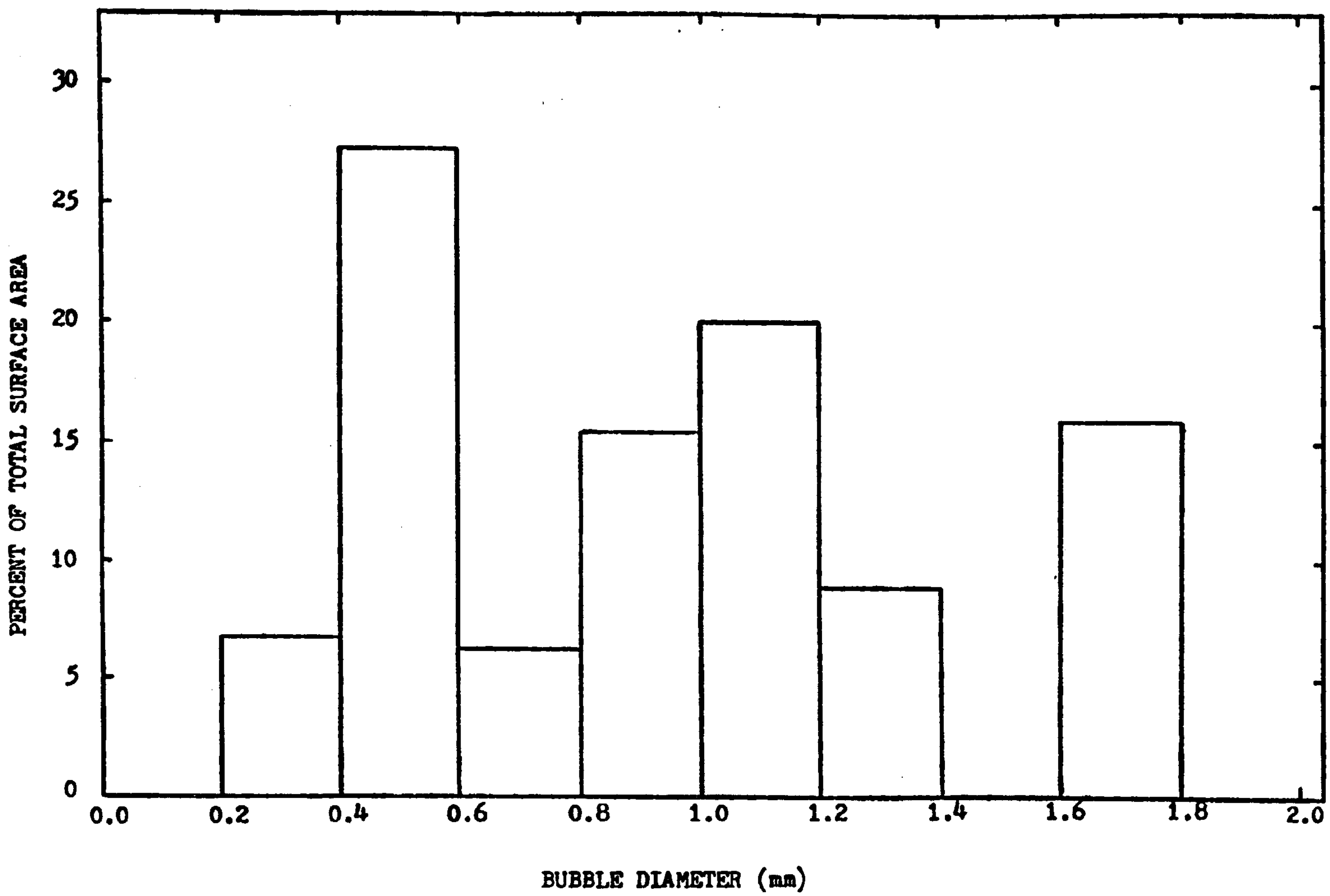

Figure 47 - Surface Area Distribution with Gas Injection into the Liquid Inlet Line (U_1 = 1.60 cm/sec, U_g = 0.05 cm/sec)

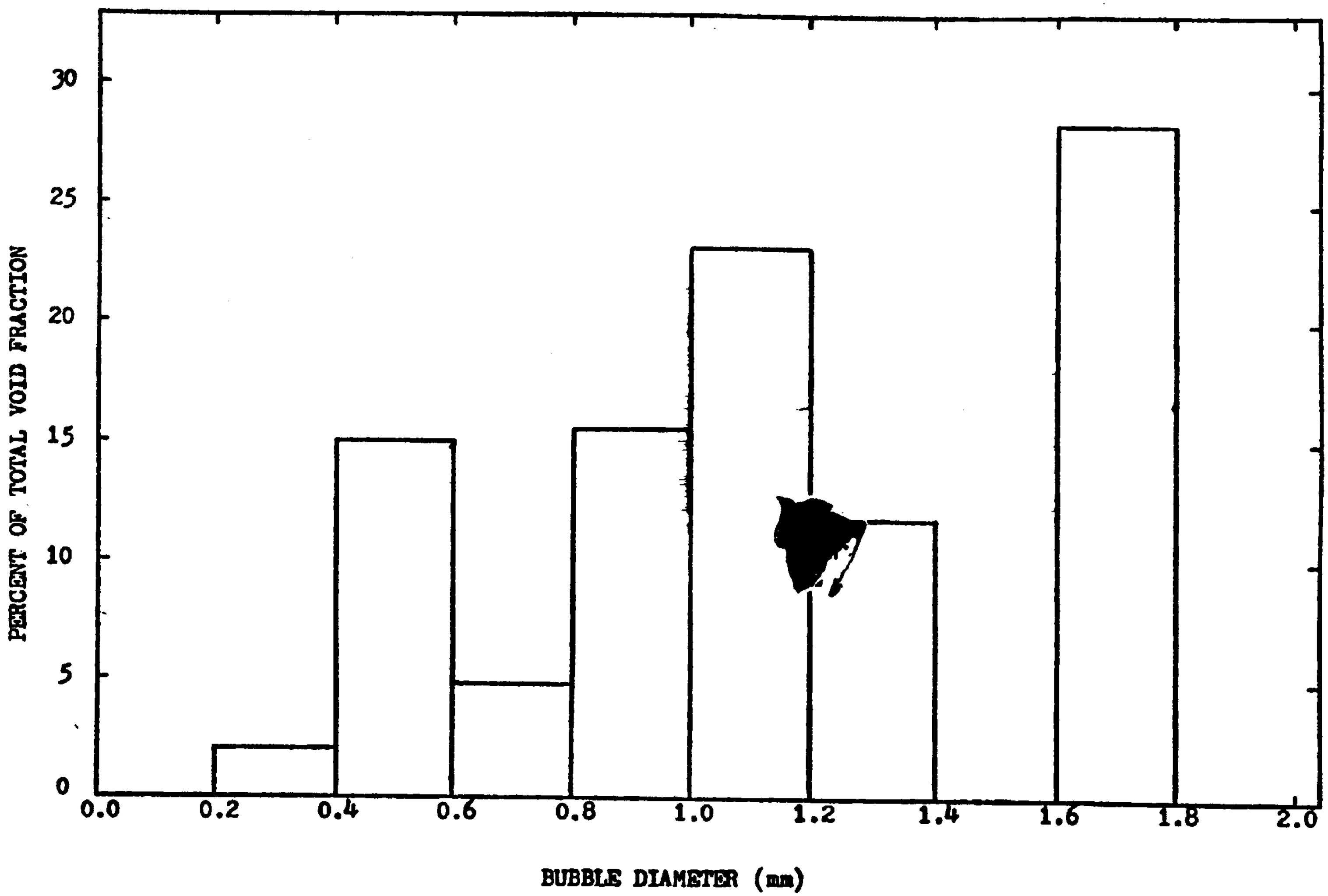

Figure 48 - Void Fraction Distribution with Gas Injection into the Liquid Inlet Line (U_1 = 1.60 cm/sec, U_g = 0.05 cm/sec)

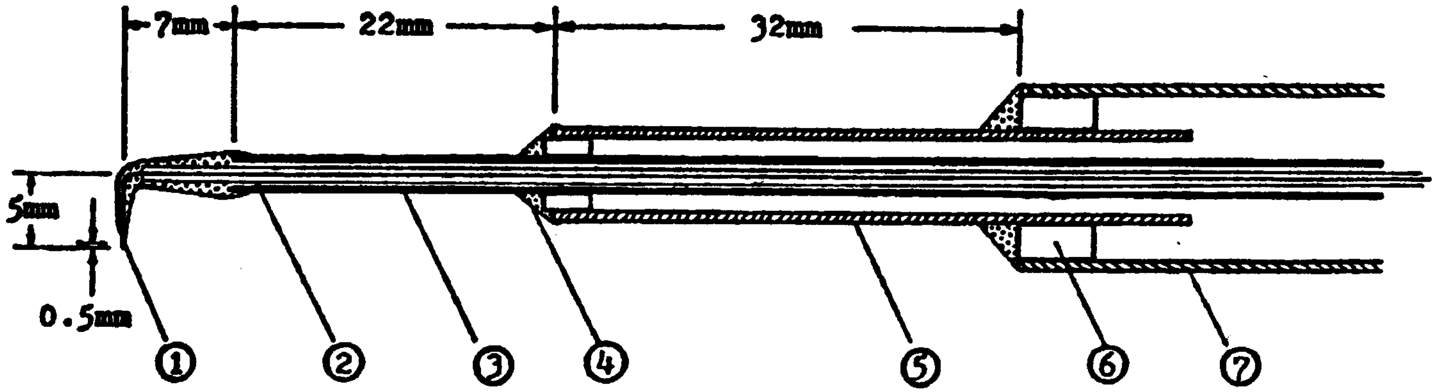

1 - 0.254 mm D music wire
2 - 1.02 mm I.D., 0.15 mm thick teflon tube
3 - 2.42 mm O.D. stainless steel tube
4 - Epoxy for sealing
5 - 6.3 mm O.D. stainless steel tube
6 - Rubber tube for fitting
7 - 12.7 mm O.D. stainless steel tube

Figure 49 - Resistivity Probe

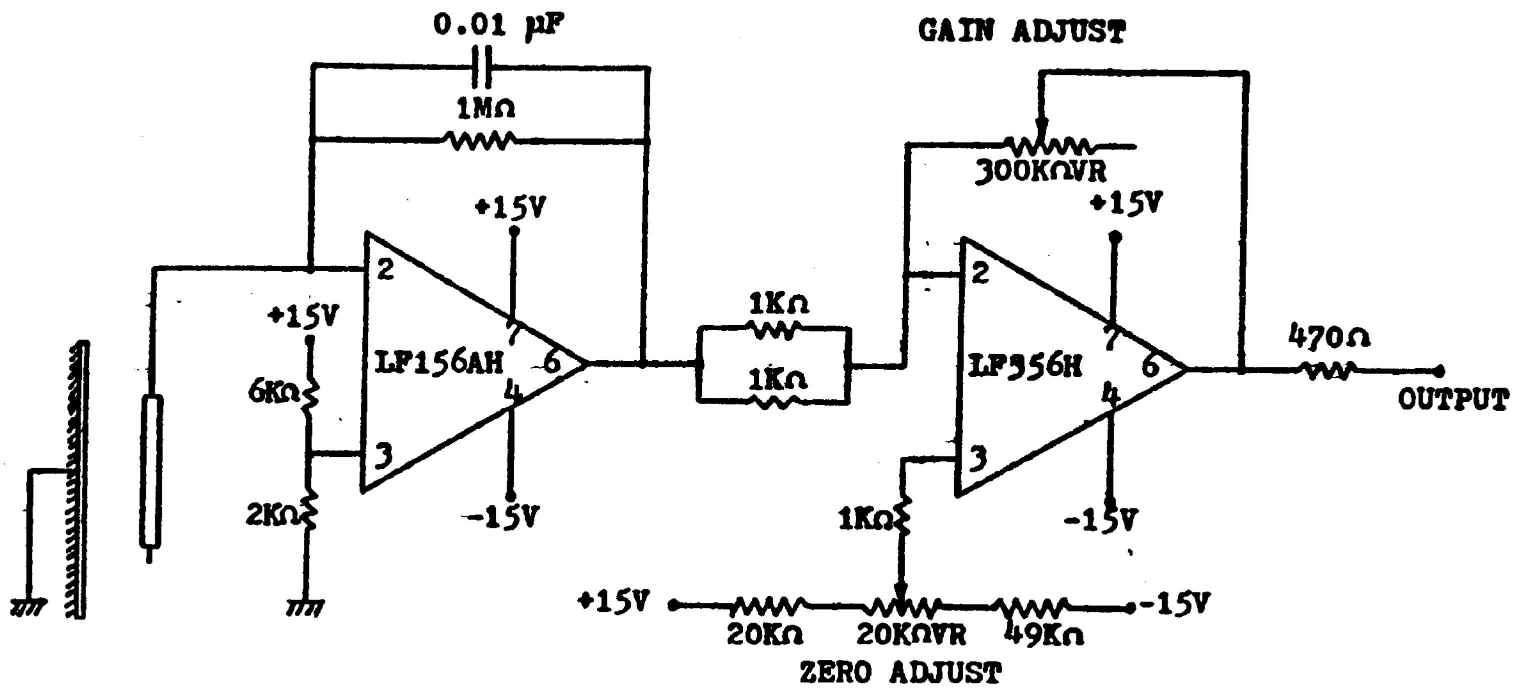

Figure 50 - Diagram of the Probe Circuit

Figure 51

PDU Reactor System and Sampling Location

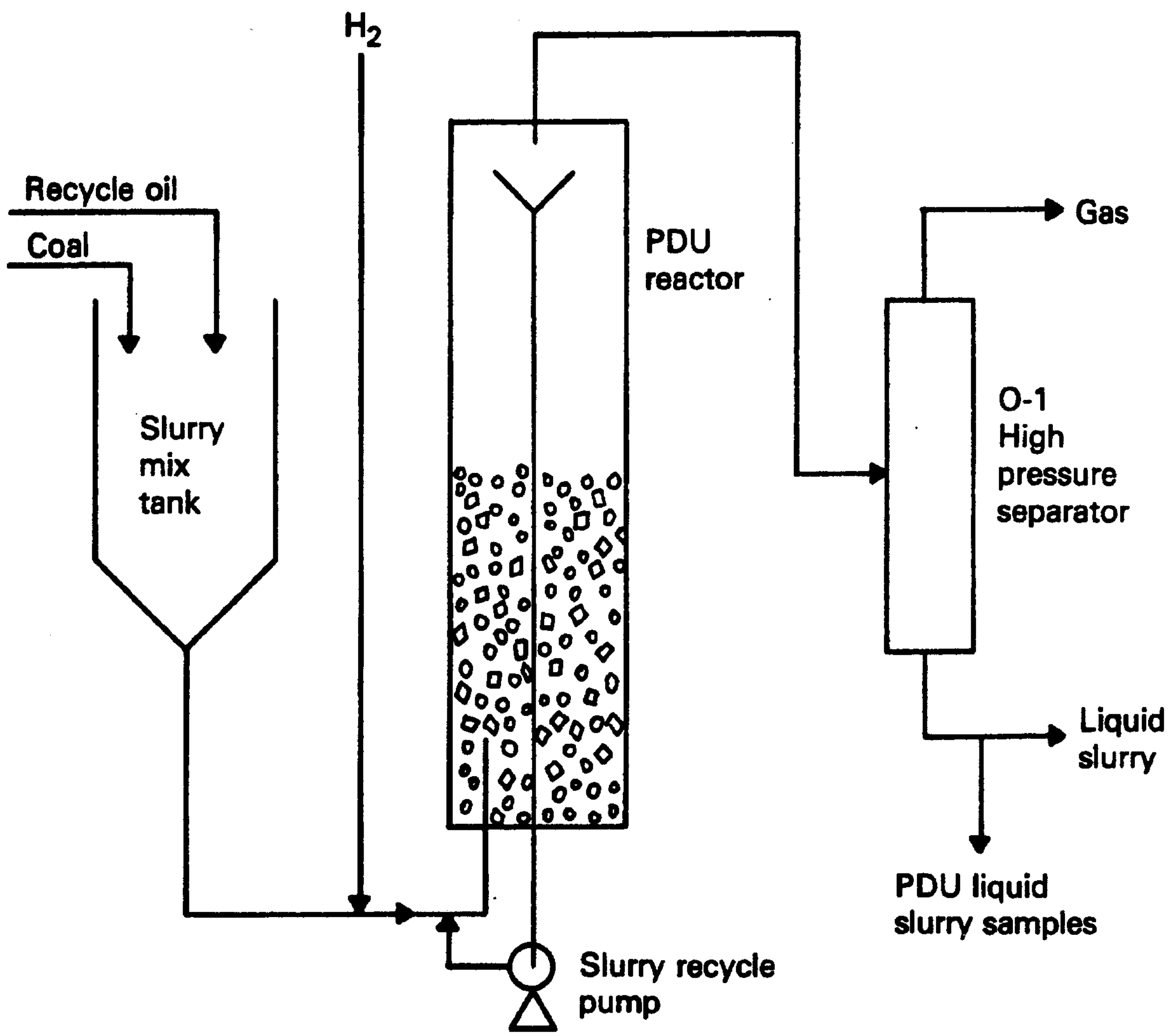

Figure 52

Side View of PDU Density Gauge Assembly

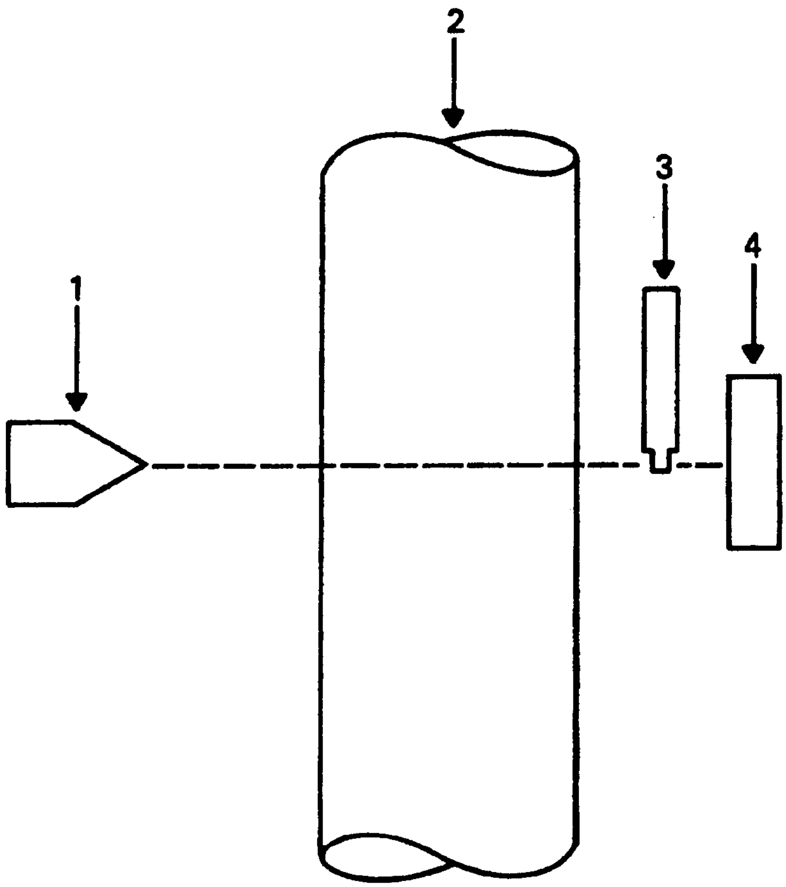

Legend

1 500 mc Cs-137 source
2 PDU reactor
3 Amoco scintillation detector
4 HRI Geiger/Muller detector

Figure 53

Top View of PDU Density Gauge Assembly

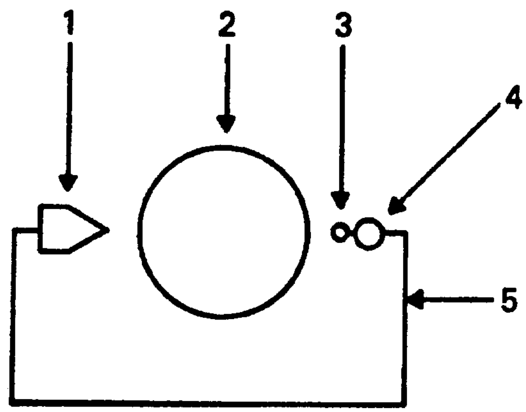

Legend

1 500 mc Cs-137 source
2 PDU reactor
3 Amoco scintillation detector
4 HRI Geiger/Muller detector
5 Traverse sled assembly

Figure 54

Gamma Ray Detection System Schematic

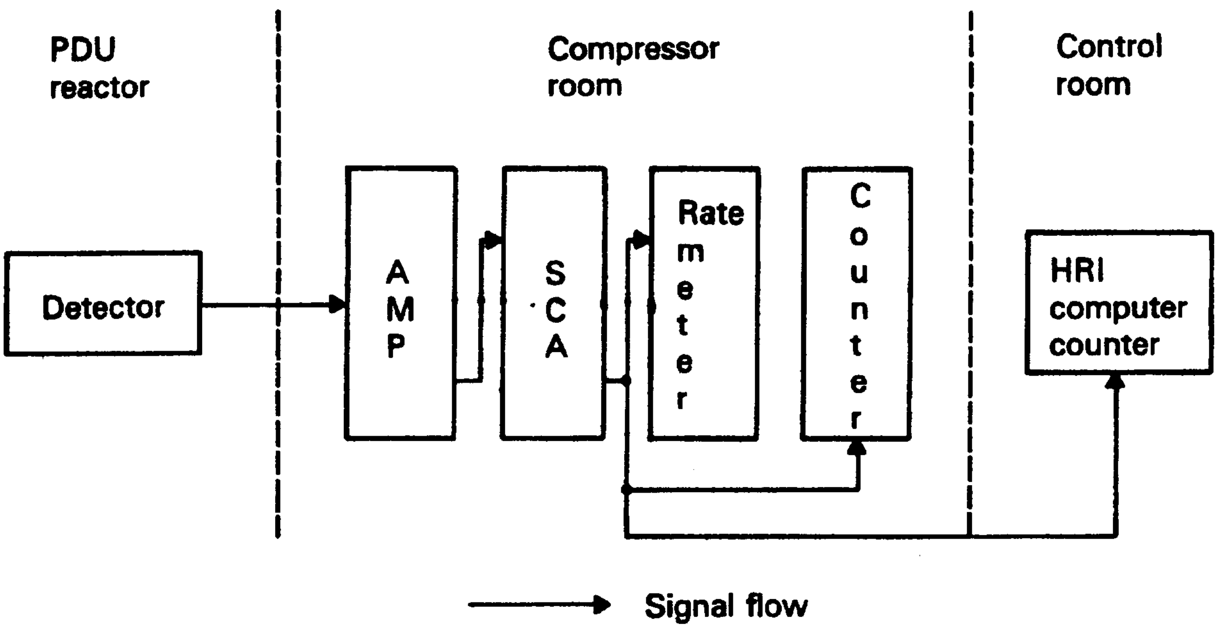

Notes

The SCA puts out a ⎍ pulse if the signal from the amplifier is in the proper energy range. One pulse corresponds to one detected gamma-ray photon.

The rate meter is an analog indicator of the SCA pulse rate (counts/sec).

Figure 55

Energy Window Criteria

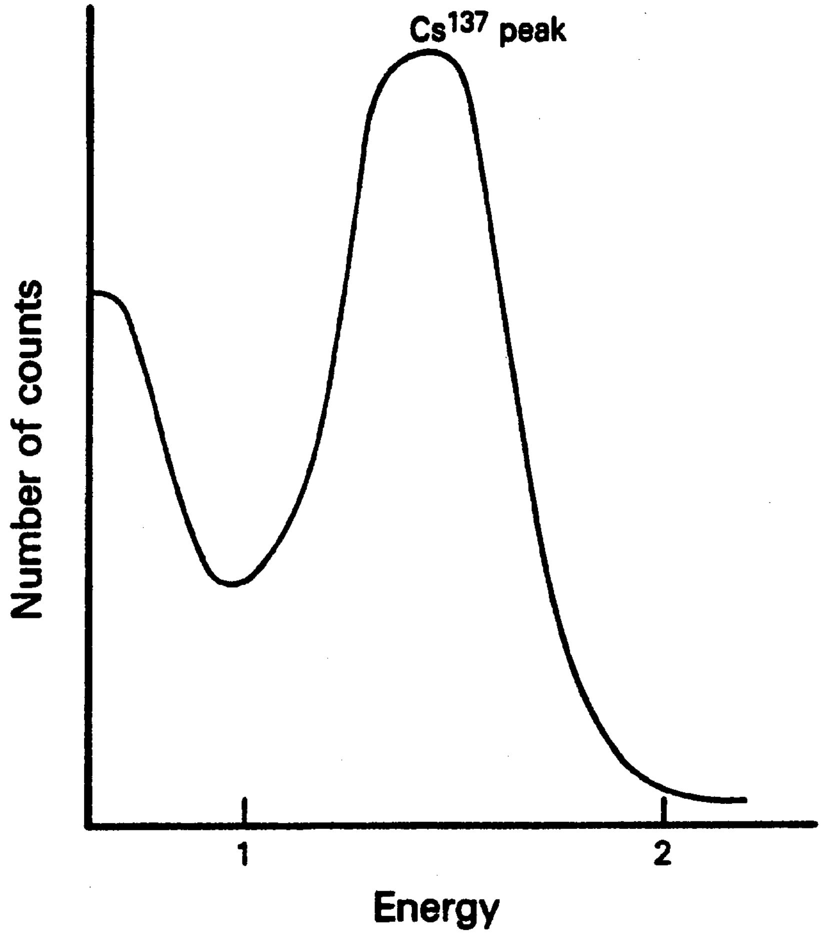

1. Lower edge: Minimum between background and Cs^{137} peak.
2. Upper edge: Defined as the energy where count rate = 10% of maximum rate.

Figure 56

Apparent Shift of Cs-137 Photopeak with Detector Temperature

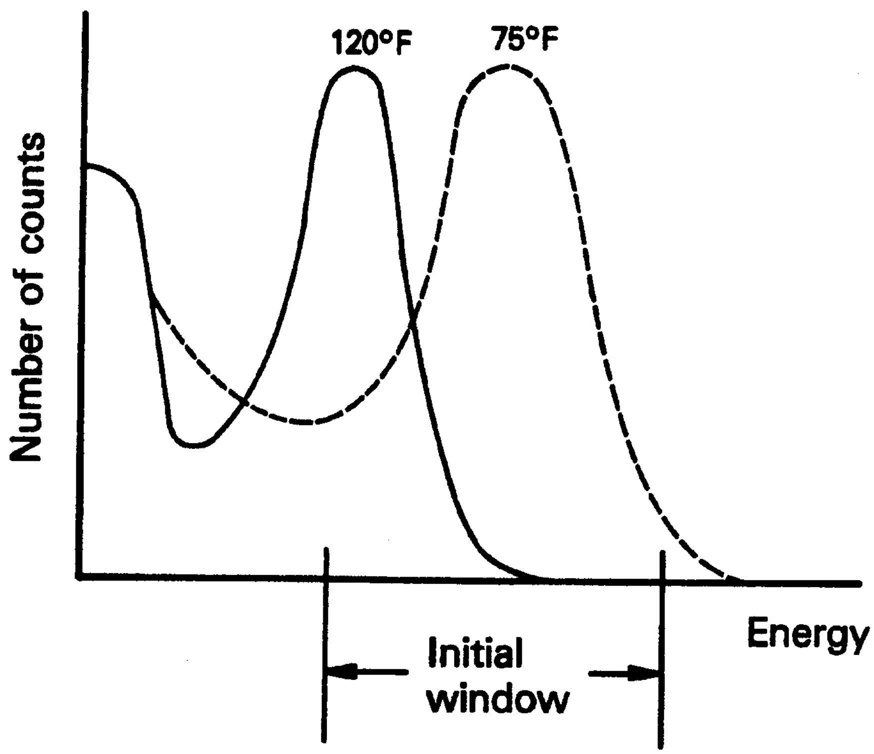

FIGURE 57

PDU-10 ZERO GAMMA RAY SCAN

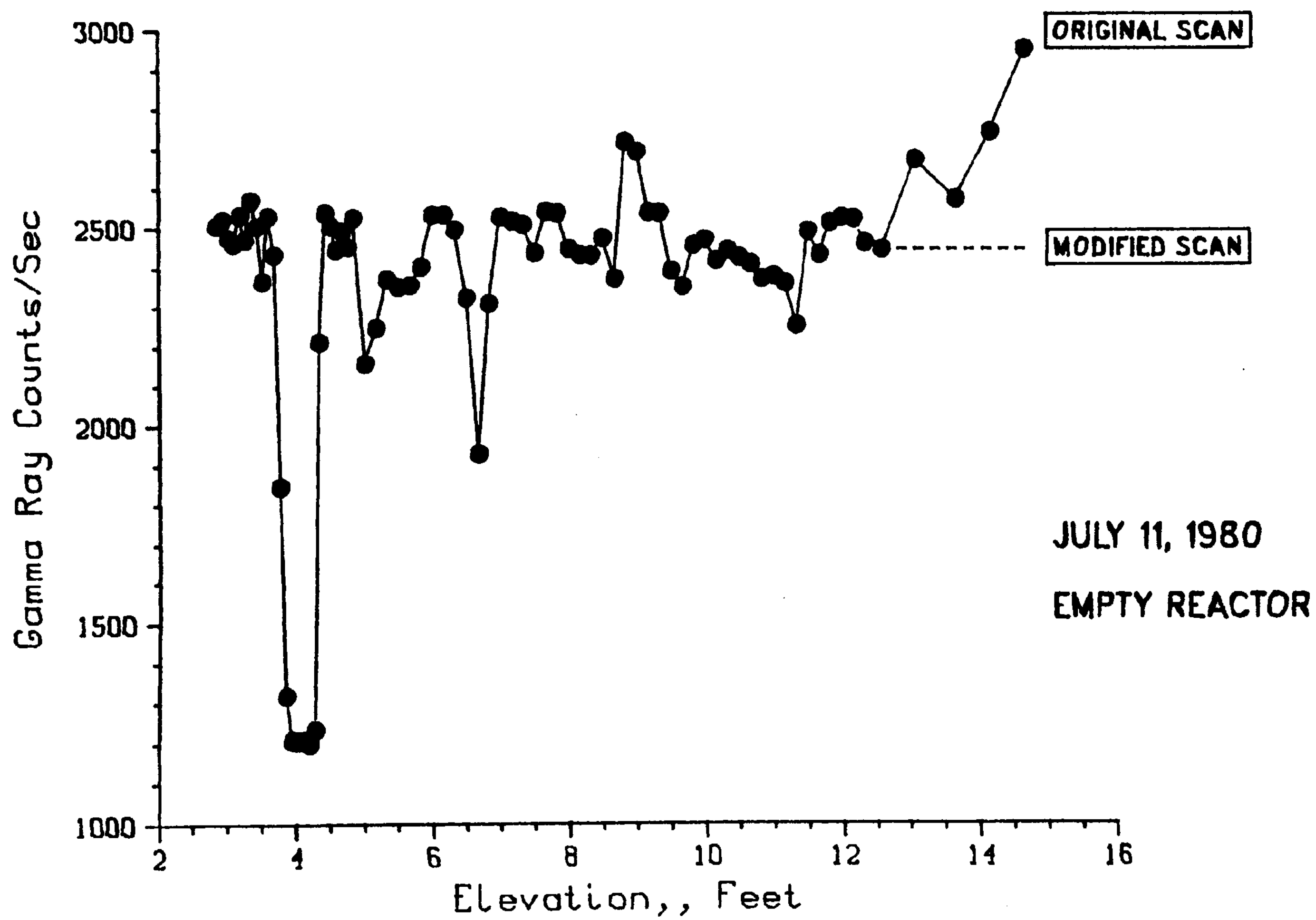

Figure 58

BATTELLE VISCOMETER SCHEMATIC

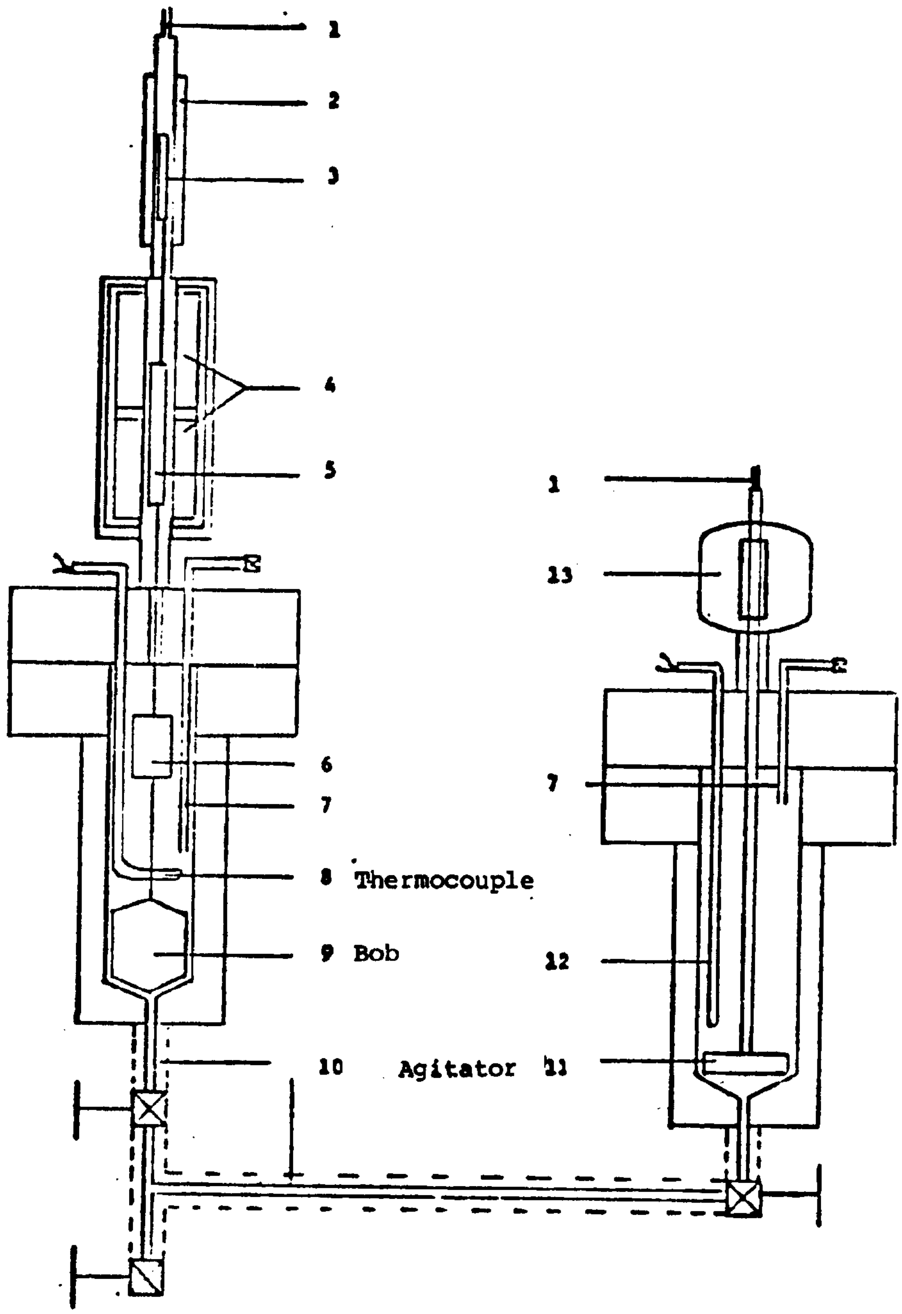

FIGURE 59

PDU-10 REACTOR LIQUID SLURRY VISCOSITY VS TEMPERATURE , AMOCO SAMPLE #5

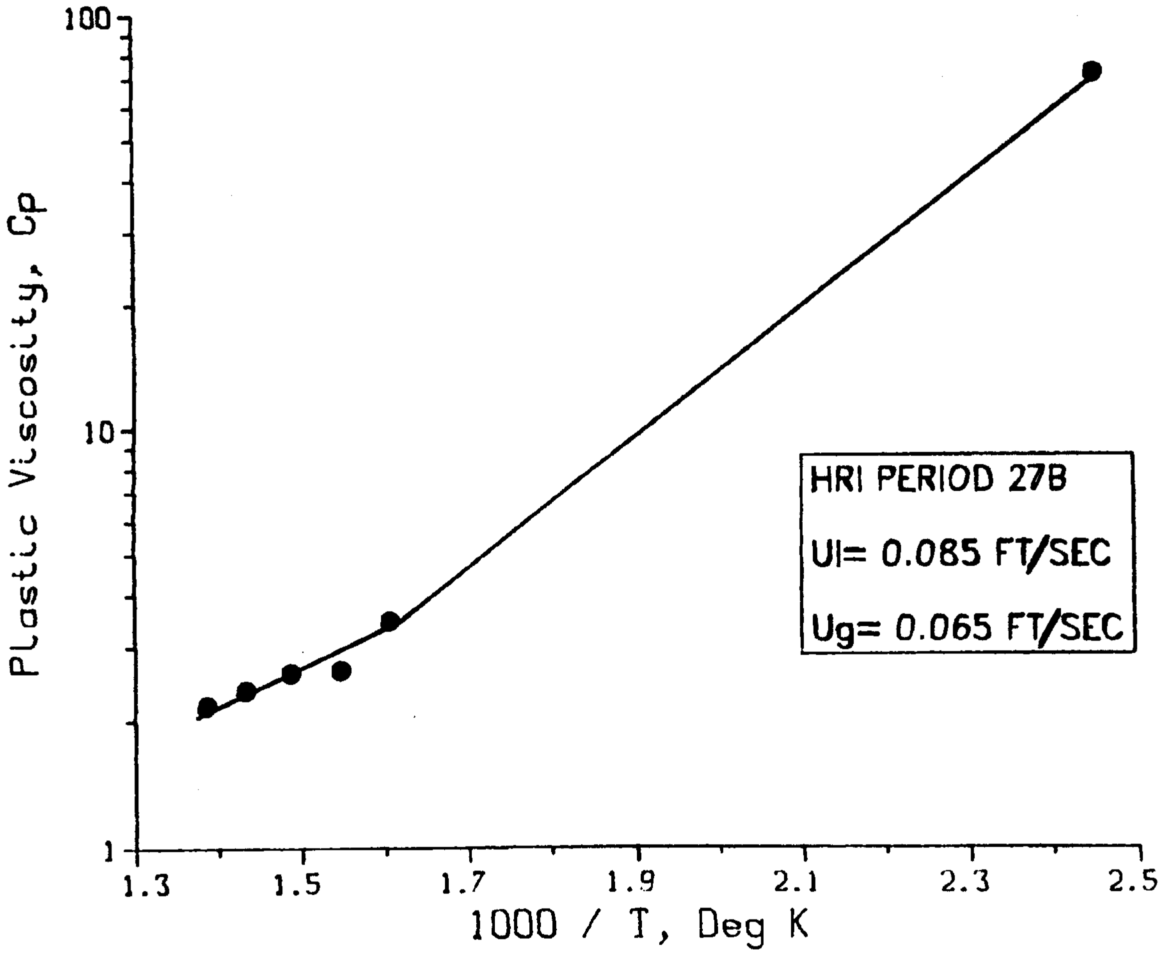

FIGURE 60

PDU-10 REACTOR LIQUID SLURRY
YIELD STRESS VS TEMPERATURE , AMOCO SAMPLE #5

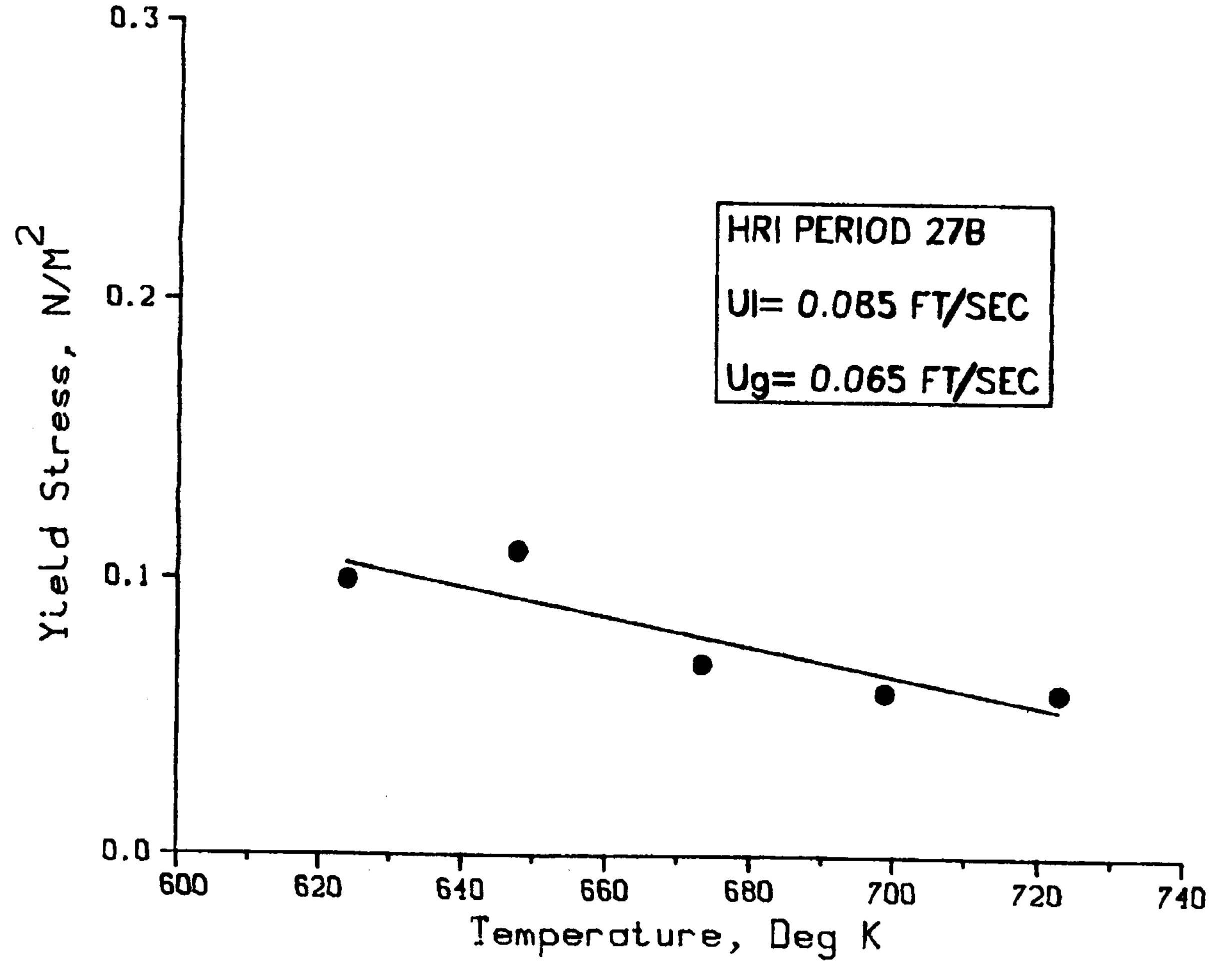

FIGURE 61

PDU-10 REACTOR LIQUID SLURRY DENSITY VS TEMPERATURE , AMOCO SAMPLE #5

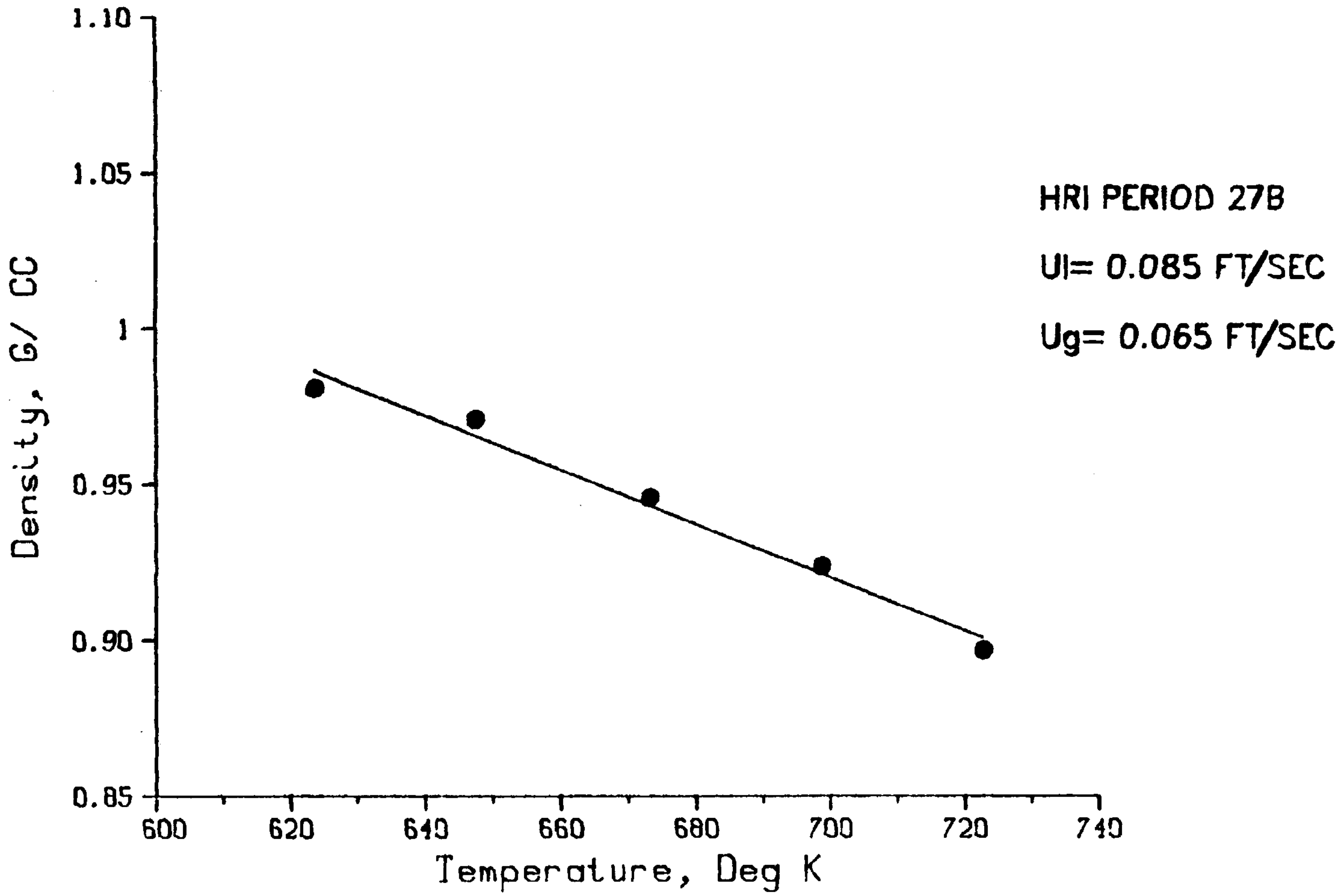

FIGURE 62

PDU-10 REACTOR LIQUID SLURRY
HYSTERESIS OF VISCOSITY VS TEMPERATURE , AMOCO SAMPLE #8

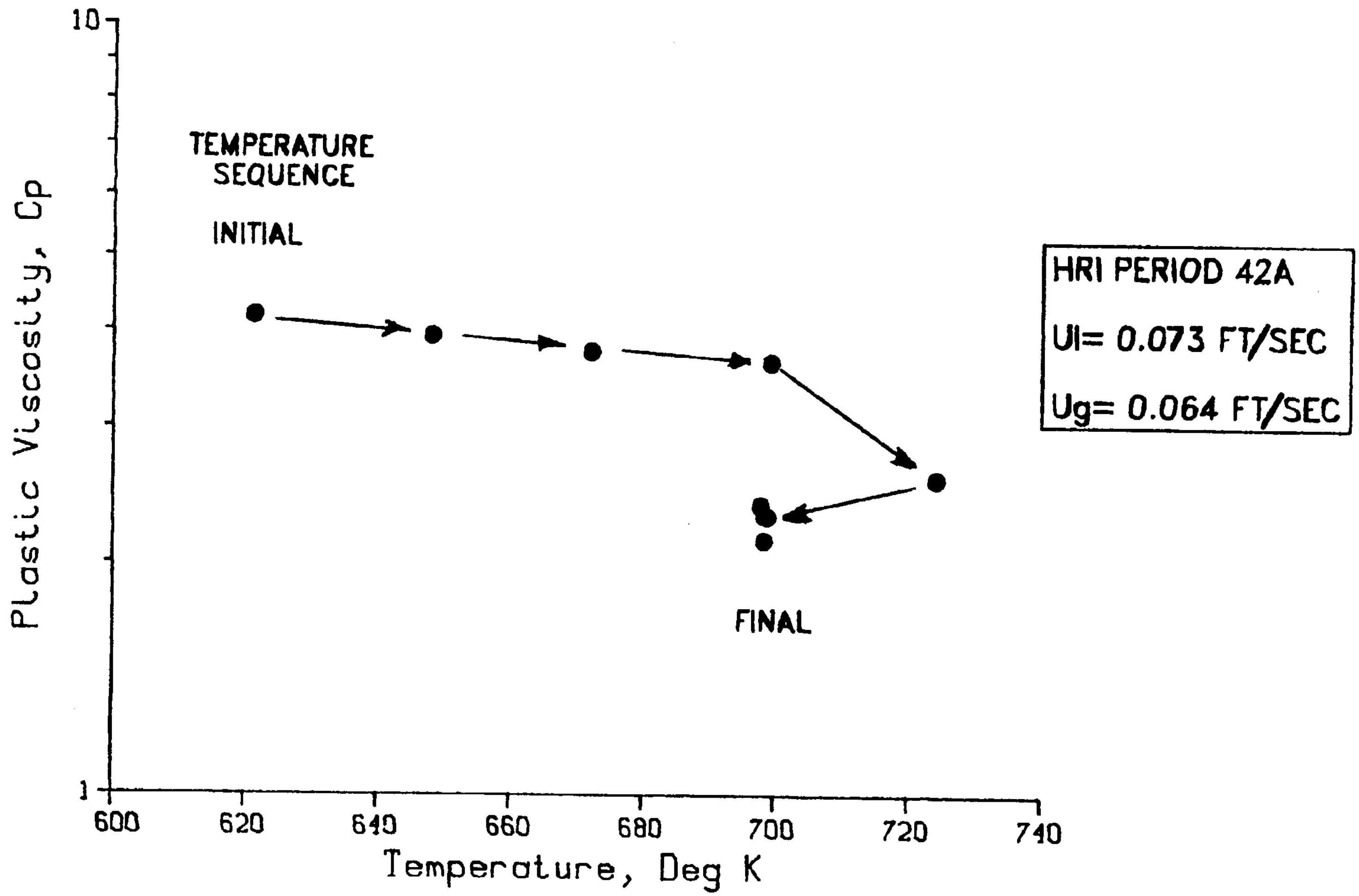

FIGURE 63

CHANGE OF PLASTIC VISCOSITY WITH TIME AT 725 K PDU LIQUID SAMPLE AMOCO-15

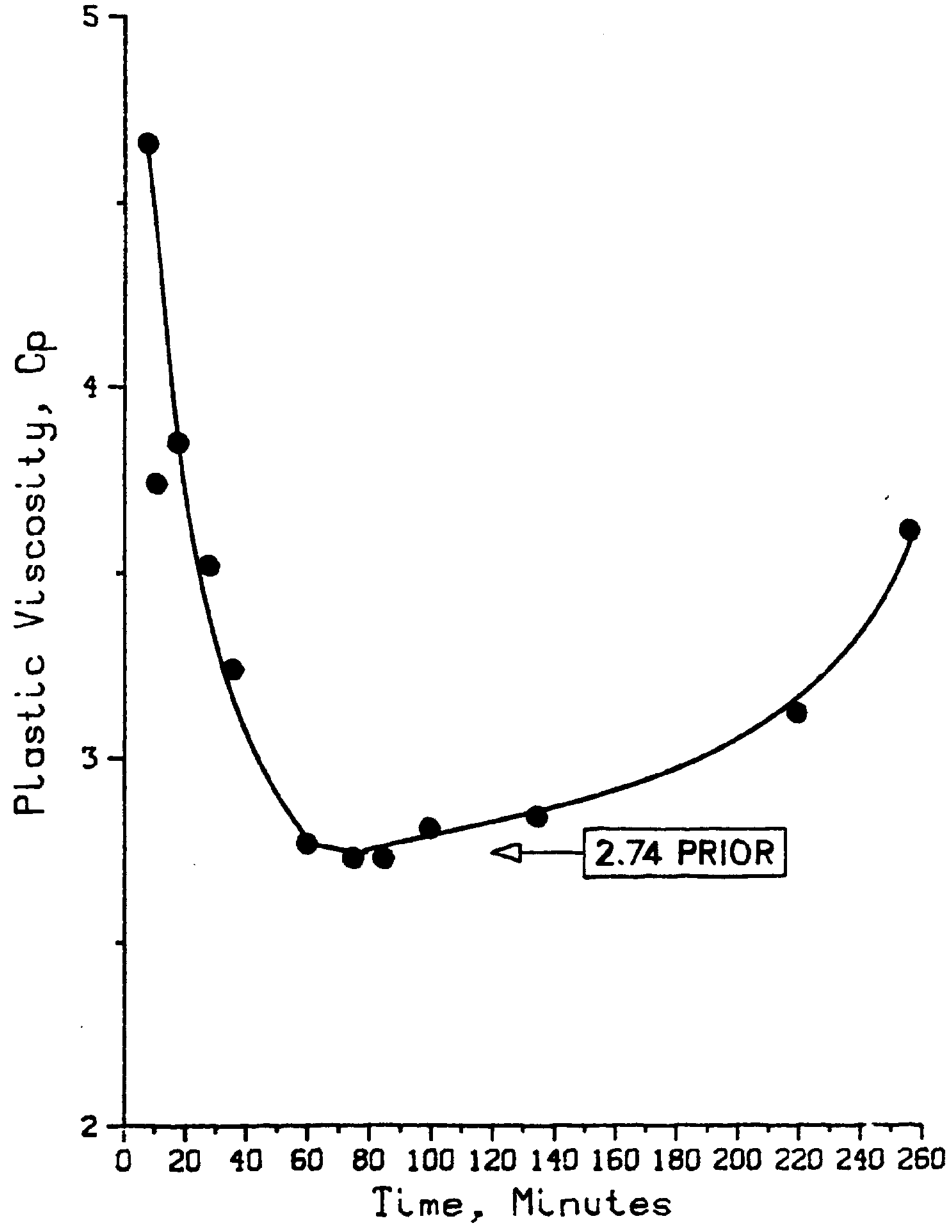

FIGURE 64

CHANGE OF YIELD STRESS WITH TIME AT 725 K PDU LIQUID SAMPLE AMOCO-15

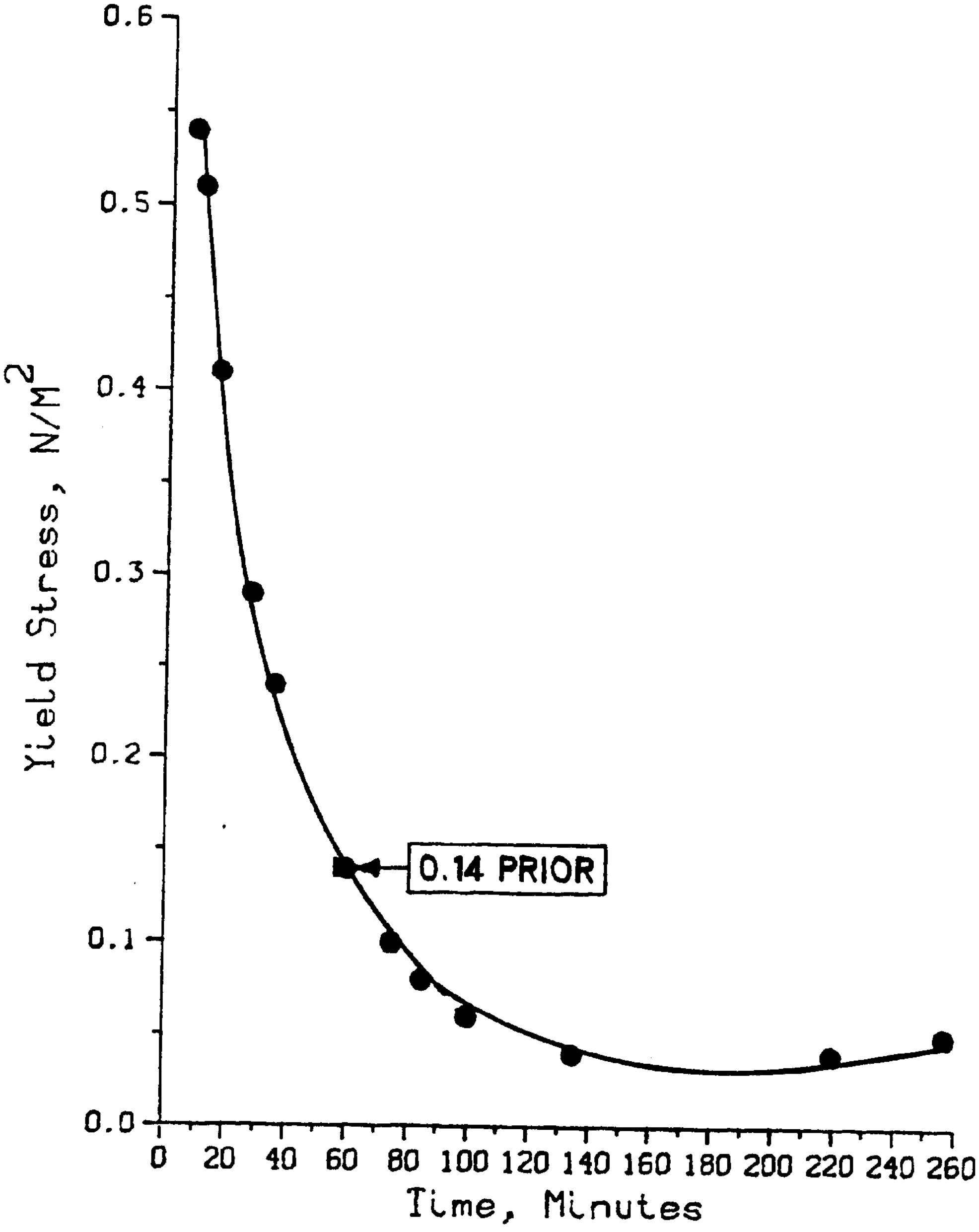

FIGURE 65

CHANGE OF SLURRY DENSITY WITH TIME AT 725 K PDU LIQUID SAMPLE AMOCO-15

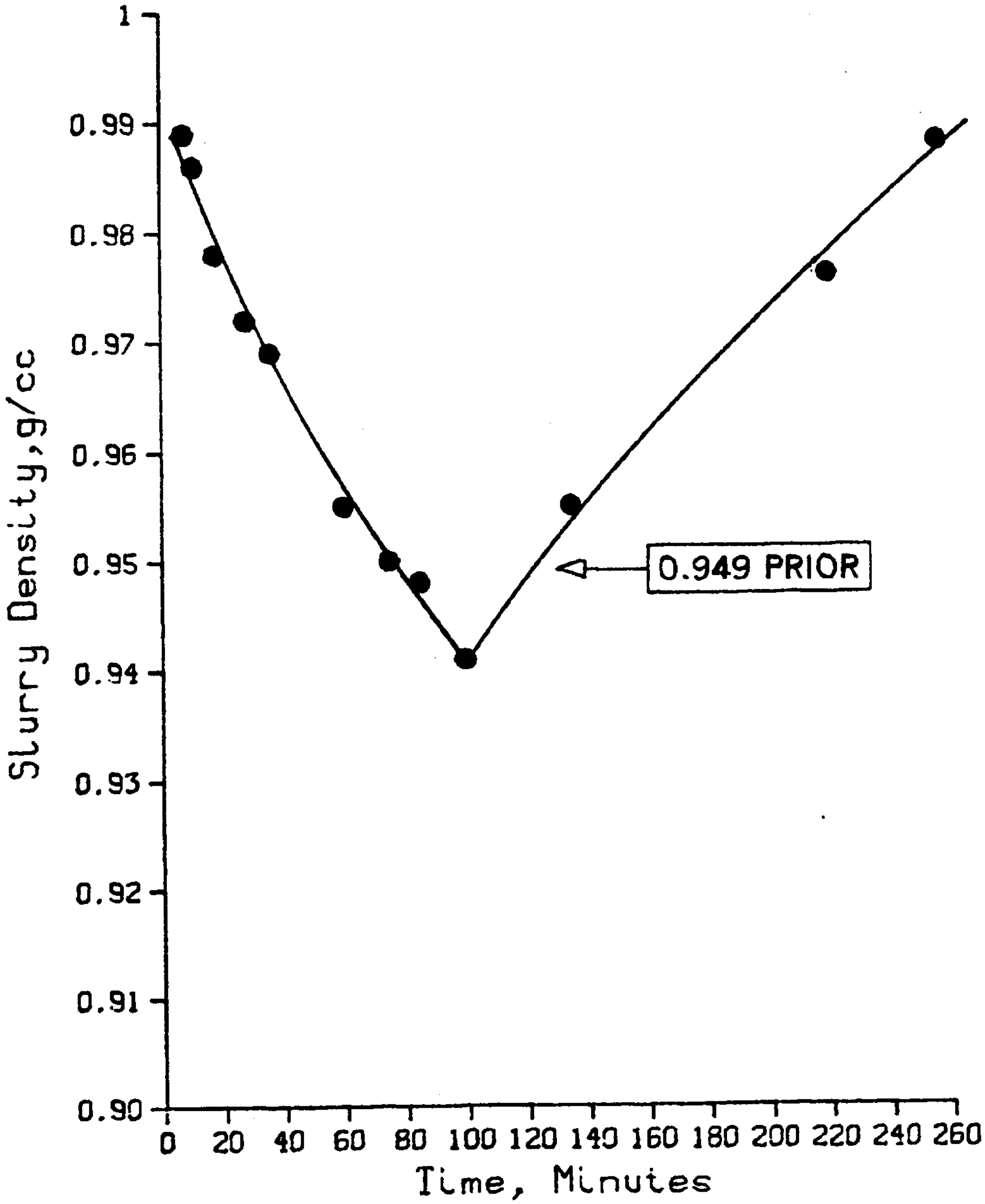

FIGURE 66

COMPARISON OF VISCOSITY OF ASPHALTENES AND PREASPHALTENES

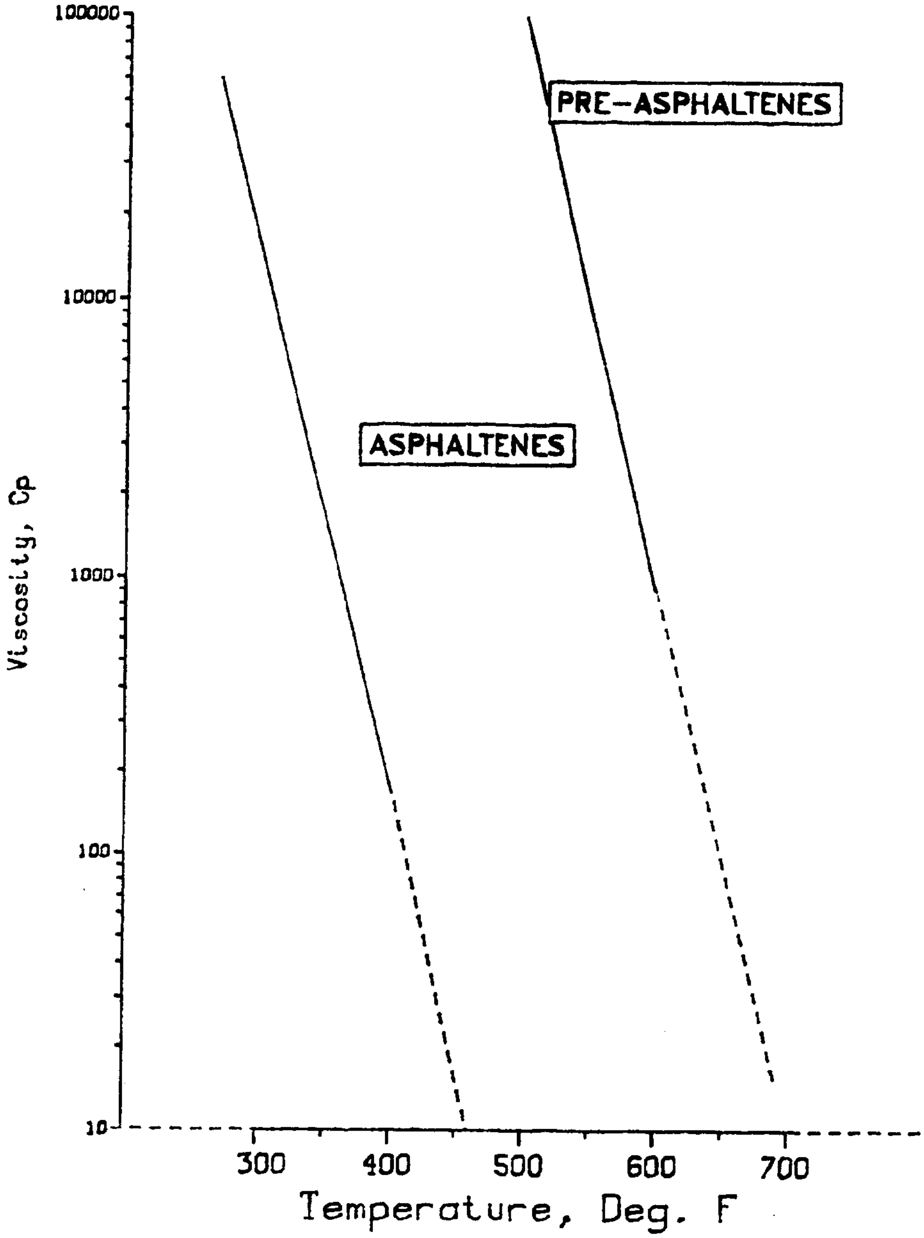

Figure 67

OAK RIDGE NATIONAL LABORATORY
VISCOMETER SCHEMATIC

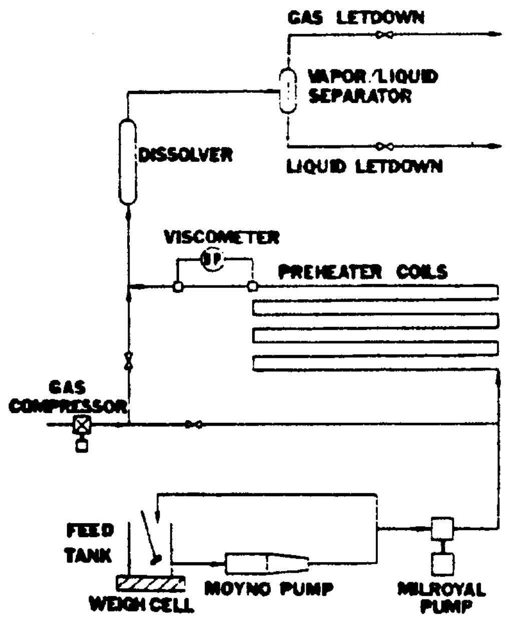

Schematic flow diagram of coal liquids flow system.

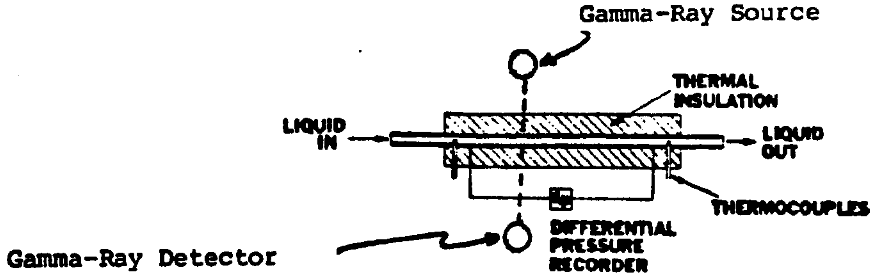

Schematic flow diagram of pipeline viscometer.

FIGURE 68

COMPARISON OF BATTELLE AND ORNL VISCOMETER TEMPERATURE HISTORIES

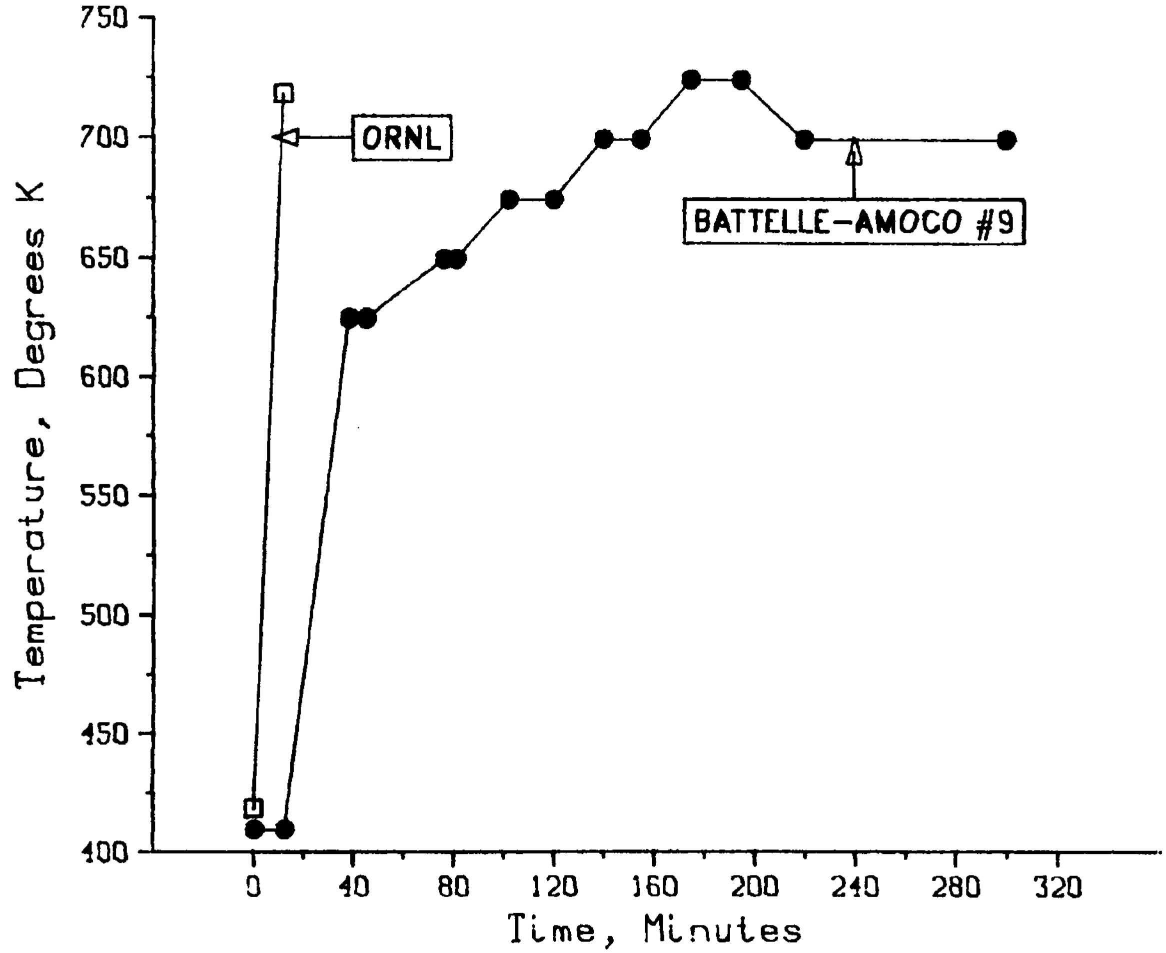

Figure 69

-182 TRENDS OF PLASTIC VISCOSITY VERSUS TIME (BATTELLE VISCOMETER)

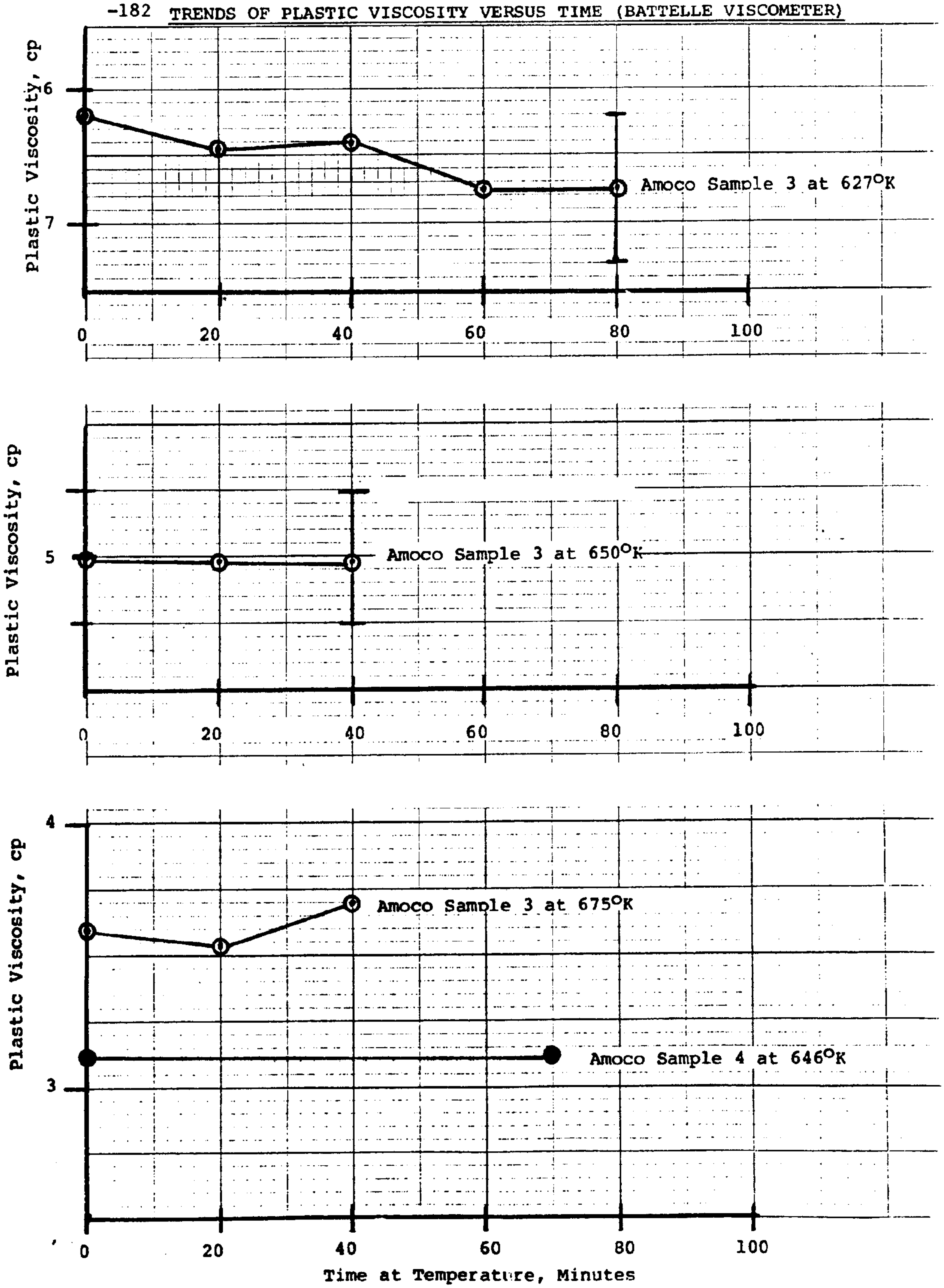

FIGURE 70

PDU-10 REACTOR LIQUID SLURRY VISCOSITY CORRELATION

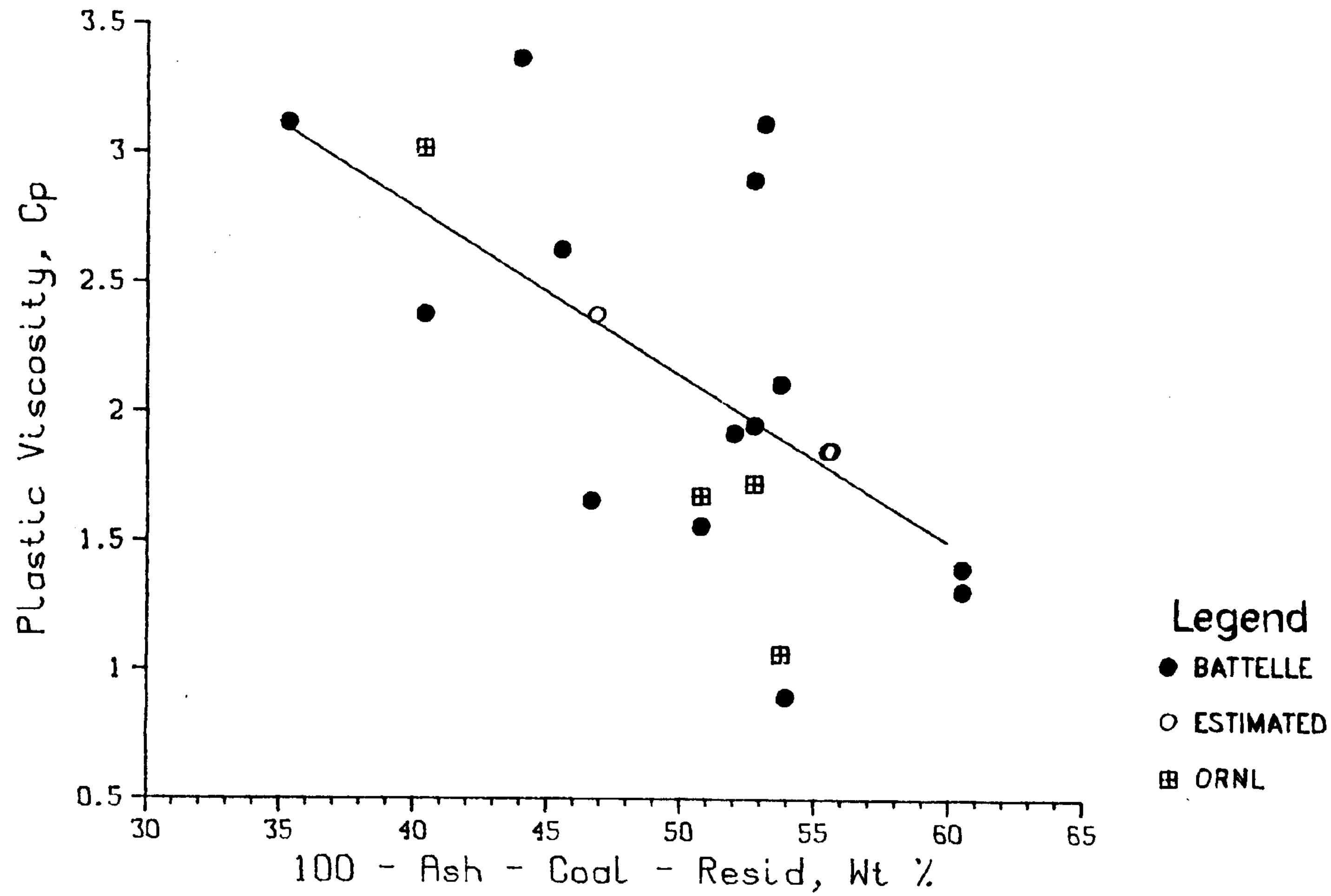

FIGURE 71

PDU-10 REACTOR LIQUID SLURRY DENSITY CORRELATION

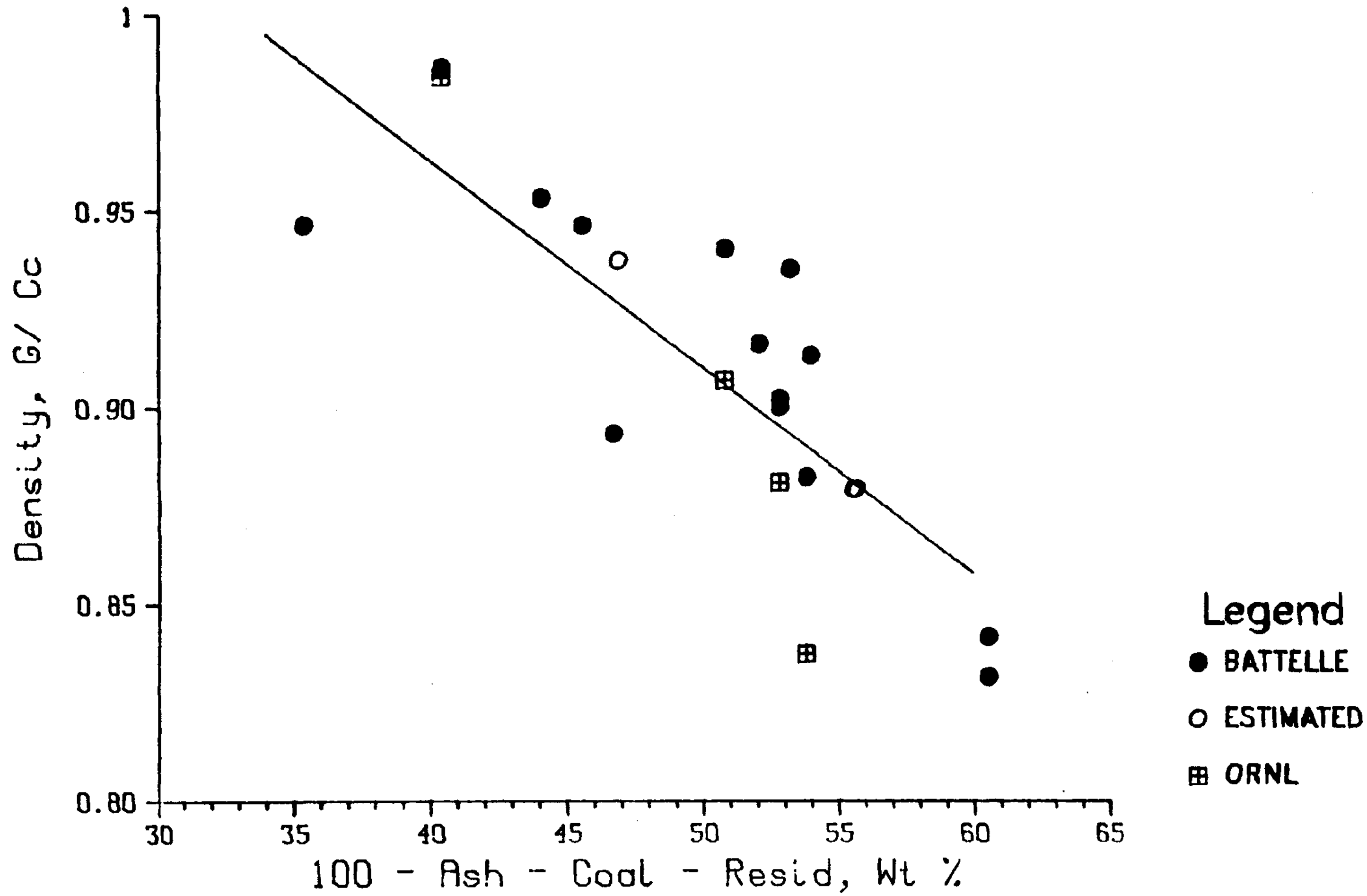

FIGURE 72

PDU-10 REACTOR LIQUID SLURRY YIELD STRESS CORRELATION

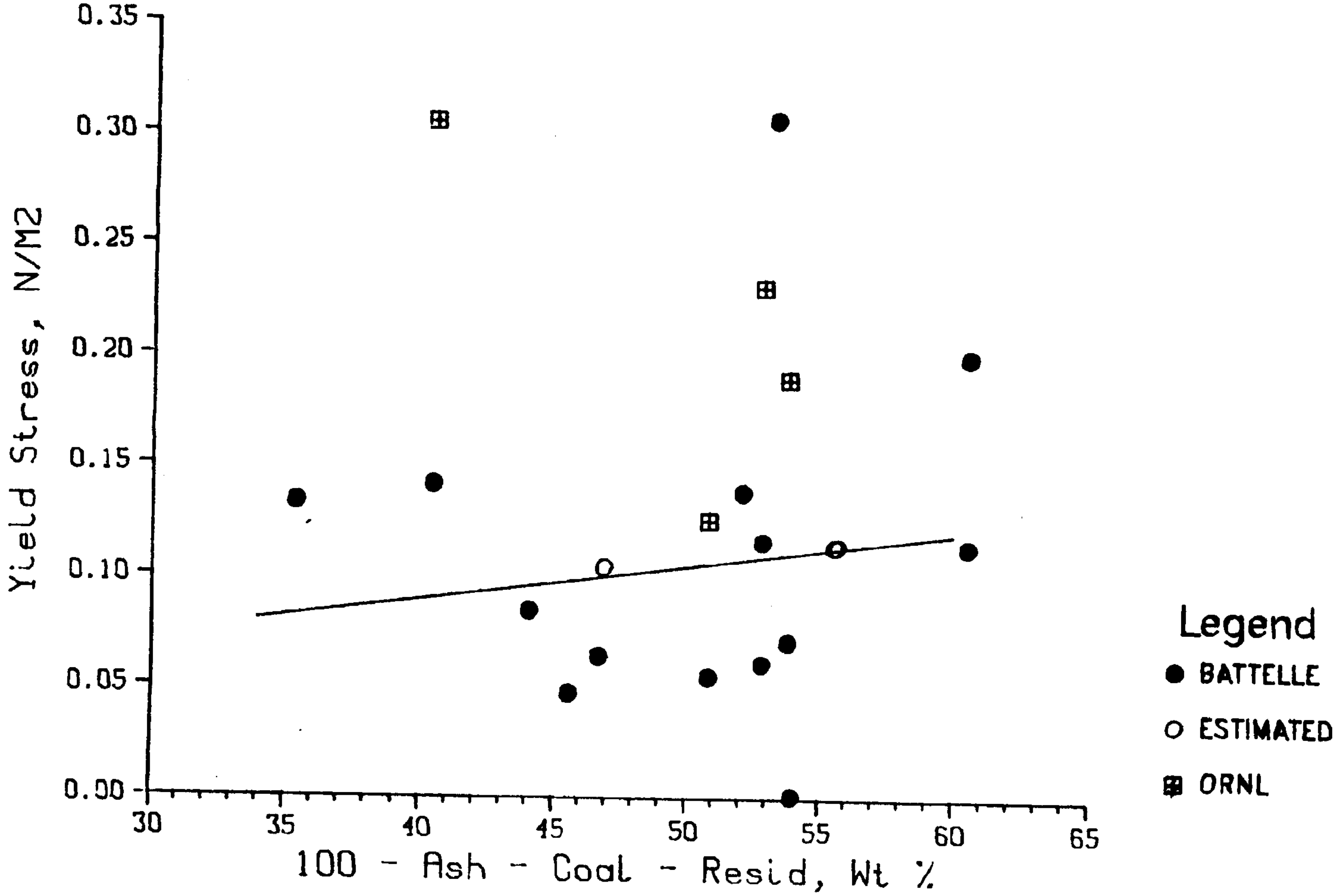

FIGURE 73

PDU-10 GAMMA RAY SCAN
I/I0 RATIO,TEST NUMBER 07
EXAMPLE OF SHARP CATALYST INTERFACE

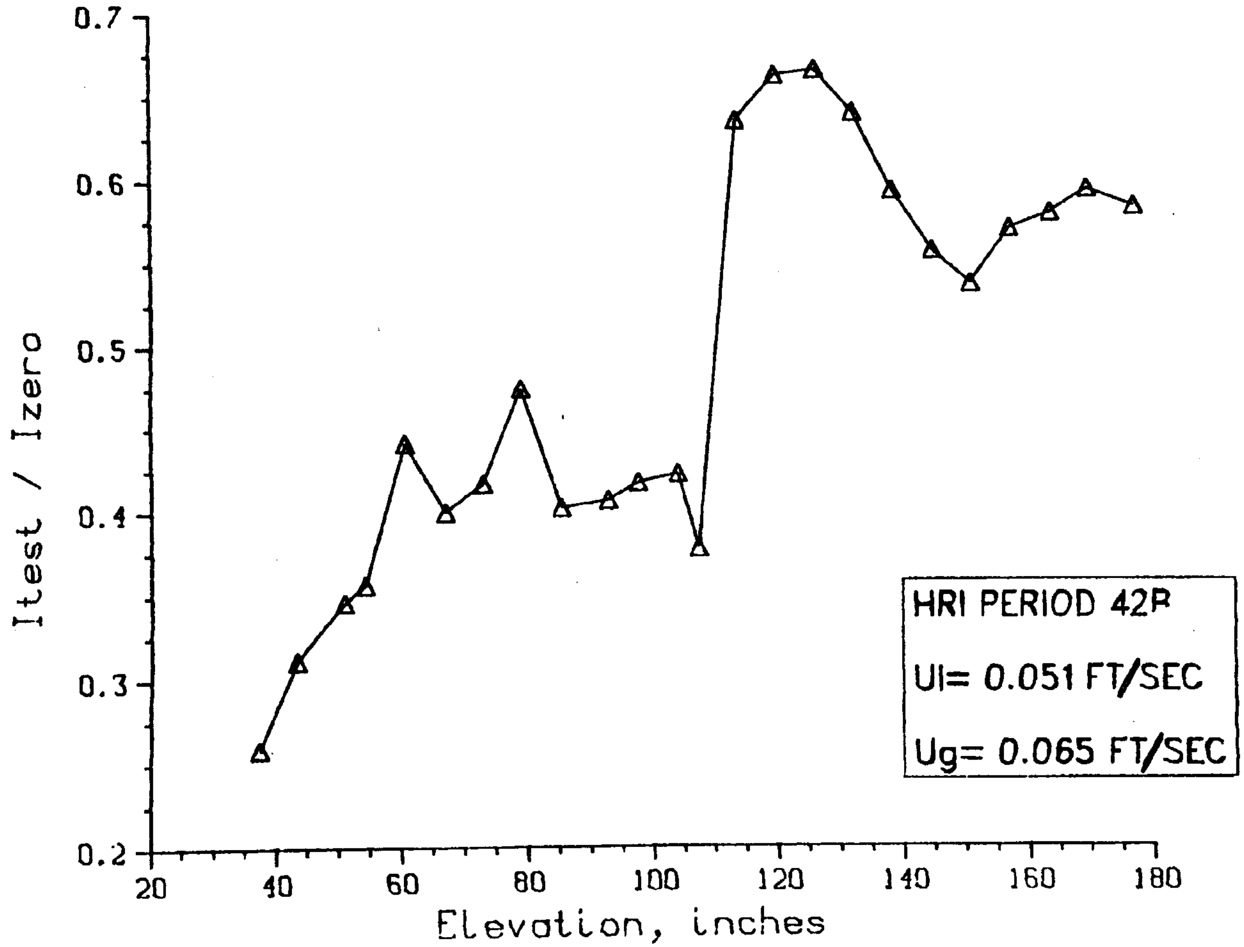

FIGURE 74

PDU-10 GAMMA RAY SCAN
I/I0 RATIO, TEST NUMBER 10
EXAMPLE OF DIFFUSE CATALYST BED INTERFACE

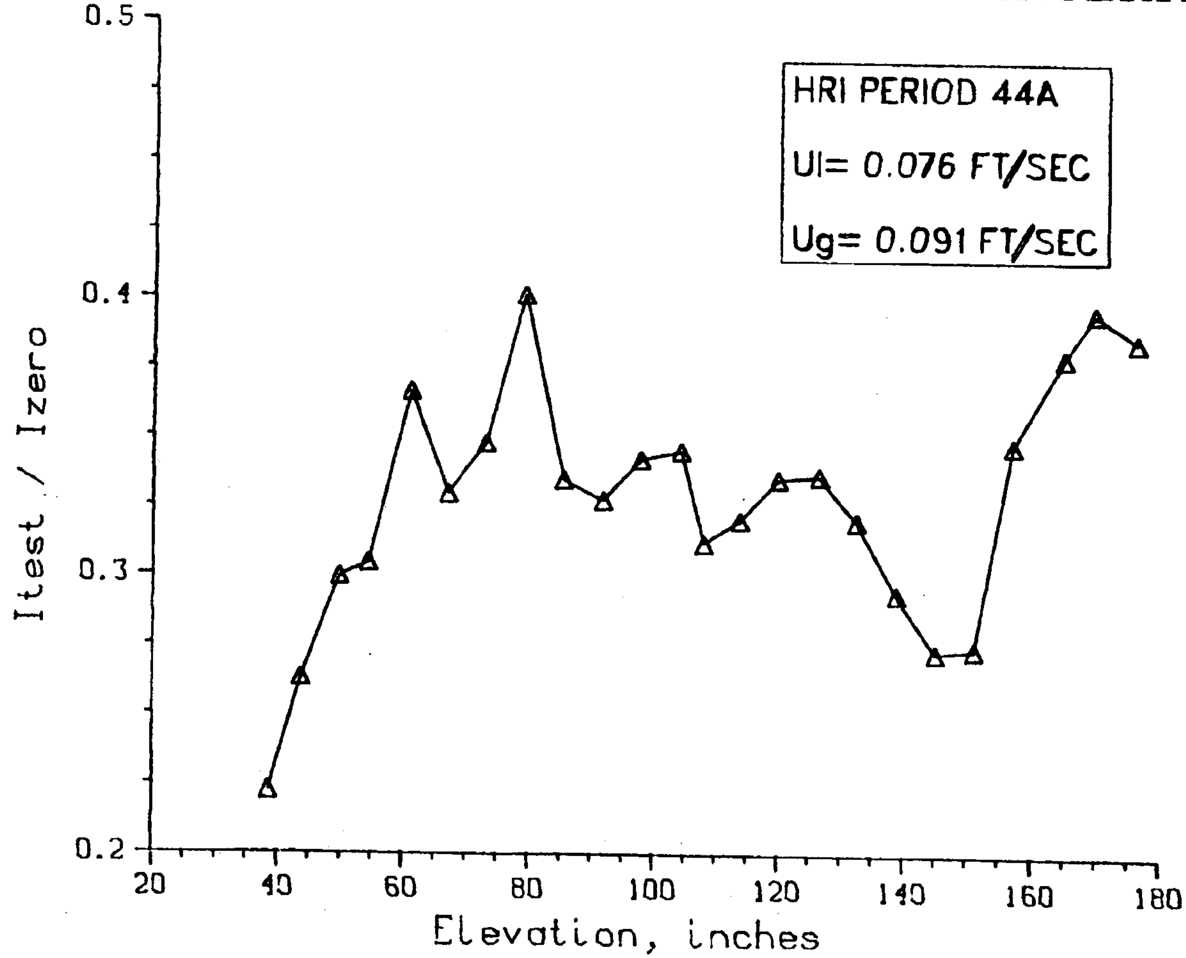

Figure 75

H-Coal PDU Reactor Elevation Reference

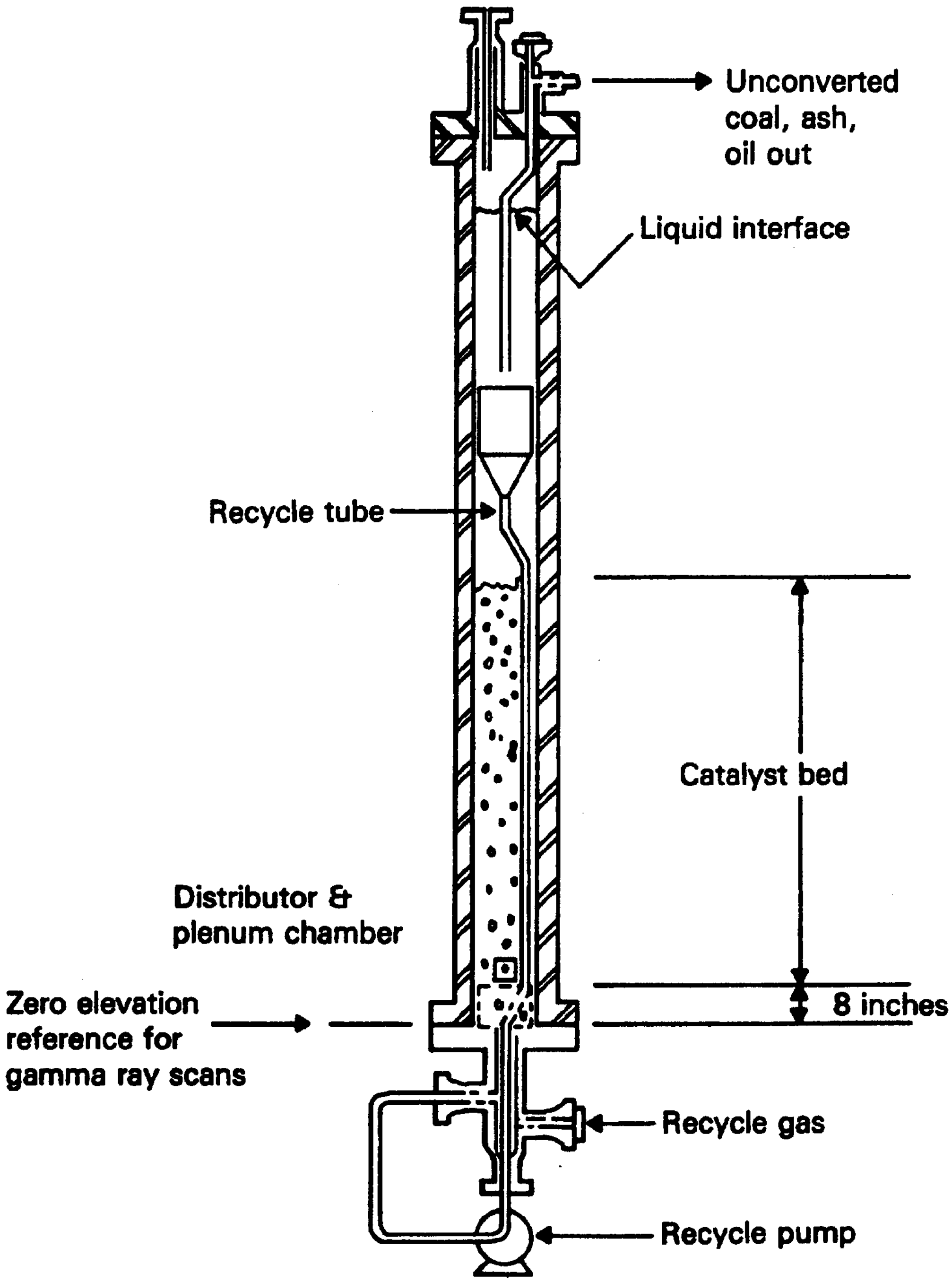

Figure 76

<u>HRI SHUTDOWN OIL DENSITY</u>

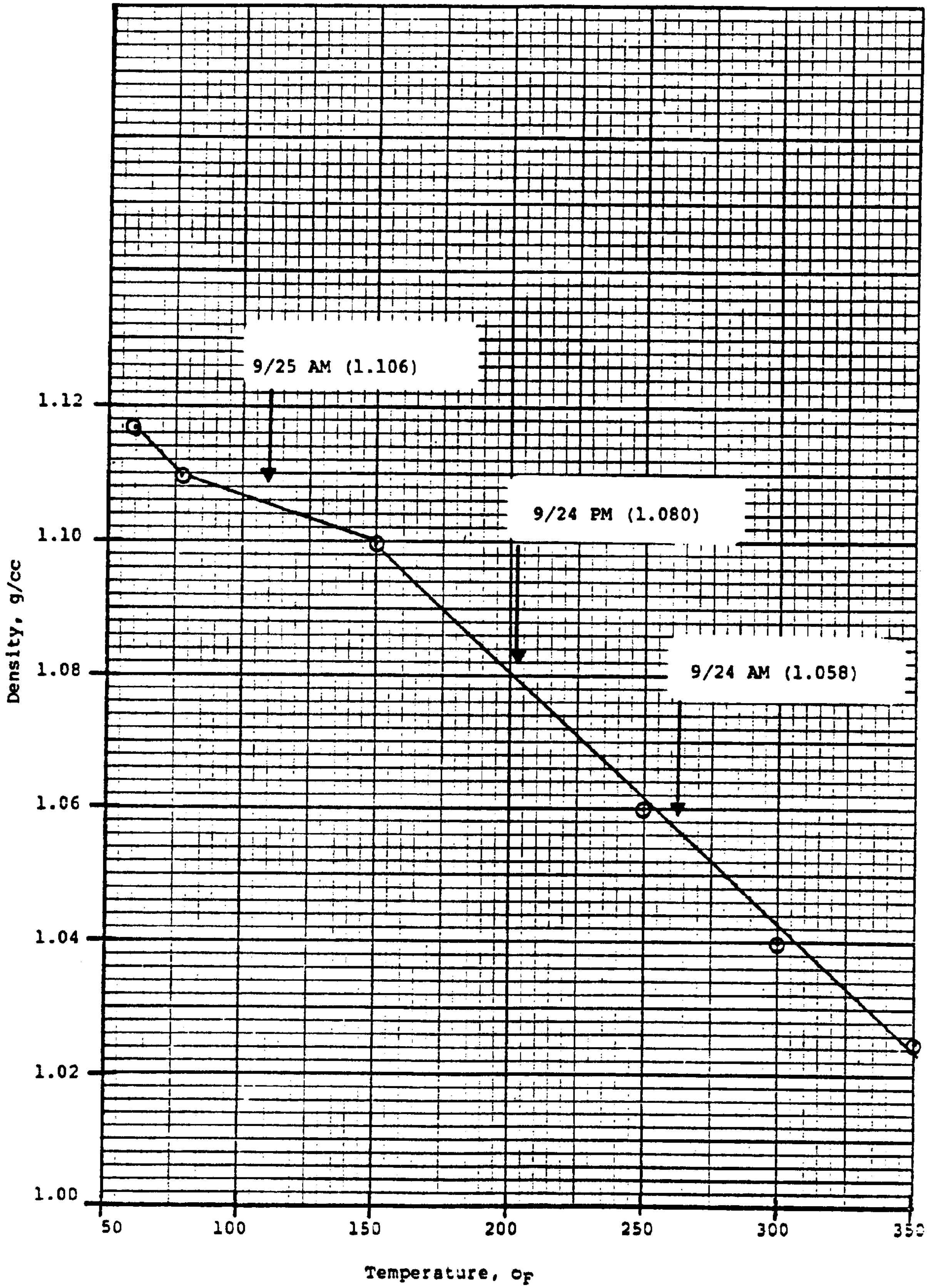

FIGURE 77

DRIFT FLUX DENSE PHASE PDU-10 FLUID DYNAMICS TESTS

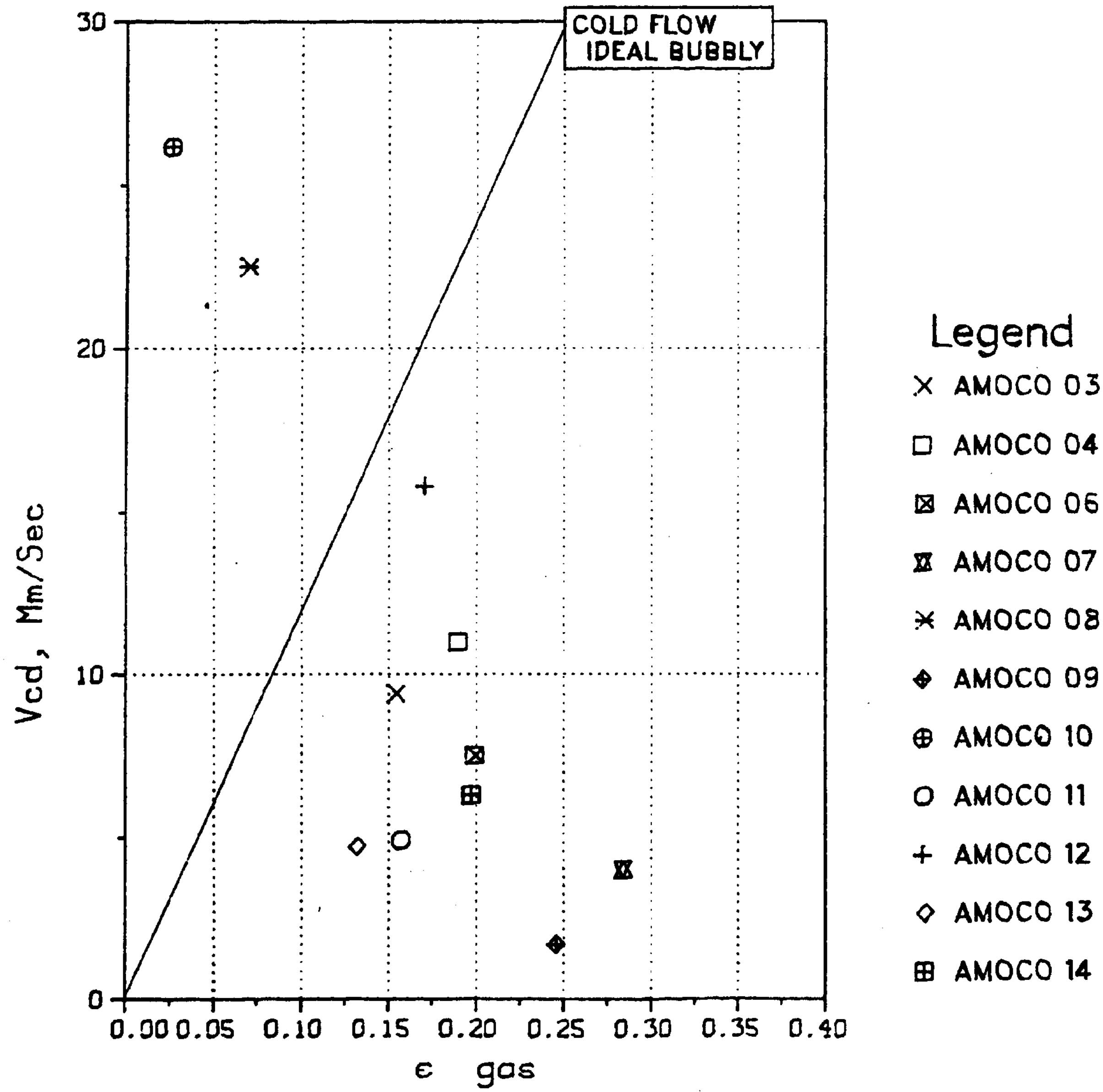

Figure 78

Bhatia-Epstein Model

- Ebullated bed assumes 3 phases
  - Gas
  - Wake
  - Particulate

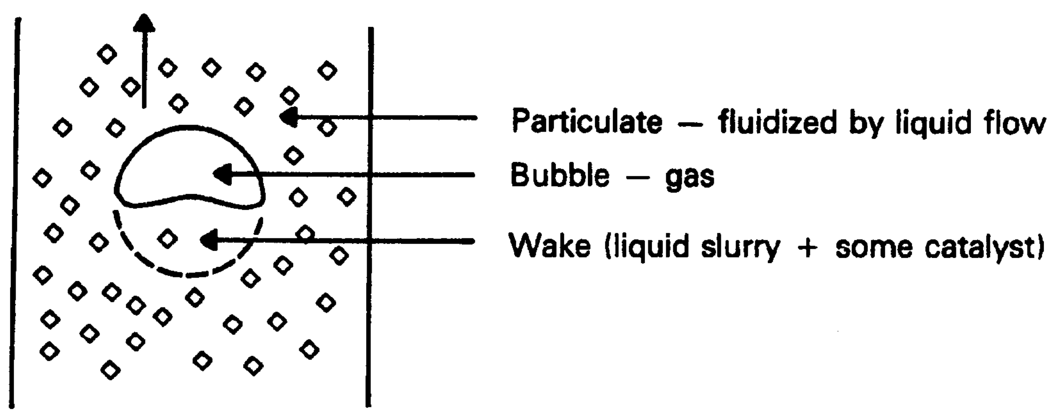

Assumptions:

- Particulate phase—liquid and catalyst only: Described by Richardson-Zaki correlation
- Bubble wake—liquids and solids: Described by wake volume ratio K_o
- Bubble rise velocity—U_{tB}

FIGURE 79

PREDICTION OF CATALYST PARTICLE TERMINAL REYNOLDS NUMBERS FOR PDU-10 TESTS AND COMPARISON WITH COLD FLOW DATA

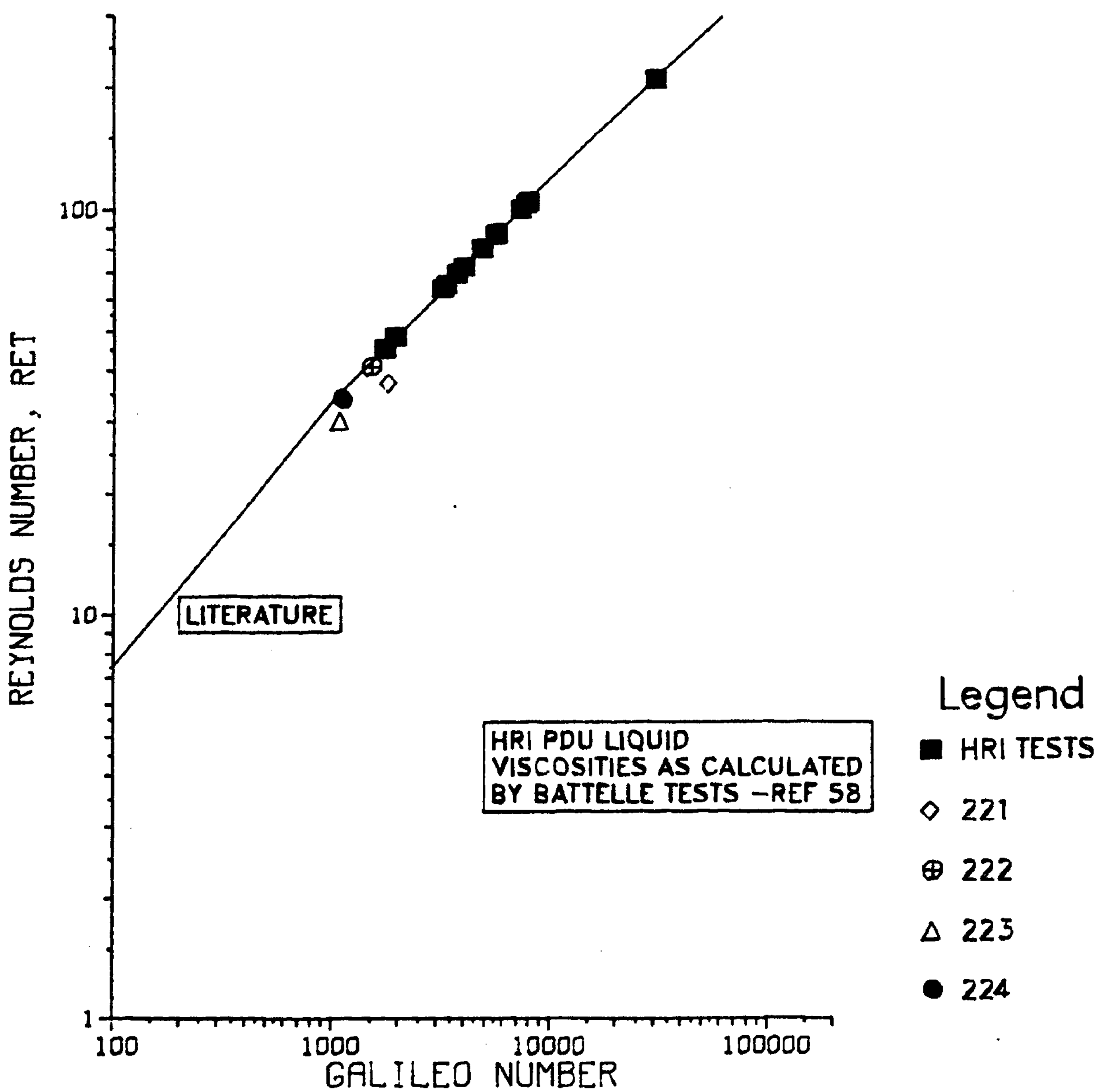

FIGURE 80

PREDICTION OF CATALYST RICHARDSON-ZAKI INDEX FOR PDU-10 TESTS AND COMPARISON WITH COLD FLOW DATA

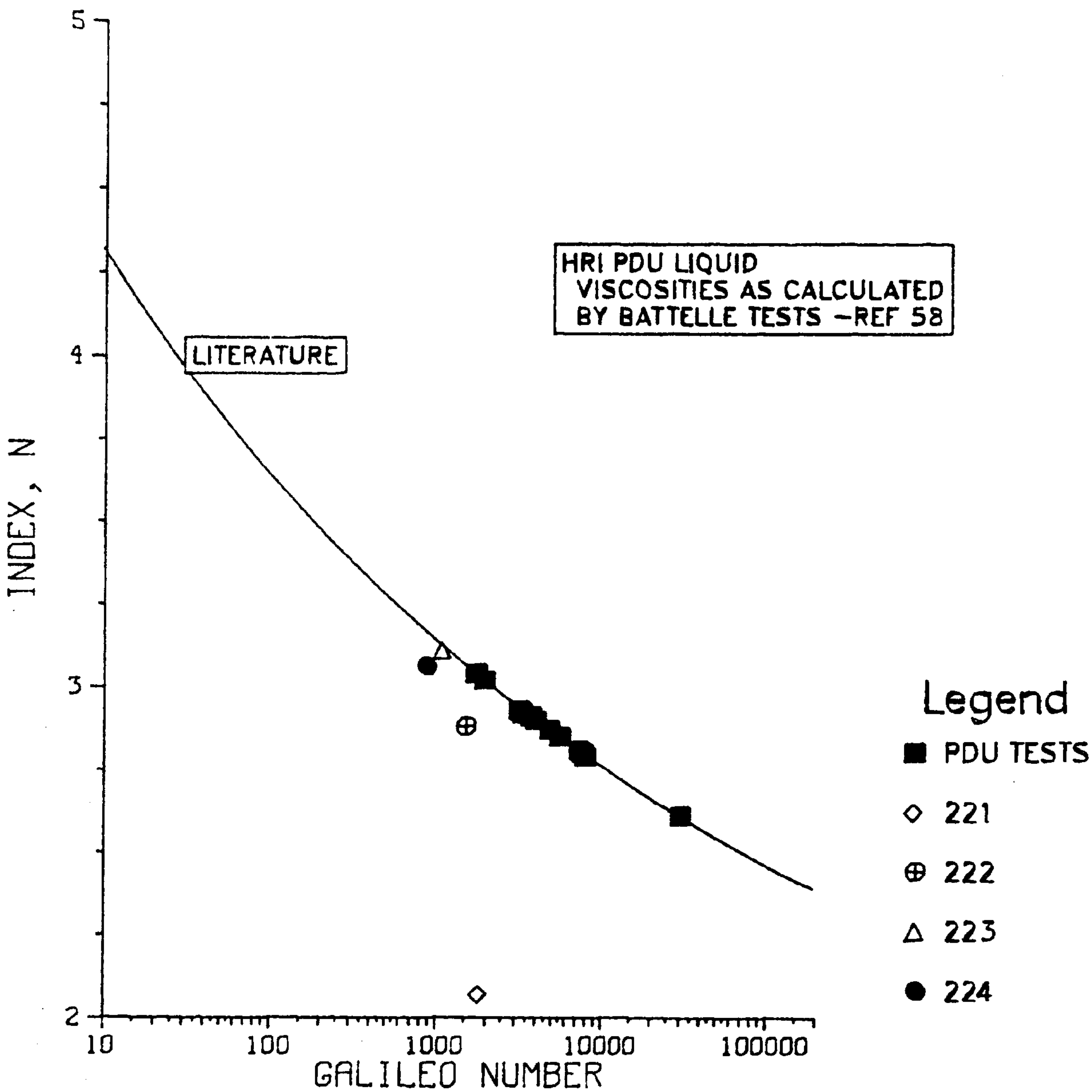

FIGURE 81

PREDICTION OF CATALYST PARTICLE TERMINAL REYNOLDS NUMBERS FOR PDU-10 TESTS AND COMPARISON WITH COLD FLOW DATA

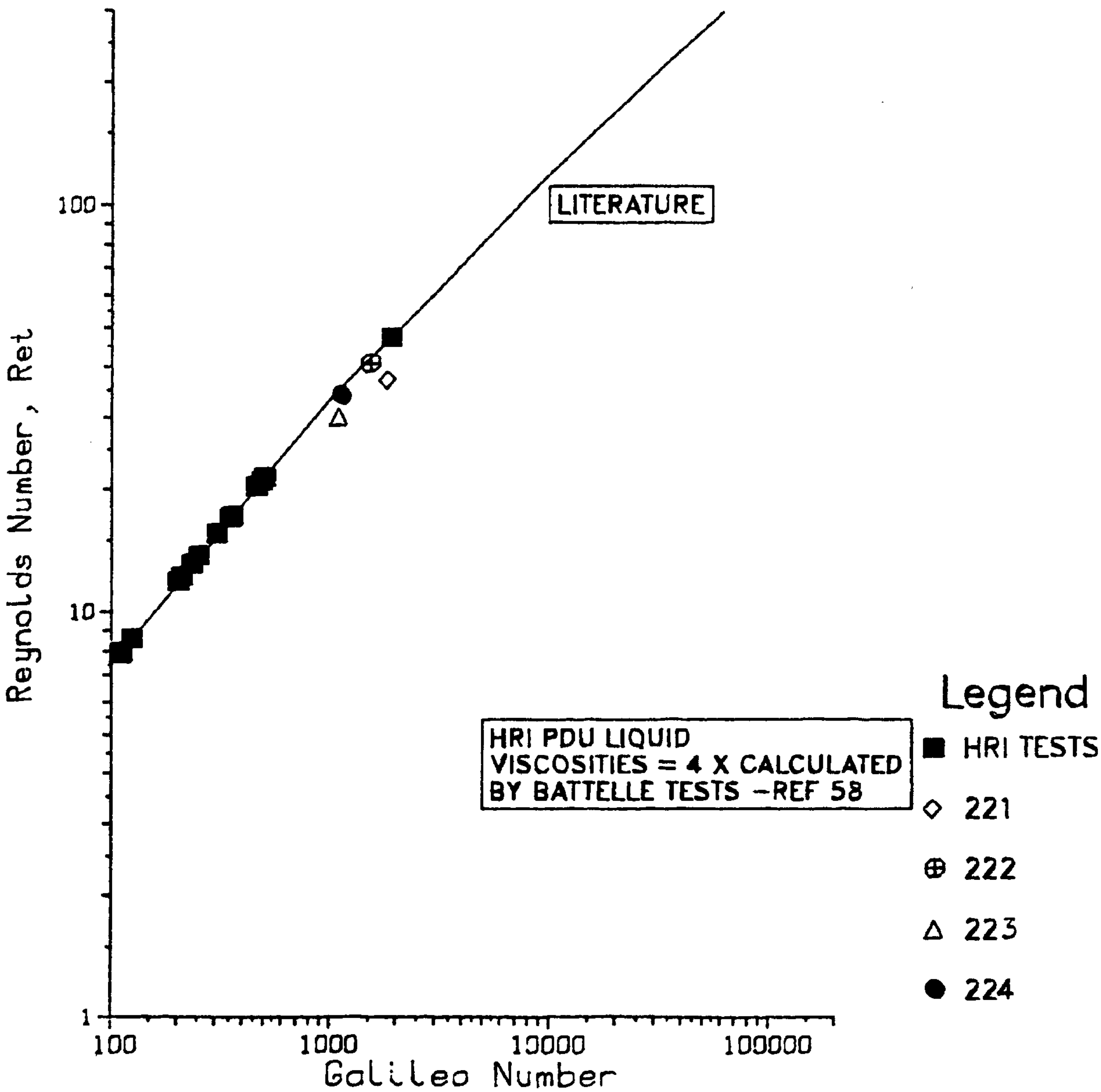

FIGURE 82

PREDICTION OF CATALYST RICHARDSON-ZAKI INDEX FOR PDU-10 TESTS AND COMPARISON WITH COLD FLOW DATA

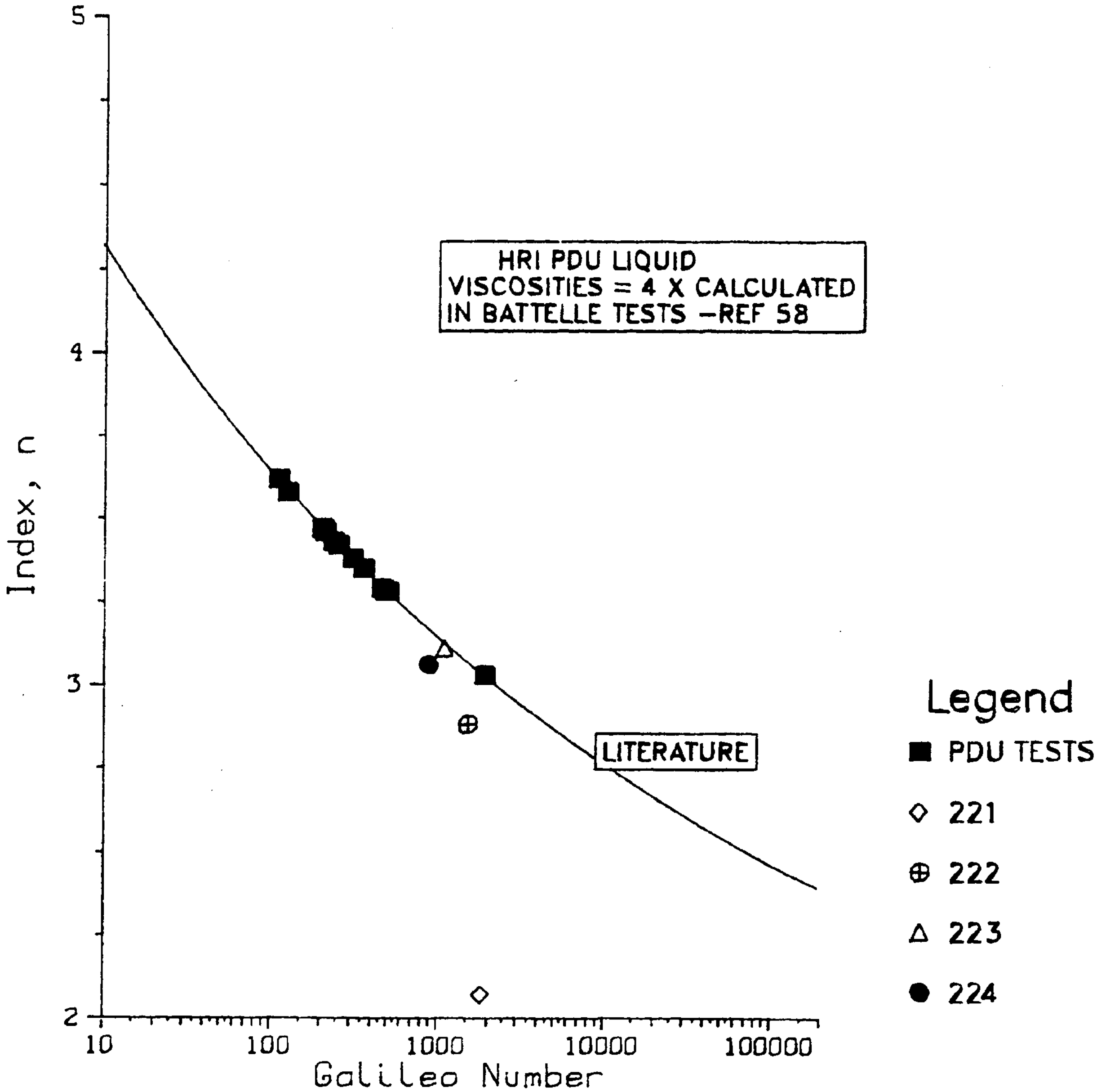

FIGURE 83

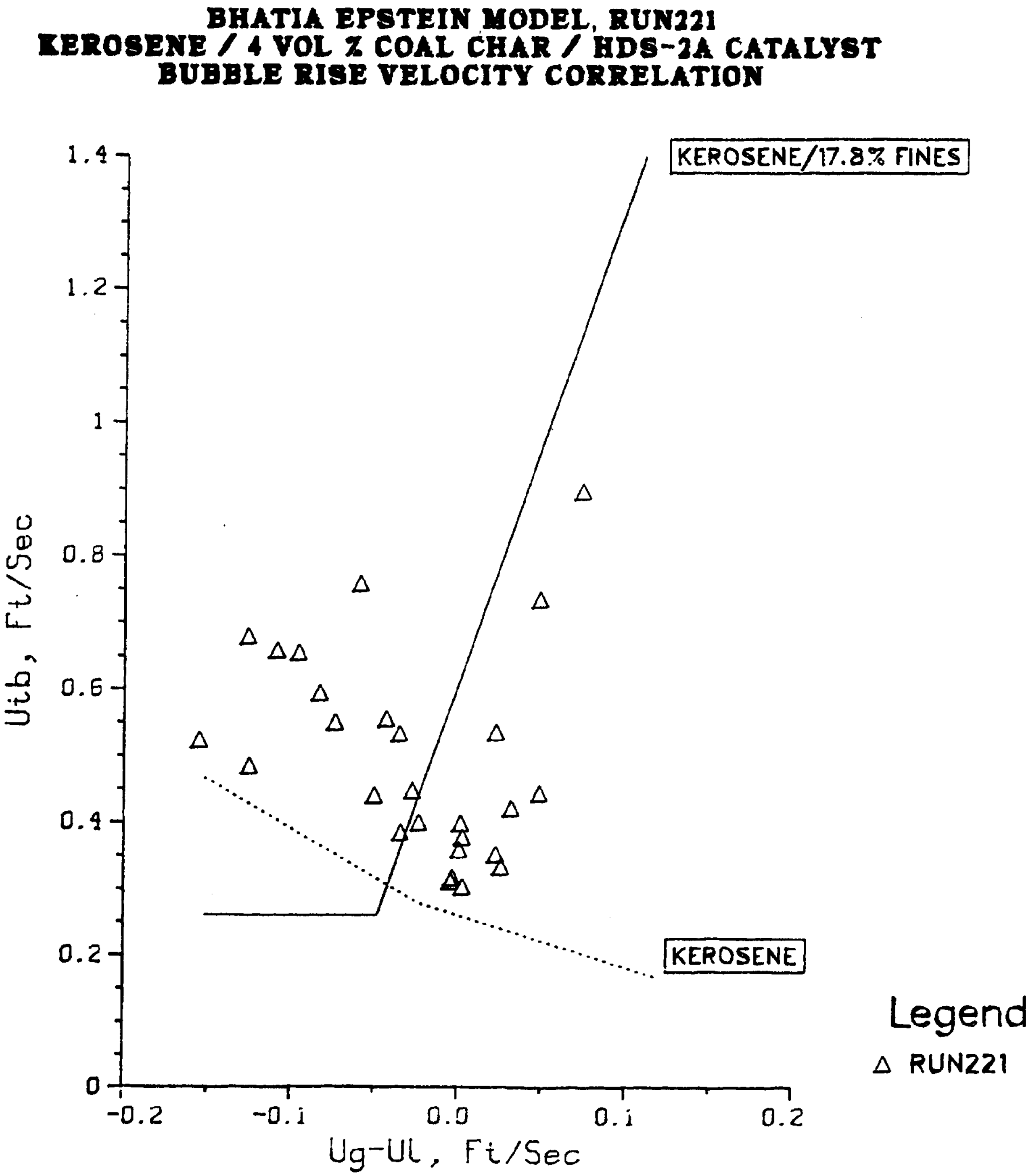
BHATIA EPSTEIN MODEL, RUN221
KEROSENE / 4 VOL % COAL CHAR / HDS-2A CATALYST
BUBBLE RISE VELOCITY CORRELATION
KEROSENE/17.8% FINES
KEROSENE
Uib, Ft/Sec
Ug-UL, Ft/Sec
1.4
1.2
1
0.8
0.6
0.4
0.2
0
-0.2
-0.1
0.0
0.1
0.2
Legend
△ RUN221

FIGURE 84

BHATIA EPSTEIN MODEL, RUN222
KEROSENE / 9.8 VOL % COAL CHAR / HDS-2A CATALYST
BUBBLE RISE VELOCITY CORRELATION

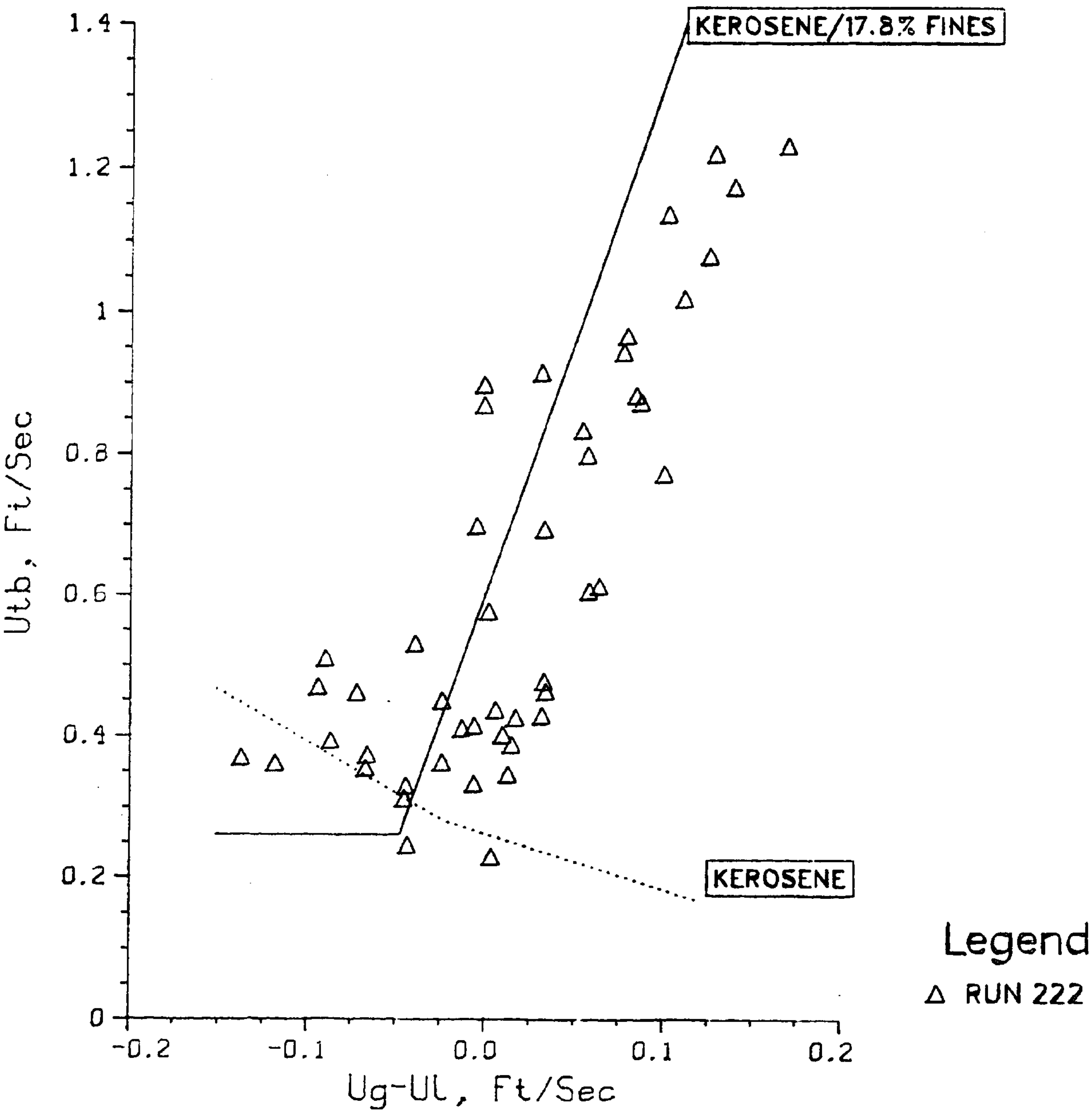

FIGURE 85

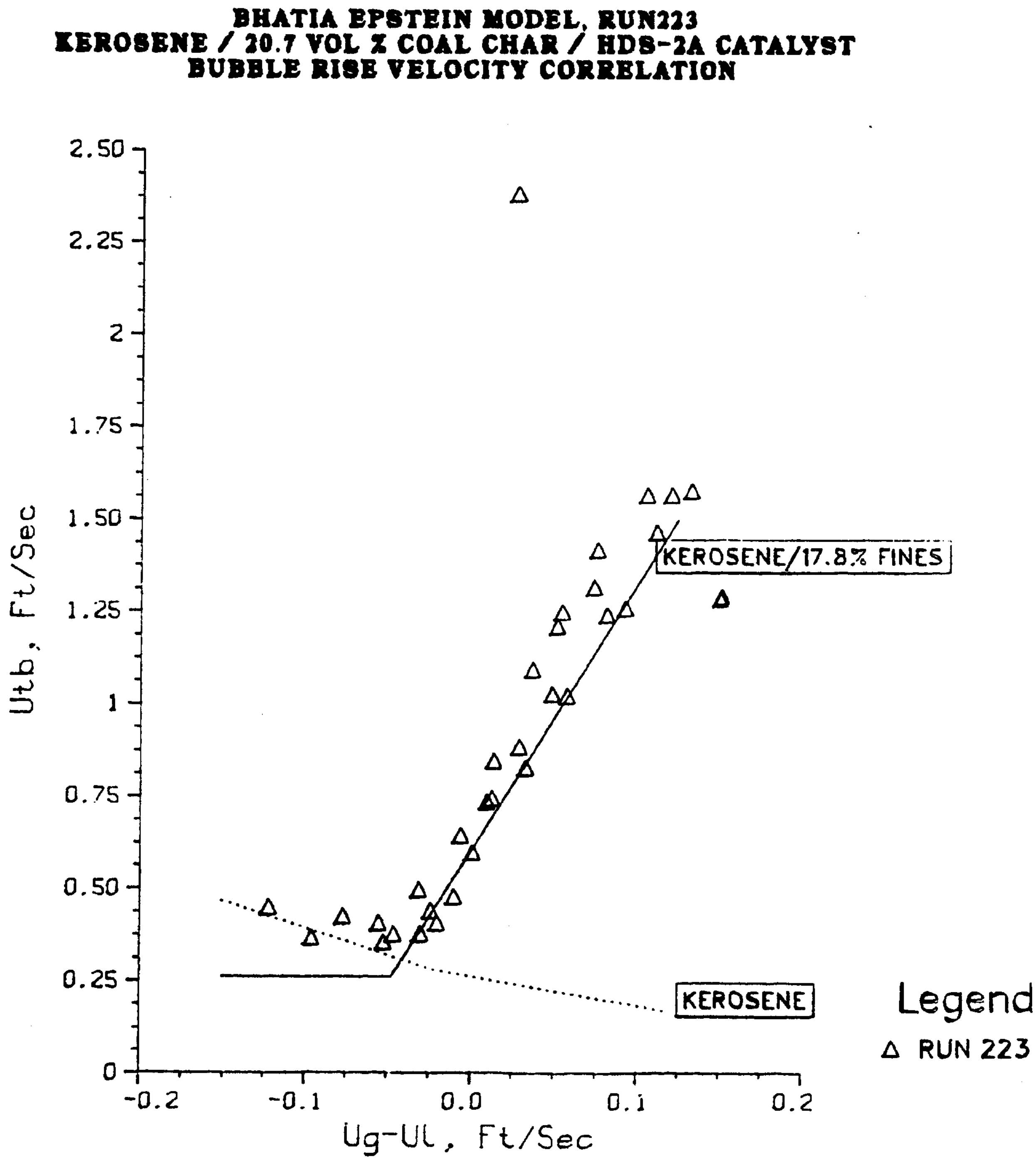
BHATIA EPSTEIN MODEL, RUN223
KEROSENE / 20.7 VOL % COAL CHAR / HDS-2A CATALYST
BUBBLE RISE VELOCITY CORRELATION
2.50
2.25
2
1.75
1.50
1.25
1
0.75
0.50
0.25
0
Utb, Ft/Sec
-0.2
-0.1
0.0
0.1
0.2
Ug-UL, Ft/Sec
KEROSENE/17.8% FINES
KEROSENE
Legend
RUN 223

FIGURE 86

BHATIA EPSTEIN MODEL, RUN224
KEROSENE / 15.4 VOL % COAL CHAR / AMOCAT-IA CATALYST
BUBBLE RISE VELOCITY CORRELATION

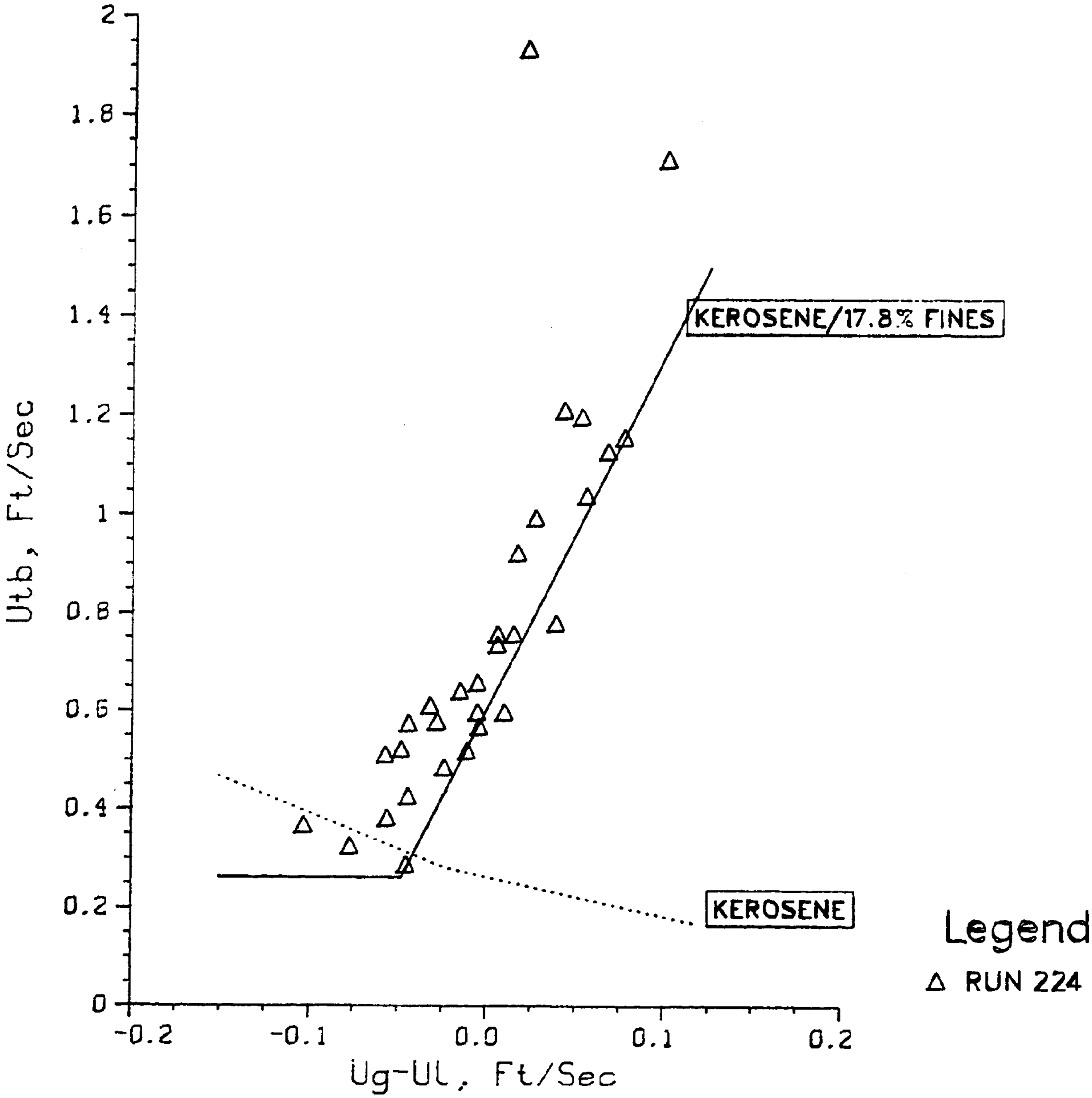

FIGURE 87

BHATIA EPSTEIN MODEL, RUN221
KEROSENE / 4 VOL % COAL CHAR / HDS-2A CATALYST
WAKE VOLUME RATIO CORRELATION

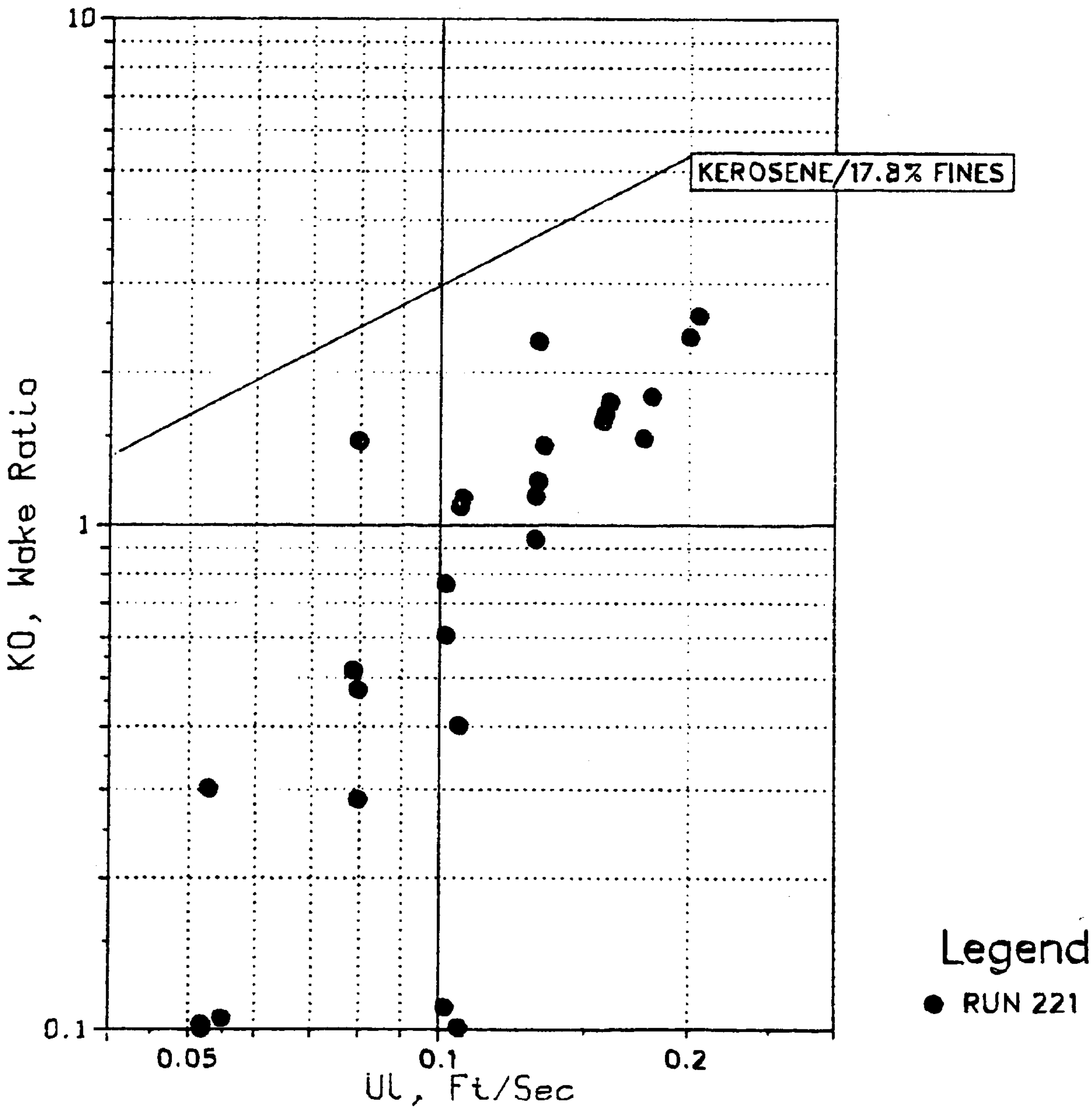

FIGURE 88

BHATIA EPSTEIN MODEL, RUN 222
KEROSENE / 9.8 VOL % COAL CHAR / HDS-2A CATALYST
WAKE VOLUME RATIO CORRELATION

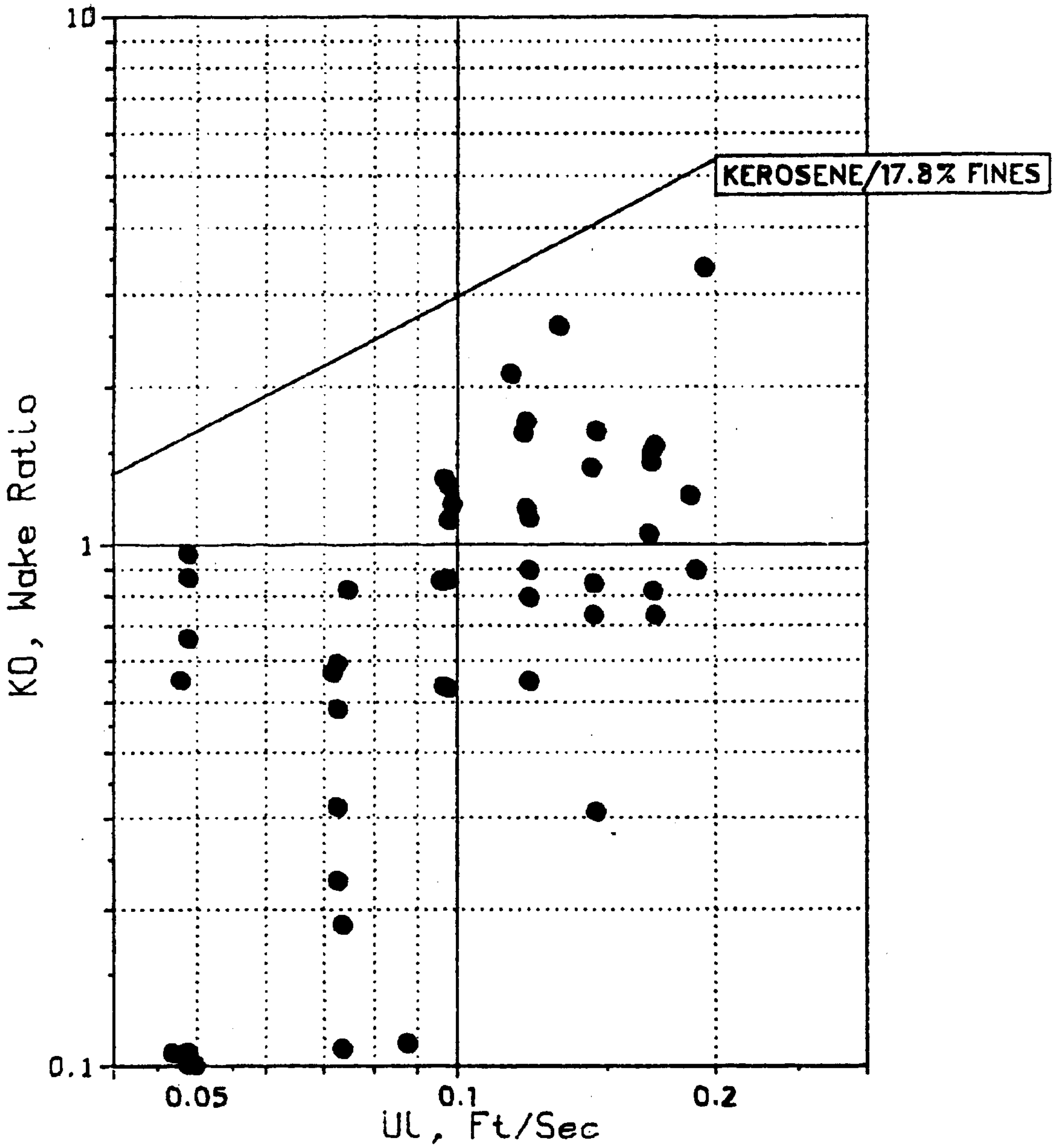

FIGURE 89

BHATIA EPSTEIN MODEL, RUN 223
KEROSENE / 20.7 VOL % COAL CHAR / HDS-2A CATALYST
WAKE VOLUME RATIO CORRELATION

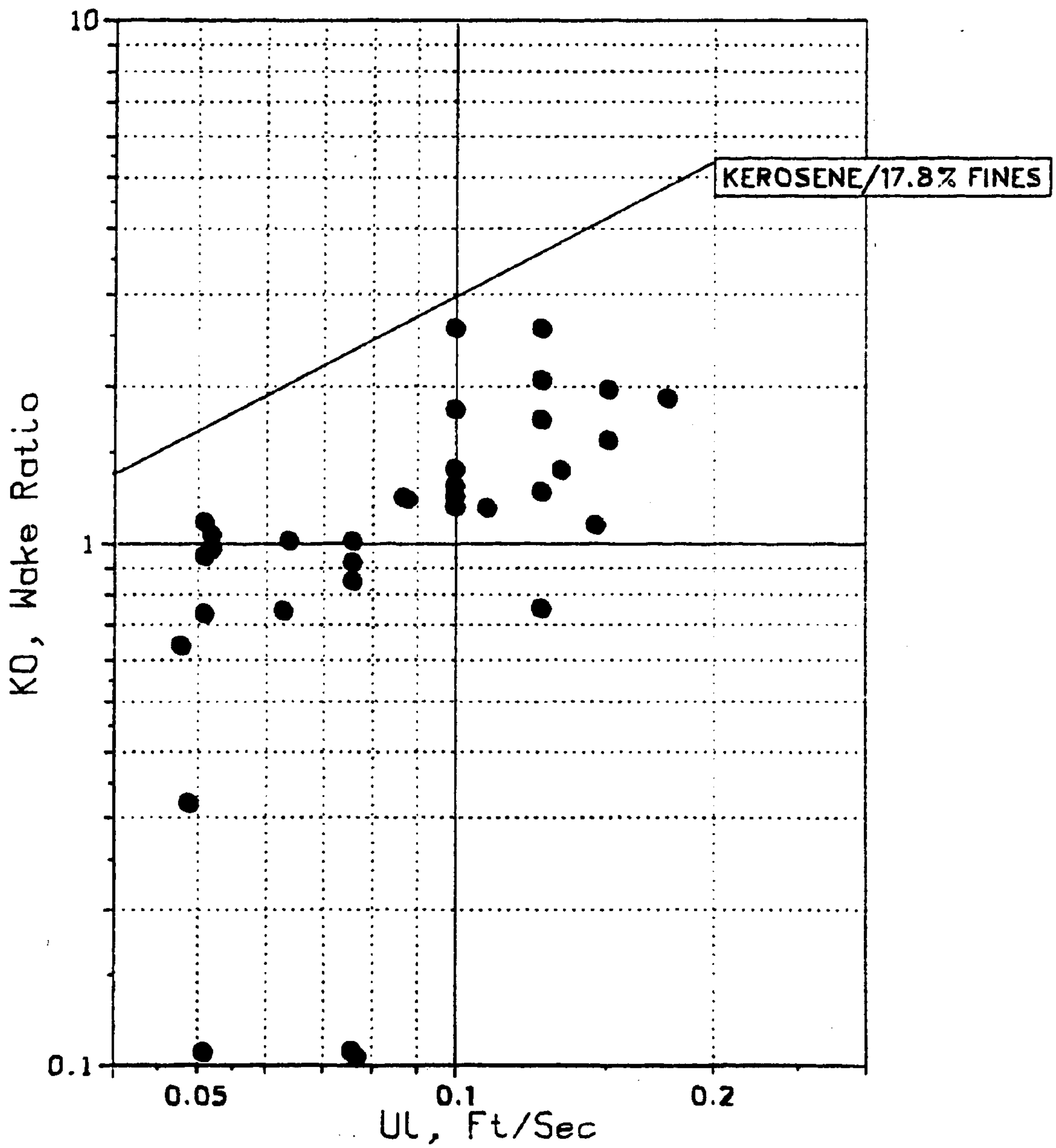

FIGURE 90

BHATIA EPSTEIN MODEL, RUN 224
KEROSENE / 15.4 VOL % COAL CHAR / AMOCAT-1 A CATALYST
WAKE VOLUME RATIO CORRELATION

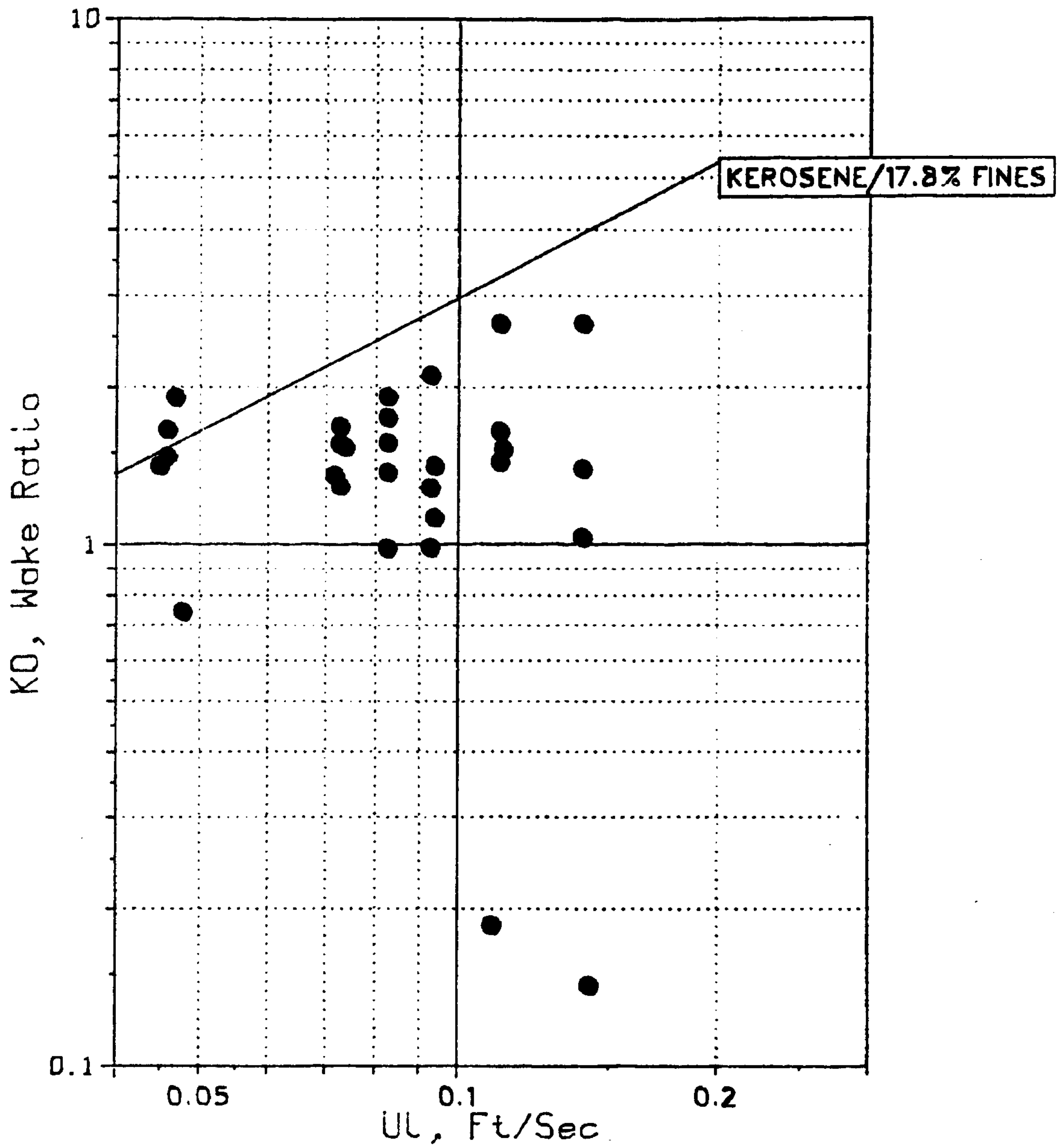

FIGURE 91

**COMPARISON OF BHATIA EPSTEIN BUBBLE RISE VELOCITIES
COLD FLOW RUN 224 VS HRI PDU-10 TESTS**

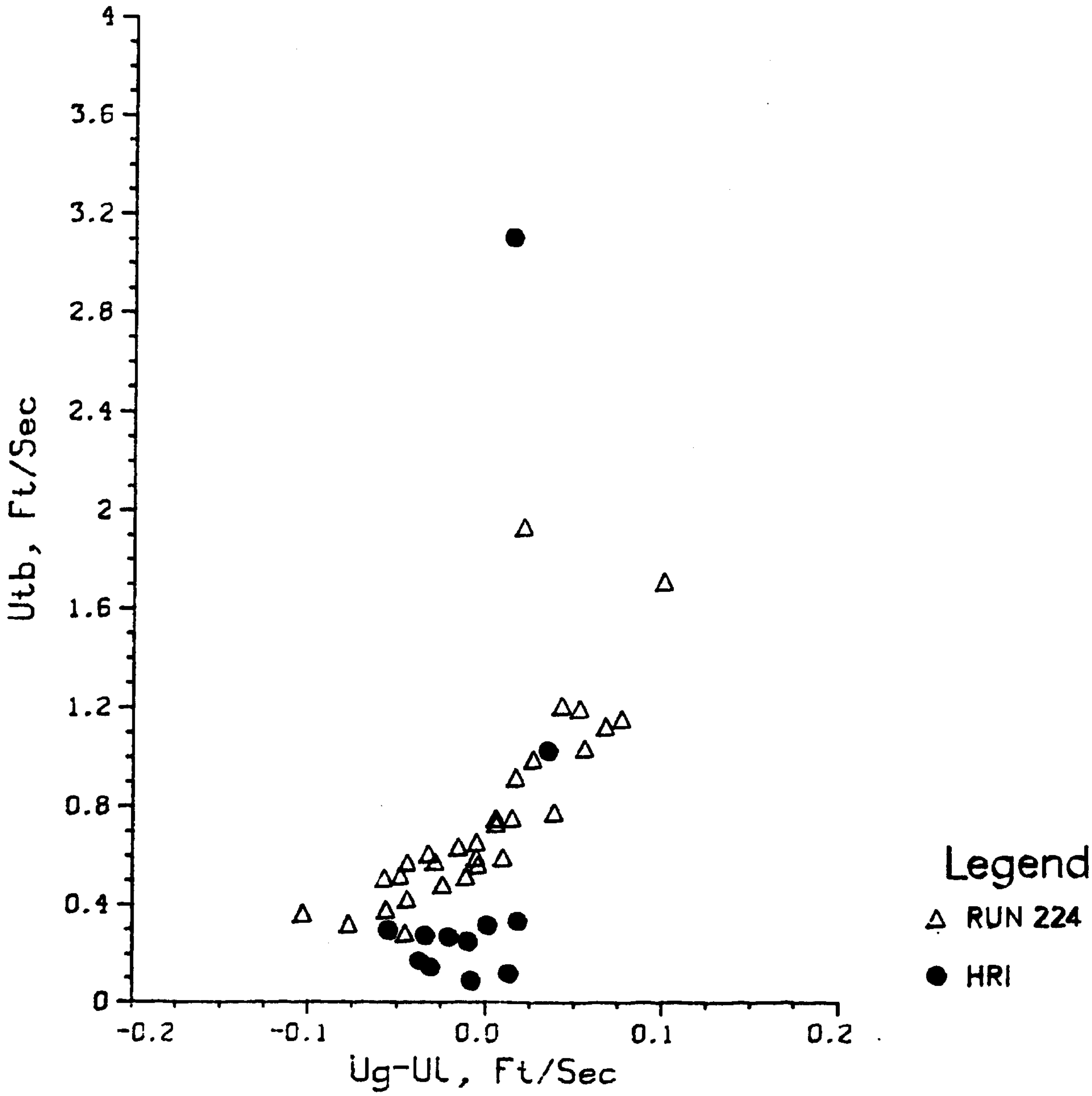

FIGURE 92

BHATIA EPSTEIN MODEL
COMPARISON OF BUBBLE RISE VELOCITIES
PDU-10 VS COLD FLOW RUN 224

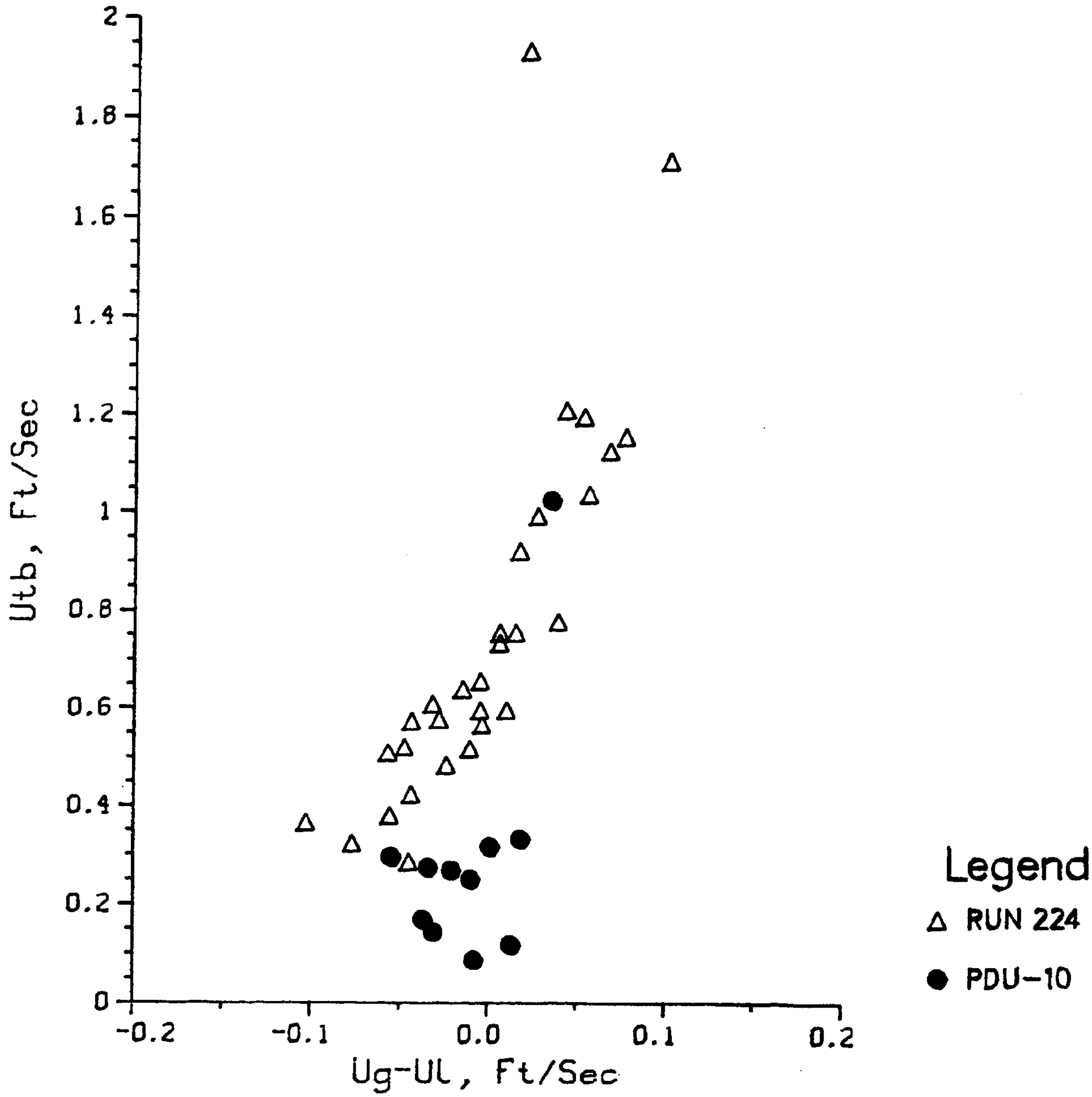

FIGURE 93

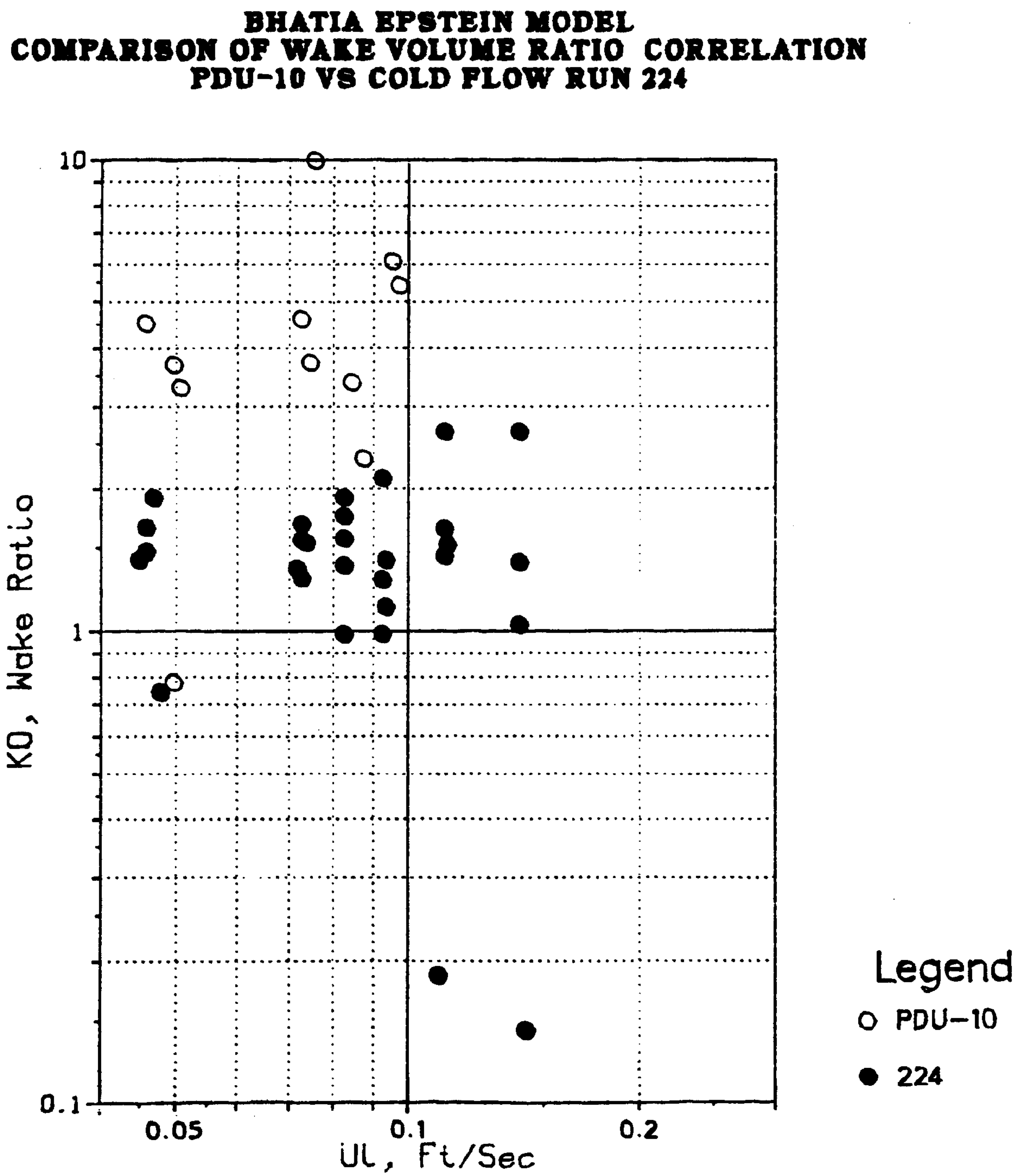
BHATIA EPSTEIN MODEL
COMPARISON OF WAKE VOLUME RATIO CORRELATION
PDU-10 VS COLD FLOW RUN 224
10
1
0.1
0.05
0.1
0.2
UL, Ft/Sec
KO, Wake Ratio
Legend
PDU-10
224